

Dear Editor:

We are truly grateful for your and other reviewers' comments on our manuscript. Based on these valuable comments, we have carefully addressed the concerns with this work. Please see our point-by-point responses to the comments and the revised manuscript for details.

Thank you very much for your concerning.

Best regards.

Sincerely yours,

Pusheng Zhao & Jing Ding

**Anonymous Referee #1**

**This paper utilizes unique data sets to predict aerosol pH in the more polluted regions of China. Overall, the paper is a significant contribution since little is known about aerosol pH in these regions and even less on size resolved pH. However, in my view, the analysis is somewhat limited. The authors have an interesting data set that could be more fully utilized to assess the pH predictions, partitioning of inorganic species and understand aerosol pH from a more fundamental standpoint.**

**Response:** Thank you for your valuable comments. Your comments have greatly improved our paper and made this work more rigorous. Please see our point-by-point responses to the comments and the revised manuscript for details. The order of the Figures or Tables in Response is the same as the corresponding Figure or Table appears in the main text and supplemental materials. Moreover, we carefully examined the grammar and expression in the text.

**A suite of important inorganic gases was measured with the MARGA, but they are not significantly discussed in the paper. This is a major oversight. For example, in the comparison of the model to measurements the particle data are shown, but no gas data. For the MOUDI, no gas data is available so the pH is estimated by an iteration method, why not use the MARGA data, which includes gases, to test the sensitivity of pH to this approach?**

**Response:** In the revised manuscript, comparisons and corresponding discussions of predicted and measured  $\text{NH}_3$ ,  $\text{HNO}_3$ ,  $\text{HCl}$ ,  $\text{NH}_4^+$ ,  $\text{NO}_3^-$ ,  $\text{Cl}^-$ ,  $\epsilon(\text{NH}_4^+)$  ( $\text{NH}_4^+ / (\text{NH}_3 + \text{NH}_4^+)$ , mol/mol),  $\epsilon(\text{NO}_3^-)$

( $\text{NO}_3^-/(\text{HNO}_3+\text{NO}_3^-)$ , mol/mol), and  $\epsilon(\text{Cl}^-)$  ( $\text{Cl}^-/(\text{HCl}+\text{Cl}^-)$ , mol/mol) based on MARGA measurement were supplemented, and the detailed information was also showed there.

The data set of MOUDI was obtained during 2013 and 2014, which was not synchronous with the online ion data (obtained in 2016 and 2017), hence an iteration method used in Fang et al. (2017) and Guo et al. (2016) was applied in this work. The MOUDI samples were mainly used to investigate the size distribution of aerosol pH.

**pH is calculated under the assumption of a completely deliquesced particle with no phase separation, all the way down to very low RH, ie, to 30%. These assumptions at low RH need to be justified. Eg, the predicted and measured partitioning of  $\text{NH}_3/\text{NH}_4^+$ ,  $\text{HNO}_3/\text{NO}_3^-$ ,  $\text{HCl}/\text{Cl}^-$  etc (ie include analysis of the gases) could be assessed as a function of pH and see if changes occur at lower RH. Discussion of phase separation in the literature under various conditions (RH, T, O/C) etc should be discussed.**

**Response:** In this work, particles were assumed in metastable, which means the aerosol is in the only liquid state. However, when the particles are exposed to the quite low RH or the ambient RH reached efflorescent RH, the state of particles may change. Figure 2 and Figure S1-S4 exhibit the comparisons between predicted and measured  $\text{NH}_3$ ,  $\text{HNO}_3$ ,  $\text{HCl}$ ,  $\text{NH}_4^+$ ,  $\text{NO}_3^-$ ,  $\text{Cl}^-$ ,  $\epsilon(\text{NH}_4^+)$  ( $\text{NH}_4^+/(\text{NH}_3+\text{NH}_4^+)$ , mol/mol),  $\epsilon(\text{NO}_3^-)$  ( $\text{NO}_3^-/(\text{HNO}_3+\text{NO}_3^-)$ , mol/mol),  $\epsilon(\text{Cl}^-)$  ( $\text{Cl}^-/(\text{HCl}+\text{Cl}^-)$ , mol/mol) based on real-time ion chromatography data, which are all colored by the corresponding RH. It can be seen that agreement between predicted and measured  $\text{NH}_3$ ,  $\text{NH}_4^+$ ,  $\text{NO}_3^-$ ,  $\text{Cl}^-$  were pretty well. However, measured and predicted partitioning of  $\text{HNO}_3$  and  $\text{HCl}$  showed significant discrepancies ( $R^2$  of 0.28 and 0.18), which may be attributed to the much lower gas concentrations compared with the particle concentrations, as well as the gas denuder measurement uncertainties from particle collection artifacts (Guo et al., 2018). Obviously, more scatter points deviate from the 1:1 line when ISORROPIA-II runs at  $\text{RH} \leq 30\%$ , which is much evident in winter and spring. For data with  $\text{RH} \leq 30\%$ , the predictions were significantly improved when assuming aerosol in stable mode (solid + liquid) (Figure S5-S6). However, the aerosol liquid water was almost zero and cannot be used to predict aerosol pH. It reveals that it is not reasonable to predict the aerosol pH using the thermodynamic model when the RH is relatively low. Consequently, in the revised manuscript, the results were only discussed for data with RH higher than 30%. **(Page 8 and 9, line 195-217, in the**

**revised manuscript)**

A new section (Section 3.3 Gas-particle separation) was added in the revised manuscript. Table 2 exhibited the measured  $\epsilon(\text{NH}_4^+)$ ,  $\epsilon(\text{NO}_3^-)$ , and  $\epsilon(\text{Cl}^-)$  at different RH levels. The measured  $\epsilon(\text{NH}_4^+)$ ,  $\epsilon(\text{NO}_3^-)$ , and  $\epsilon(\text{Cl}^-)$  increased with the elevated RH in all four seasons, indicating more  $\text{NH}_4^{\text{T}}$ ,  $\text{NO}_3^{\text{T}}$ , and  $\text{Cl}^{\text{T}}$  were partitioned into particle phase at higher RH. In winter and spring,  $\text{NO}_3^{\text{T}}$  and  $\text{Cl}^{\text{T}}$  were dominated by particle phases. Whereas in summer and autumn, more than half of the  $\text{NO}_3^{\text{T}}$  and  $\text{Cl}^{\text{T}}$  were partitioned into the gaseous phase. When the RH reaches above 60%, more than 90% of  $\text{NO}_3^{\text{T}}$  and 70% of  $\text{Cl}^{\text{T}}$  were in the particle phase for all four seasons. Compared with  $\epsilon(\text{NO}_3^-)$  and  $\epsilon(\text{Cl}^-)$ , the  $\epsilon(\text{NH}_4^+)$  was pretty lower, which may attribute to the higher  $\text{NH}_3$  mass concentration in the atmosphere. In winter, the average  $\epsilon(\text{NH}_4^+)$  were much higher than that in other seasons with the relatively lower  $\text{NH}_3$  mass concentration. **(Page 14, line 357-371, in the revised manuscript)**

**Greater utilization of the gas data could also help the authors understand fundamentally what is driving pH and the sensitivities to various parameters. This could include the use of S curves, as done extensively by Guo et al, to go beyond just simple variation of one variable at a time. Eg, why in the sensitivity analysis do changes in HNO3 not affect pH, but changes in NH3 do? These, and possibly other, more detailed analysis would reduce the sense that the authors simply run the thermodynamic model and plotted results.**

**Response:** In the real ambient air, the thermodynamic process of the aerosol is complicated, it is not easy to tell the effect of one factor on aerosol pH. The ISORROPIA-II can well predict the effect of an input variable on output data. Thus, in this paper, we focus on the sensitivity analysis of single-factor variation, which can reflect the variation tendency of aerosol pH caused by the change of each variable. When running the ISO-II model, the total nitrate ( $\text{NO}_3^{\text{T}}$ , gas+aerosol), total ammonium ( $\text{NH}_4^{\text{T}}$ , gas+aerosol), and total chloride ( $\text{Cl}^{\text{T}}$ , gas+aerosol) are input, and the gas and aerosol phase of these three components would be reapporitioned and output. In view of this, it is more reasonable to analyze the impact of  $\text{NO}_3^{\text{T}}$ ,  $\text{NH}_4^{\text{T}}$ , and  $\text{Cl}^{\text{T}}$  on aerosol pH, rather than the impact of a single gas or aerosol phase of  $\text{NO}_3^{\text{T}}$ ,  $\text{NH}_4^{\text{T}}$ , and  $\text{Cl}^{\text{T}}$  on aerosol pH. In the revised manuscript, the data analysis for the sensitivities of aerosol pH to  $\text{SO}_4^{2-}$ ,  $\text{NO}_3^{\text{T}}$ ,  $\text{NH}_4^{\text{T}}$ ,  $\text{Cl}^{\text{T}}$ , RH, and T were fully reorganized and reinspected. More discussions about gas-particle partitioning were added to this section. The impacts of  $\text{NO}_3^{\text{T}}$ ,  $\text{NH}_4^{\text{T}}$ , and  $\text{Cl}^{\text{T}}$  on  $\epsilon(\text{NH}_4^+)$ ,  $\epsilon(\text{NO}_3^-)$ , and  $\epsilon(\text{Cl}^-)$  were also discussed.

More detailed information was shown in the revised manuscript.

The  $\text{SO}_4^{2-}$  and T are two crucial factors affecting aerosol pH variation. Aerosol pH is also sensitive to  $\text{NH}_4^+$  when  $\text{NH}_4^+$  is in a lower range and sensitive to RH only in summer. Figure 7-9 and S12-S17 show how these factors affect the ALWC,  $\text{H}_{\text{air}}^+$ , and aerosol acidity over four seasons.

**(Page 15, line 380-391, in the revised manuscript)**

**RH:** RH has a different impact on aerosol pH in different seasons. In winter, aerosol pH decreased with the increasing RH, whereas the aerosol pH increased with the increasing RH in summer. In spring and autumn, the RH between 30~83% had little impact on aerosol pH. The explanation for this is that the increased RH actually dilutes the solution and promotes ionization, releasing  $\text{H}_{\text{air}}^+$  and increasing ALWC as well, but the gradient was different. In winter, variation in  $\text{H}_{\text{air}}^+$  caused by RH changes was much larger than variation in ALWC, whereas it showed an opposite tendency in summer. In autumn and spring, variation in  $\text{H}_{\text{air}}^+$  caused by RH changes was slightly higher than variation in ALWC. The different impact of RH on aerosol pH indicated that the dilution effect of ALWC on  $\text{H}_{\text{air}}^+$  is obvious only in summer, the high RH during the severe haze in winter could increase the aerosol acidity. **(Page 15, line 397-406, in the revised manuscript)**

**T:** At high ambient temperature,  $\epsilon(\text{NH}_4^+)$ ,  $\epsilon(\text{NO}_3^-)$ , and  $\epsilon(\text{Cl}^-)$  all showed a decreased tendency (Figure 10 and S19). And  $\text{NH}_4^+$ ,  $\text{NO}_3^-$ , and  $\text{Cl}^-$  were volatilized partially, the procedure of  $\text{NH}_4^+ \rightarrow \text{NH}_3$  released one  $\text{H}^+$  to particle phase, whereas the procedure of  $\text{NO}_3^- \rightarrow \text{HNO}_3$  and  $\text{Cl}^- \rightarrow \text{HCl}$  needs one  $\text{H}^+$  from the particle phase. Compared with the loss of  $\text{NO}_3^-$  from  $\text{NH}_4\text{NO}_3$  as well as  $\text{Cl}^-$  from  $\text{NH}_4\text{Cl}$ , greater loss of  $\text{NH}_4^+$  from  $\text{NH}_4\text{NO}_3$ ,  $\text{NH}_4\text{Cl}$ , and  $(\text{NH}_4)_2\text{SO}_4$  resulted in a net increase in particle  $\text{H}^+$  and lower pH. In addition, molality-based equilibrium constants ( $H^*$ ) of  $\text{NH}_3\text{-NH}_4^+$  partitioning decreased faster with increasing temperature when compared with that of  $\text{HNO}_3\text{-NO}_3^-$  partitioning, resulting in a net increase in particle  $\text{H}^+$  (Guo et al., 2018). Moreover, higher ambient temperature tends to lower ALWC, which further decrease the aerosol pH. The wide range of ambient temperature in autumn made a significant impact on aerosol pH in the sensitivity analysis.

**(Page 15 and 16, line 407-416, in the revised manuscript)**

**$\text{SO}_4^{2-}$ :**  $\text{SO}_4^{2-}$  has a key role in aerosol acidity, especially in winter and spring (Figure 9, S14, S17). More  $\text{H}^+$  are released into particle phase during the formation of  $\text{SO}_4^{2-}$ , forming one  $\text{SO}_4^{2-}$  can release two  $\text{H}^+$ . In the sensitivity test, the aerosol pH decreases about 1.6 (4.1 to 2.5), 4.9 (5.1 to

0.2), 1.0 (3.6 to 2.6), and 0.9 (4.0 to 3.1) unit with  $\text{SO}_4^{2-}$  concentration goes up from 0 to  $40 \mu\text{g m}^{-3}$  in spring, winter, summer, and autumn, respectively. In spring and winter, the ALWC is low, the variation of  $\text{SO}_4^{2-}$  mass concentration could generate dramatic changes in  $\text{H}_{\text{air}}^+$ . In section 3.1, the aerosol pH was lowest in summer whereas highest in winter, which was consistent with the  $\text{SO}_4^{2-}$  mass fraction in total ions. The  $\text{SO}_4^{2-}$  mass fraction in total ions in summer was highest among four seasons with  $32.4\% \pm 11.1\%$ , whereas it was lowest in winter with  $20.9\% \pm 4.4\%$ . **(Page 16, line 418-425, in the revised manuscript)**

**$\text{NO}_3^{\text{T}}$ :** The impact of  $\text{NO}_3^-$  on aerosol pH was also different, which is related to the averages of input  $\text{NH}_4^{\text{T}}$  in different seasons. In winter, the aerosol pH decreased with increasing  $\text{NO}_3^{\text{T}}$  concentration, whereas little impact was found in summer (Figure 9). In spring and autumn, the aerosol pH increases first and then drops with the increasing  $\text{NO}_3^{\text{T}}$  concentration (Figure S14, S17). In winter, the  $\text{NH}_4^{\text{T}}$  mass concentration was low. As  $\text{NO}_3^{\text{T}}$  increases, all  $\text{NH}_3$  was converted into  $\text{NH}_4^+$  ( $\epsilon(\text{NH}_4^+) \approx 1$ ). However,  $\text{HNO}_3$  continues to dissolve and releases  $\text{H}_{\text{air}}^+$ , resulting in the decrease of aerosol pH. In summer, the averages of  $\text{NO}_3^{\text{T}}$  and  $\text{Cl}^{\text{T}}$  was relatively low but the  $\text{NH}_4^{\text{T}}$  was excessive, the highest  $\epsilon(\text{NH}_4^+)$  was only 0.6 with the corresponding highest  $\text{NO}_3^{\text{T}}$ . The excessive  $\text{NH}_3$  could provide continuous buffering to the increasing  $\text{NO}_3^{\text{T}}$ , together with a significant dilution of ALWC on  $\text{H}_{\text{air}}^+$ , leads to the little changes in aerosol pH. In spring and autumn, the increasing aerosol pH with elevated  $\text{NO}_3^{\text{T}}$  in lower range attributed to the dilution of ALWC to  $\text{H}_{\text{air}}^+$ .  $\text{H}_{\text{air}}^+$  concentration increased exponentially with elevated  $\text{NO}_3^{\text{T}}$  concentration, especially at higher  $\text{NO}_3^{\text{T}}$  concentrations, whereas the ALWC increase linearly with elevated  $\text{NO}_3^{\text{T}}$  concentration (Figure S12-S17), hence ALWC plays a dominant role when the  $\text{NO}_3^{\text{T}}$  concentration is low. With the further increase of  $\text{NO}_3^{\text{T}}$ , the variation in  $\text{H}_{\text{air}}^+$  caused by  $\text{NO}_3^{\text{T}}$  addition is larger than variation in ALWC, leading to the decrease of aerosol pH. Besides, the relationship between  $\text{NO}_3^{\text{T}}$  and  $\epsilon(\text{NH}_4^+)$  in the sensitivity analysis showed that decreasing  $\text{NO}_3^{\text{T}}$  could lower the  $\epsilon(\text{NH}_4^+)$  effectively (Figure 11 and S20), which helps  $\text{NH}_3$  maintain in the gas phase. **(Page 16 and 17, line 426-443, in the revised manuscript)**

**$\text{NH}_4^{\text{T}}$ :** The relationship between aerosol pH and  $\text{NH}_4^{\text{T}}$  was nonlinear.  $\text{NH}_4^{\text{T}}$  in lower range had a significant impact on aerosol pH (Table S2), and higher  $\text{NH}_4^{\text{T}}$  generated limited pH change (Figure 9, S14, S17). Elevated  $\text{NH}_4^{\text{T}}$  could reduce  $\text{H}_{\text{air}}^+$  exponentially and slightly increase ALWC when the

other input parameters were held constant. As the  $\text{NH}_4^{\text{T}}$  increases,  $\text{H}_{\text{air}}^+$  are consumed swiftly during the dissolution of  $\text{NH}_3$  and the further reaction with  $\text{SO}_4^{2-}$ ,  $\text{NO}_3^-$ , and  $\text{Cl}^-$ . And the elevated  $\text{NH}_4^{\text{T}}$  increased the  $\epsilon(\text{NO}_3^-)$  and  $\epsilon(\text{Cl}^-)$  when  $\text{NO}_3^{\text{T}}$  and  $\text{Cl}^{\text{T}}$  were fixed (Figure 11 and S20), which means the elevated  $\text{NH}_4^{\text{T}}$  alters the gas-particle partition and shifts more  $\text{NO}_3^{\text{T}}$  and  $\text{Cl}^{\text{T}}$  into particle phase, leading to the deliquescence of additional nitrate and chloride and increase of ALWC. It seems that  $\text{NH}_3$  emission control is a good way to reduce  $\text{NO}_3^-$ . However, the relationship between  $\text{NH}_4^{\text{T}}$  and  $\epsilon(\text{NO}_3^-)$  in the sensitivity analysis (Figure 11 and S20) showed that the  $\epsilon(\text{NO}_3^-)$  response to  $\text{NH}_4^{\text{T}}$  control is highly nonlinear, which means the decrease of nitrate is effective only when the  $\text{NH}_4^{\text{T}}$  is greatly reduced. The same result was obtained from Guo et al (2018) using the S curve method. **(Page 17, line 445-457, in the revised manuscript)**

The ratio of  $[\text{TA}]/2[\text{TS}]$  provides a qualitative description for the ammonia abundance, where  $[\text{TA}]$  and  $[\text{TS}]$  are the total (gas + aqueous + solid) molar concentrations of ammonia and sulfate. The rich-ammonia is defined as  $[\text{TA}] > 2[\text{TS}]$ , while if the  $[\text{TA}] \leq 2[\text{TS}]$ , then it is defined as poor-ammonia (Seinfeld and Pandis, 2016). In this work, the ratio of  $[\text{TA}]/2[\text{TS}]$  is much higher than 1 and belongs to rich-ammonia (Figure. S21). Although  $\text{NH}_3$  in the NCP is abundant, the aerosol pH is far from neutral, which may attribute to the limited ALWC. Compared to the liquid water content in clouds and precipitation, ALWC is much lower, hence the dilution of aerosol liquid water to  $\text{H}_{\text{air}}^+$  is weak. **(Page 17, line 458-465, in the revised manuscript)**

**$\text{Cl}^{\text{T}}$ :**  $\text{Cl}^{\text{T}}$  has a relatively larger impact on aerosol pH in winter and spring compared to summer and autumn. Except for winter, the  $\text{Cl}^{\text{T}}$  mass concentration was generally lower than  $10 \mu\text{g m}^{-3}$ , which accounted for the little impact on aerosol pH. On account of the low level of  $\text{Cl}^{\text{T}}$ , the dilution of ALWC on  $\text{H}_{\text{air}}^+$  plays a dominant role, generating the aerosol pH increase with elevated  $\text{Cl}^{\text{T}}$ . However, similar to  $\text{NO}_3^{\text{T}}$ , higher  $\text{Cl}^{\text{T}}$  could decrease the aerosol pH. **(Page 17 and 18, line 466-470, in the revised manuscript)**

**$\text{Ca}^{2+}$ :** In fine particles,  $\text{Ca}^{2+}$  mass concentration was generally low. In the output of ISORROPIA-II, Ca existed as  $\text{CaSO}_4$  (slightly soluble). Elevated  $\text{Ca}^{2+}$  concentration could increase the aerosol pH by decreasing  $\text{H}_{\text{air}}^+$  and ALWC (Figure. S18), the decreased  $\text{H}_{\text{air}}^+$  results from the buffering capacity of  $\text{Ca}^{2+}$  to the acid species, while the decreased ALWC result from the weak water solubility of  $\text{CaSO}_4$ . As discussed in Section 3.1, on clean conditions, the aerosol pH could reach

6~7 when the mass fraction of  $\text{Ca}^{2+}$  was high, hence the role of mineral ions on aerosol pH could not be ignored in seasons (such as spring) or regions where mineral dust was an important source of fine particles. Due to the strict control measures for road dust, construction sites, and other bare ground, the nonvolatile cations in  $\text{PM}_{2.5}$  decreased significantly in NCP. (Page 18, line 471-479, in the revised manuscript)

**Table 2.** The averaged ambient temperature and  $\epsilon(\text{NH}_4^+)$ ,  $\epsilon(\text{NO}_3^-)$ ,  $\epsilon(\text{Cl}^-)$  at different ambient RH levels in four seasons.

	RH	T, °C	$\epsilon(\text{NH}_4^+)$	$\epsilon(\text{NO}_3^-)$	$\epsilon(\text{Cl}^-)$
Spring	$\leq 30\%$	$24.8 \pm 3.7$	$0.17 \pm 0.14$	$0.84 \pm 0.12$	$0.67 \pm 0.24$
	30~60 %	$20.6 \pm 3.8$	$0.25 \pm 0.14$	$0.91 \pm 0.06$	$0.82 \pm 0.16$
	$>60\%$	$15.8 \pm 2.7$	$0.28 \pm 0.12$	$0.96 \pm 0.03$	$0.96 \pm 0.06$
Winter	$\leq 30\%$	$5.4 \pm 5.3$	$0.31 \pm 0.13$	$0.78 \pm 0.12$	$0.89 \pm 0.14$
	30~60 %	$1.0 \pm 3.6$	$0.50 \pm 0.21$	$0.89 \pm 0.10$	$0.97 \pm 0.03$
	$>60\%$	$-1.9 \pm 2.1$	$0.60 \pm 0.20$	$0.96 \pm 0.03$	$0.99 \pm 0.01$
Summer	$\leq 30\%$	$35.6 \pm 0.4$	$0.06 \pm 0.02$	$0.35 \pm 0.20$	$0.39 \pm 0.17$
	30~60 %	$29.6 \pm 4.2$	$0.17 \pm 0.11$	$0.65 \pm 0.23$	$0.43 \pm 0.16$
	$>60\%$	$25.2 \pm 3.8$	$0.26 \pm 0.12$	$0.90 \pm 0.12$	$0.71 \pm 0.15$
Autumn	$\leq 30\%$	$21.7 \pm 7.5$	$0.07 \pm 0.06$	$0.49 \pm 0.25$	$0.45 \pm 0.21$
	30~60 %	$20.8 \pm 6.3$	$0.21 \pm 0.14$	$0.82 \pm 0.19$	$0.67 \pm 0.21$
	$>60\%$	$14.9 \pm 5.7$	$0.30 \pm 0.19$	$0.92 \pm 0.10$	$0.86 \pm 0.13$

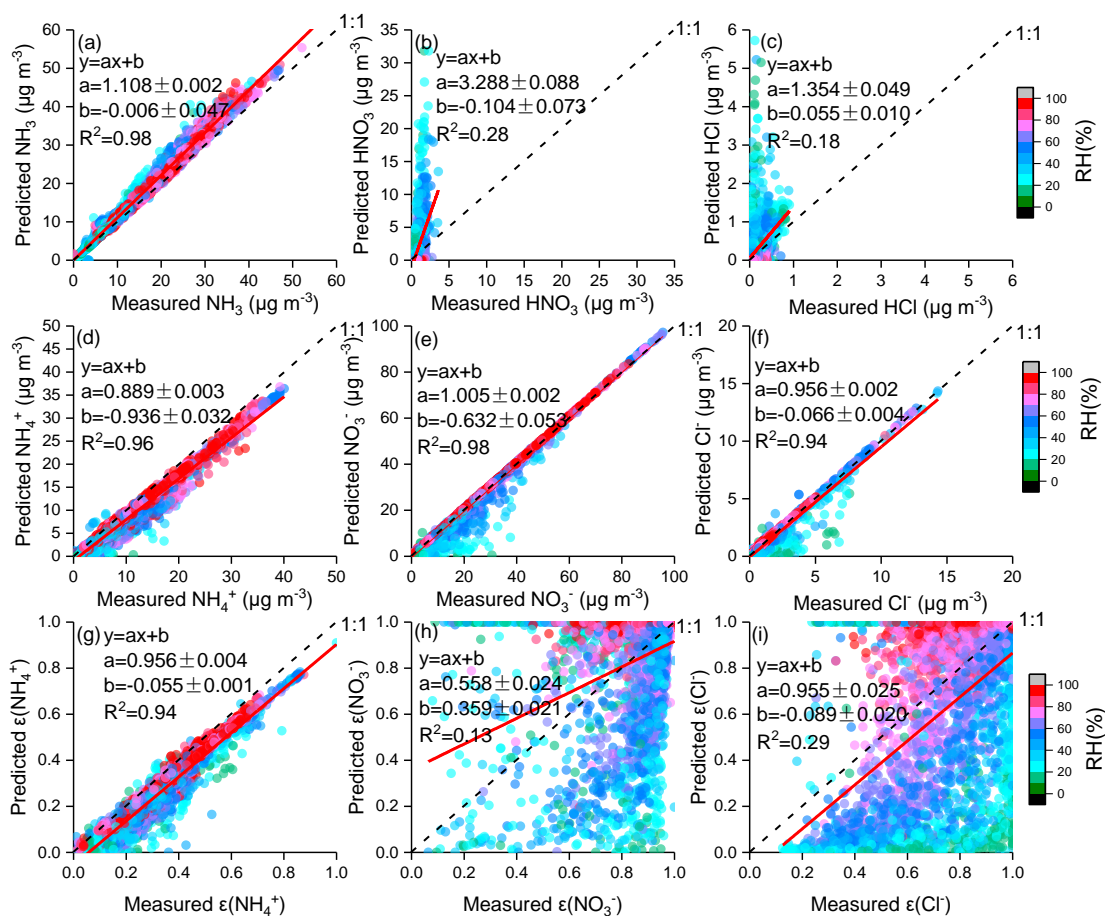


**Figure 2.** Comparisons of predicted and measured  $\text{NH}_3$ ,  $\text{HNO}_3$ ,  $\text{HCl}$ ,  $\text{NH}_4^+$ ,  $\text{NO}_3^-$ ,  $\text{Cl}^-$ ,  $\epsilon(\text{NH}_4^+)$ ,  $\epsilon(\text{NO}_3^-)$ ,  $\epsilon(\text{Cl}^-)$  colored by RH. In this Figure, the real-time data in four seasons were put together, and the comparisons for each season were shown in Figure S1-S4.



Spring

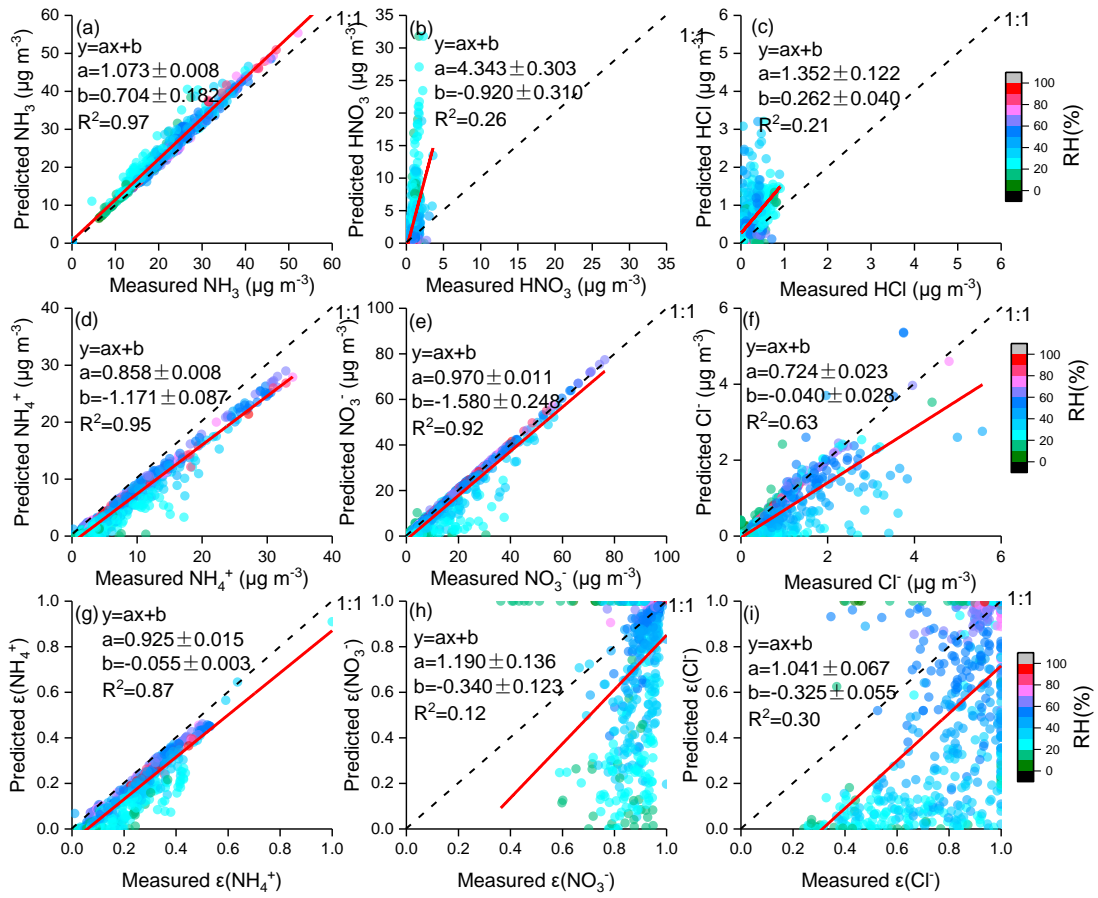


**Figure S1.** Comparisons of predicted and measured  $\text{NH}_3$ ,  $\text{HNO}_3$ ,  $\text{HCl}$ ,  $\text{NH}_4^+$ ,  $\text{NO}_3^-$ ,  $\text{Cl}^-$ ,  $\epsilon(\text{NH}_4^+)$ ,  $\epsilon(\text{NO}_3^-)$ ,  $\epsilon(\text{Cl}^-)$  colored by RH in spring.

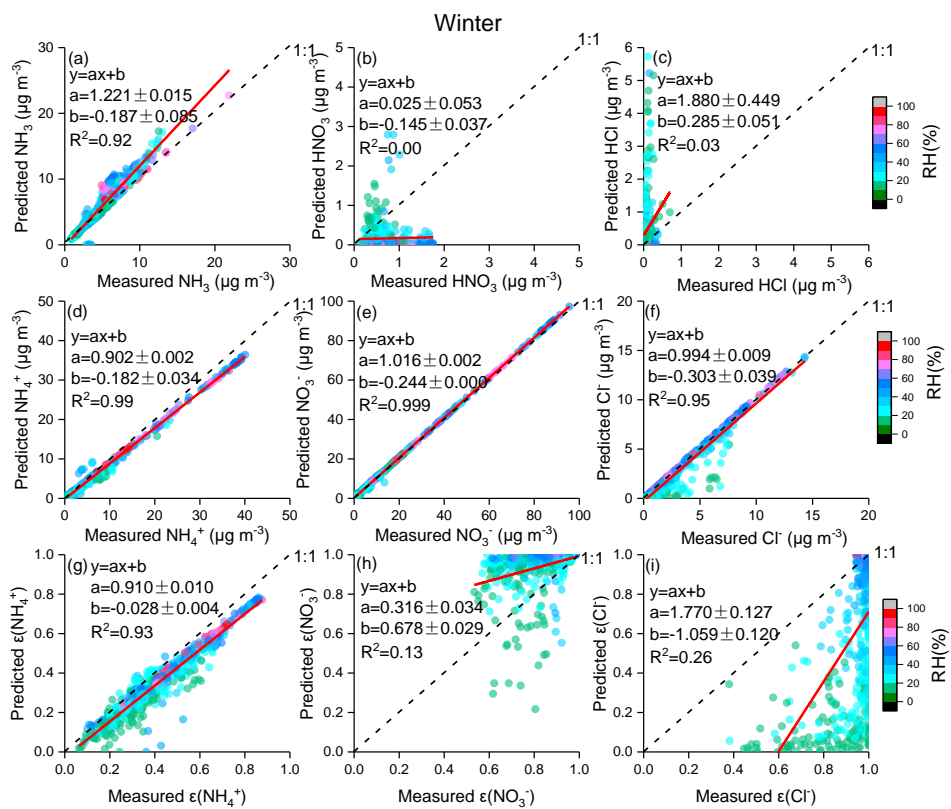


**Figure S2.** Comparisons of predicted and measured  $\text{NH}_3$ ,  $\text{HNO}_3$ ,  $\text{HCl}$ ,  $\text{NH}_4^+$ ,  $\text{NO}_3^-$ ,  $\text{Cl}^-$ ,  $\epsilon(\text{NH}_4^+)$ ,  $\epsilon(\text{NO}_3^-)$ ,  $\epsilon(\text{Cl}^-)$  colored by RH in winter.

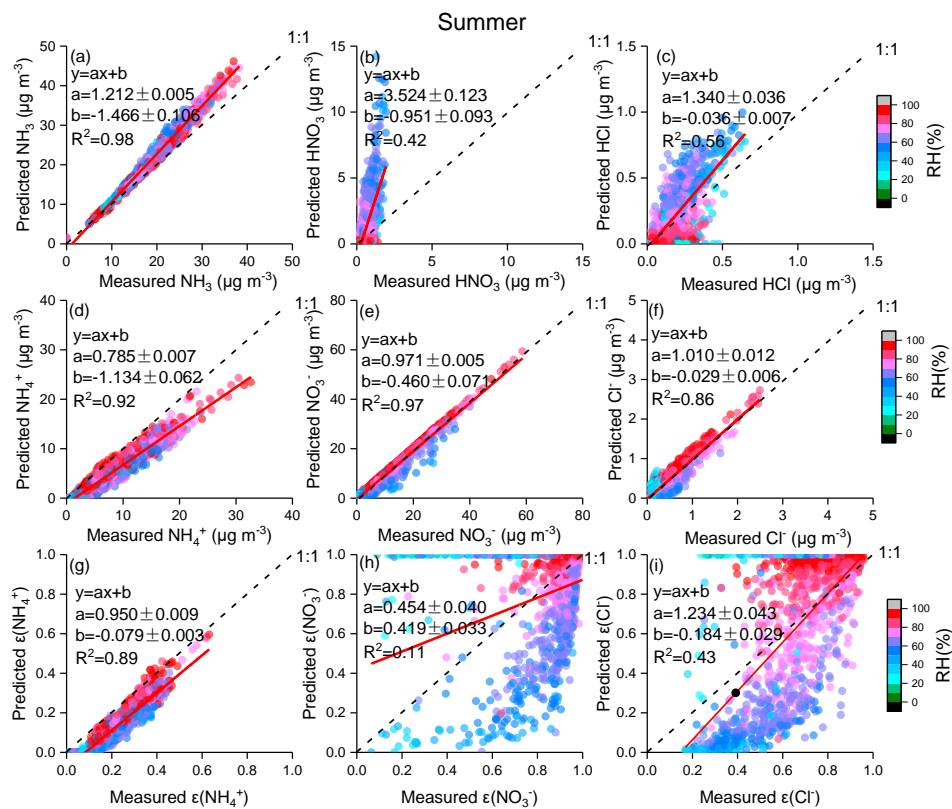


**Figure S3.** Comparisons of predicted and measured  $\text{NH}_3$ ,  $\text{HNO}_3$ ,  $\text{HCl}$ ,  $\text{NH}_4^+$ ,  $\text{NO}_3^-$ ,  $\text{Cl}^-$ ,  $\epsilon(\text{NH}_4^+)$ ,  $\epsilon(\text{NO}_3^-)$ ,  $\epsilon(\text{Cl}^-)$  colored by RH in summer.

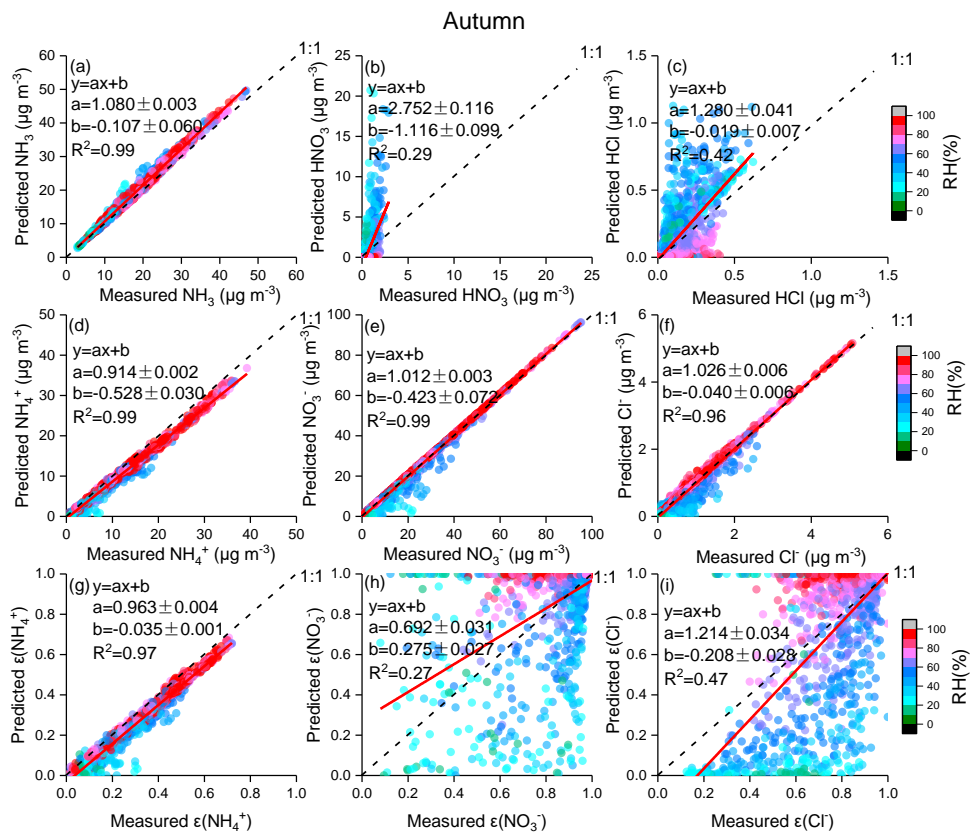


**Figure S4.** Comparisons of predicted and measured  $\text{NH}_3$ ,  $\text{HNO}_3$ ,  $\text{HCl}$ ,  $\text{NH}_4^+$ ,  $\text{NO}_3^-$ ,  $\text{Cl}^-$ ,  $\epsilon(\text{NH}_4^+)$ ,  $\epsilon(\text{NO}_3^-)$ ,  $\epsilon(\text{Cl}^-)$  colored by RH in autumn.

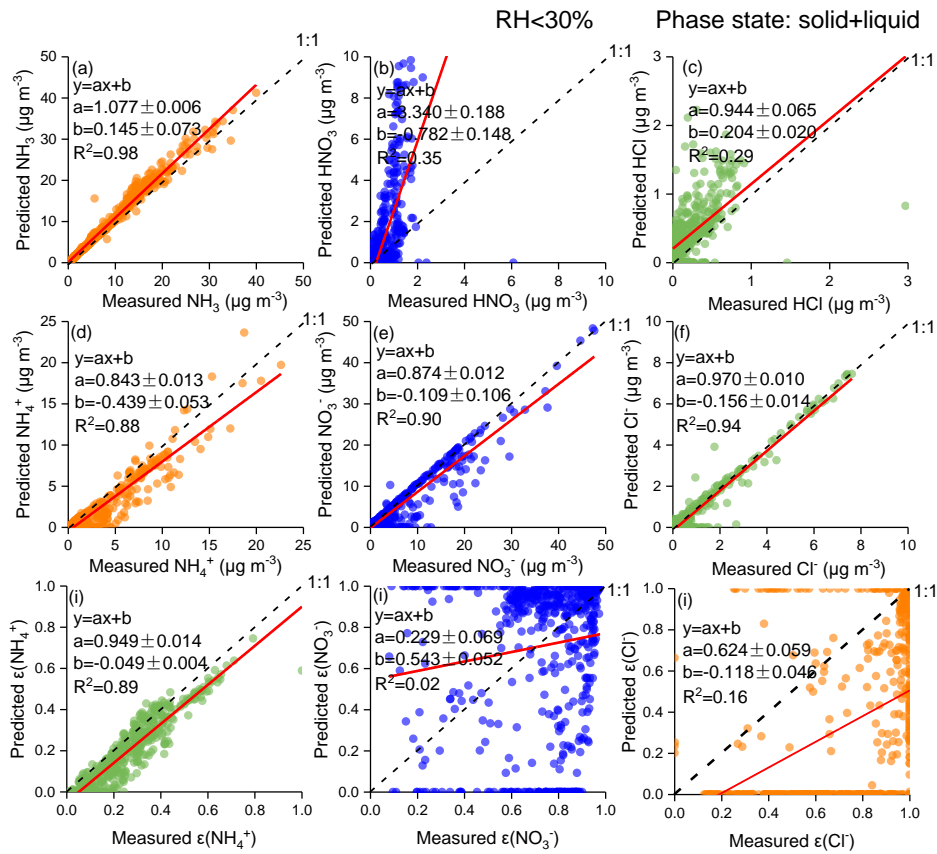


**Figure S5.** Comparisons of predicted and measured NH<sub>3</sub>, HNO<sub>3</sub>, HCl, NH<sub>4</sub><sup>+</sup>, NO<sub>3</sub><sup>-</sup>, Cl<sup>-</sup>, ε(NH<sub>4</sub><sup>+</sup>), ε(NO<sub>3</sub><sup>-</sup>), ε(Cl<sup>-</sup>) at the RH < 30%, the ISORROPIA-II runs in stable mode (solid + liquid).

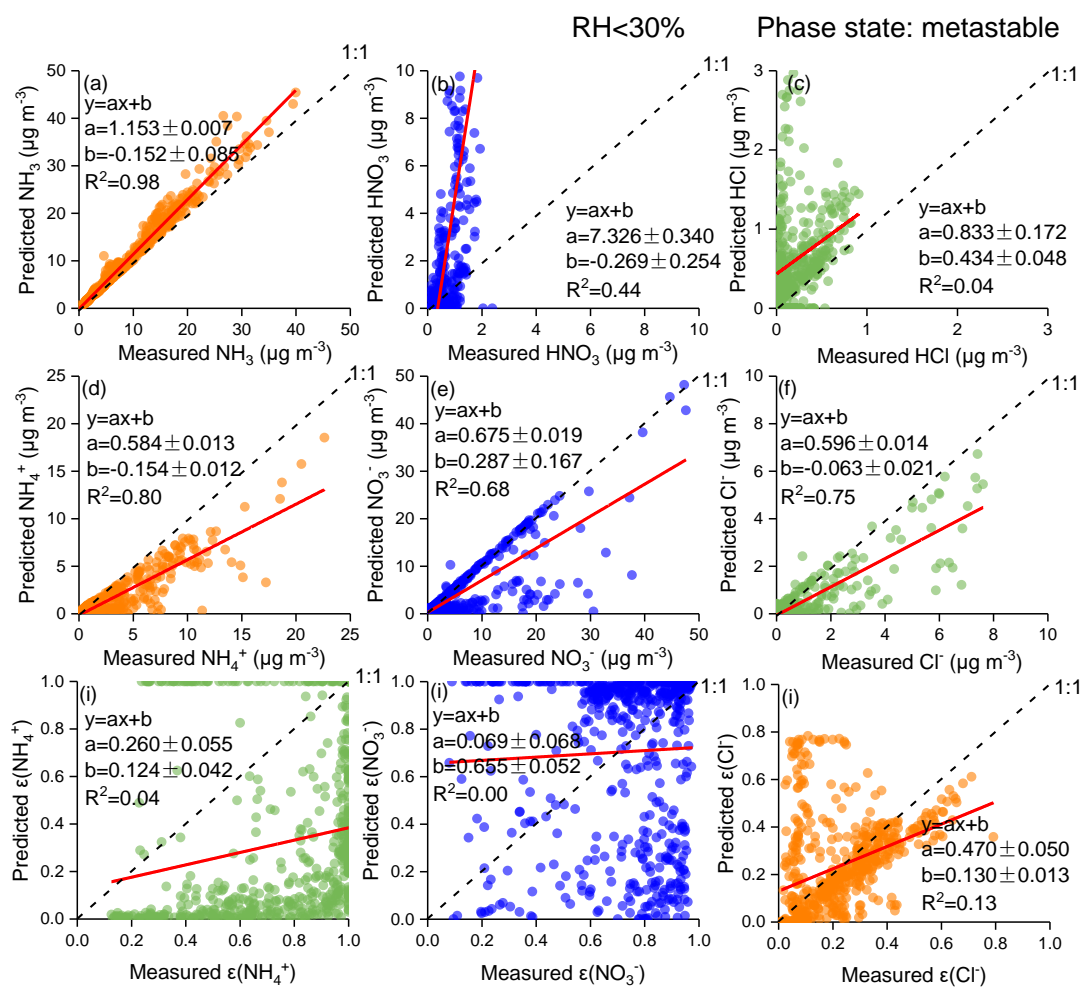


**Figure S6.** Comparisons of predicted and measured  $\text{NH}_3$ ,  $\text{HNO}_3$ ,  $\text{HCl}$ ,  $\text{NH}_4^+$ ,  $\text{NO}_3^-$ ,  $\text{Cl}^-$ ,  $\epsilon(\text{NH}_4^+)$ ,  $\epsilon(\text{NO}_3^-)$ ,  $\epsilon(\text{Cl}^-)$  at the  $\text{RH}<30\%$ , the ISORROPIA-II runs in metastable mode.

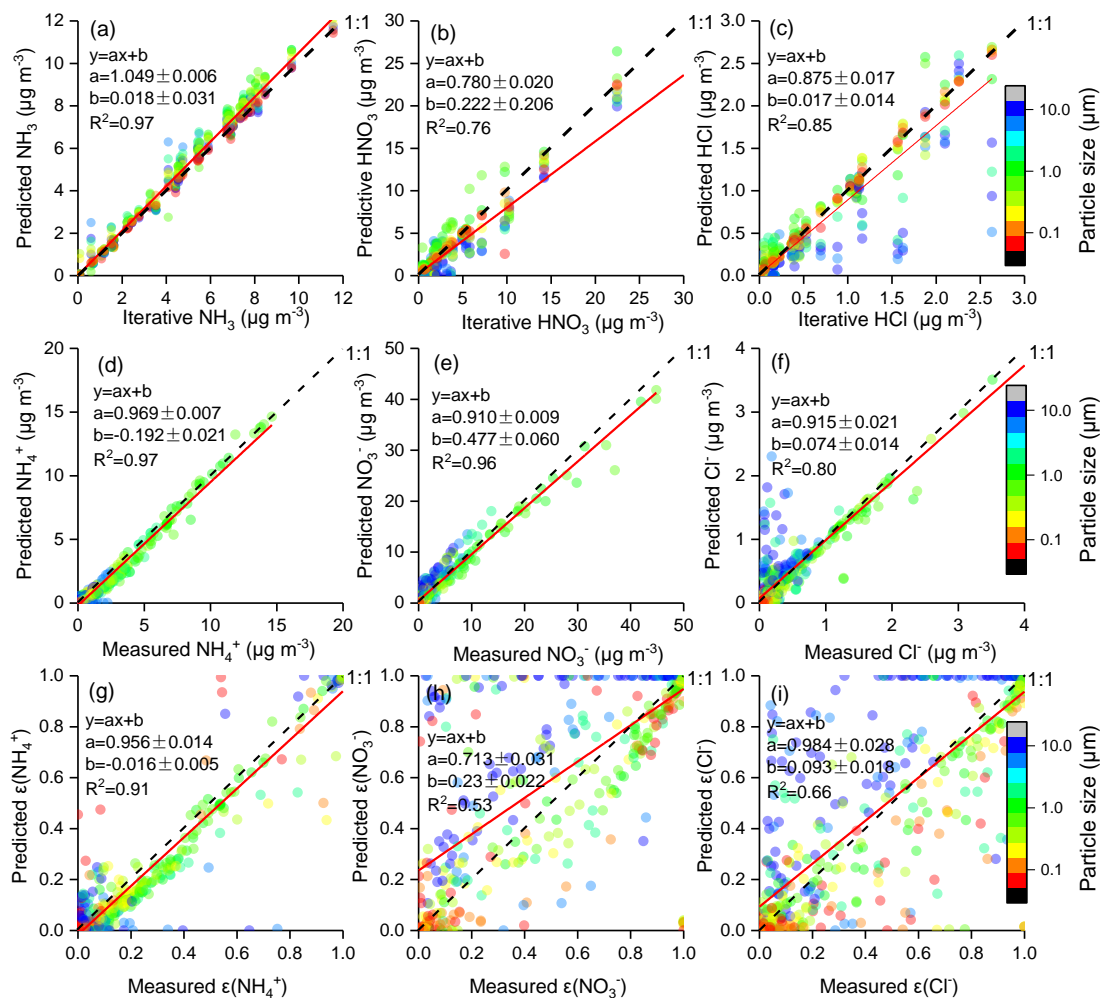


**Figure 3.** Comparisons of predicted and iterative  $\text{NH}_3$ ,  $\text{HNO}_3$ ,  $\text{HCl}$ , as well as the predicted and measured  $\text{NH}_4^+$ ,  $\text{NO}_3^-$ ,  $\text{Cl}^-$ ,  $\epsilon(\text{NH}_4^+)$ ,  $\epsilon(\text{NO}_3^-)$ ,  $\epsilon(\text{Cl}^-)$  colored by particle size. In this Figure, all MOUDI data were put together.

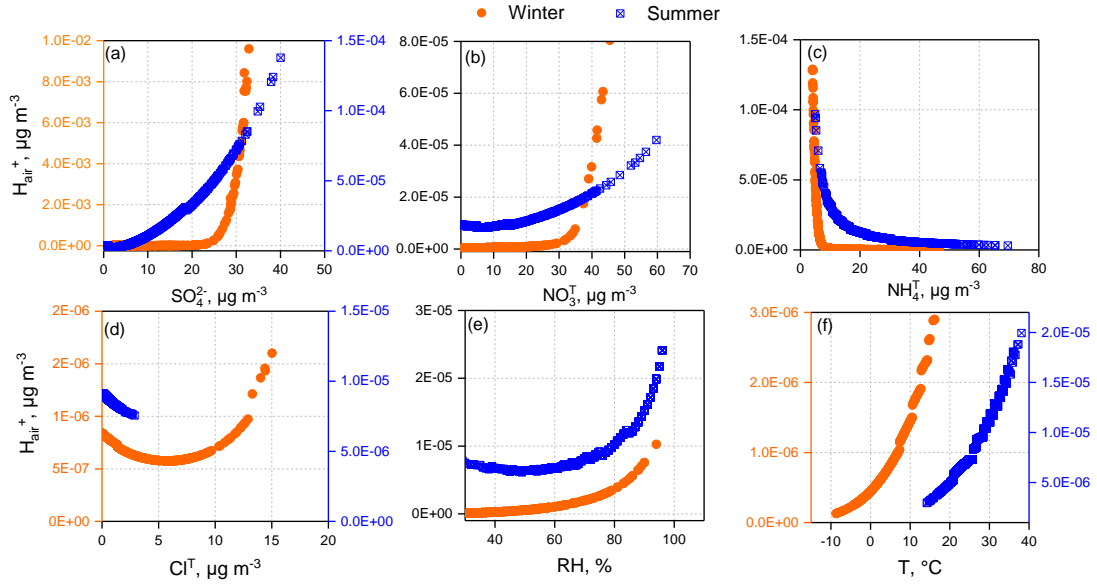


**Figure 7.** Sensitivities of  $H_{air}^+$  to  $\text{SO}_4^{2-}$ ,  $\text{NO}_3^T$ ,  $\text{NH}_4^T$ ,  $\text{Cl}^T$ , as well as meteorological parameters (RH, T) in summer and winter.

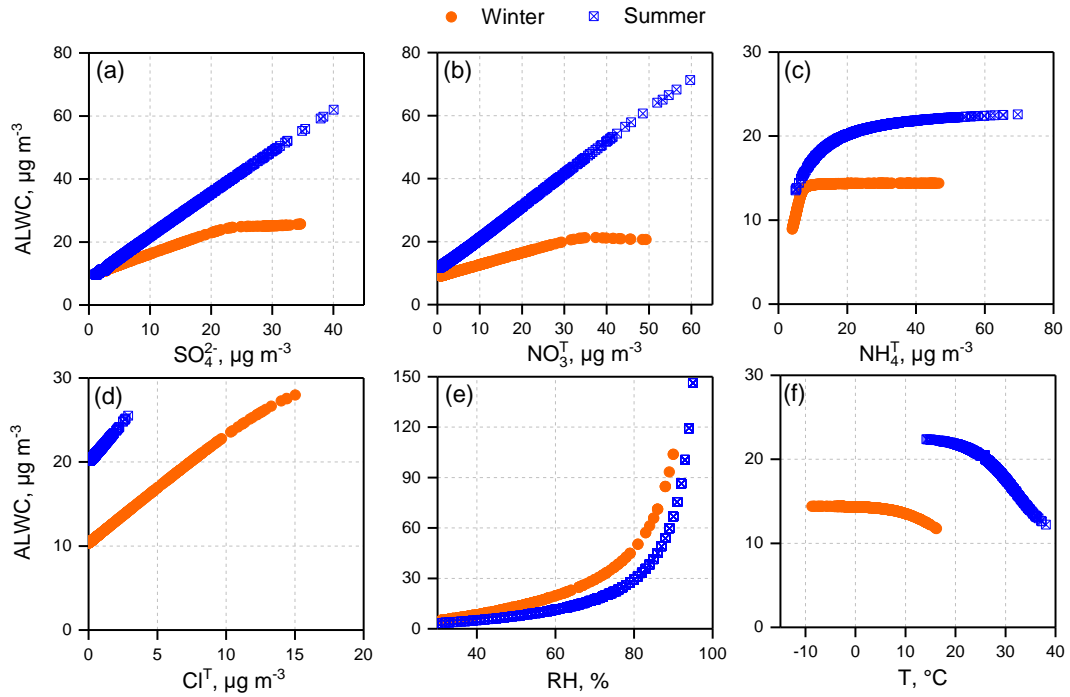


**Figure 8.** Sensitivities of ALWC to  $\text{SO}_4^{2-}$ ,  $\text{NO}_3^T$ ,  $\text{NH}_4^T$ ,  $\text{Cl}^T$ , as well as meteorological parameters (RH, T) in summer and winter.



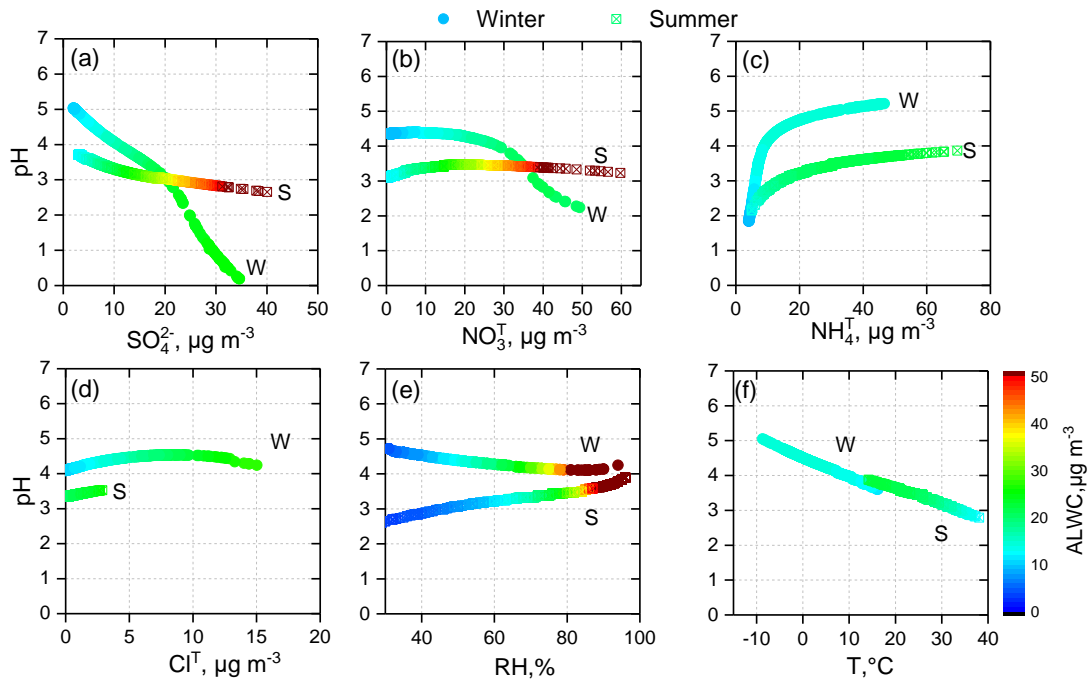


**Figure 9.** Sensitivities of aerosol pH to  $\text{SO}_4^{2-}$ ,  $\text{NO}_3^-$ ,  $\text{NH}_4^+$ ,  $\text{Cl}^-$ , as well as meteorological parameters (RH, T) in summer and winter.

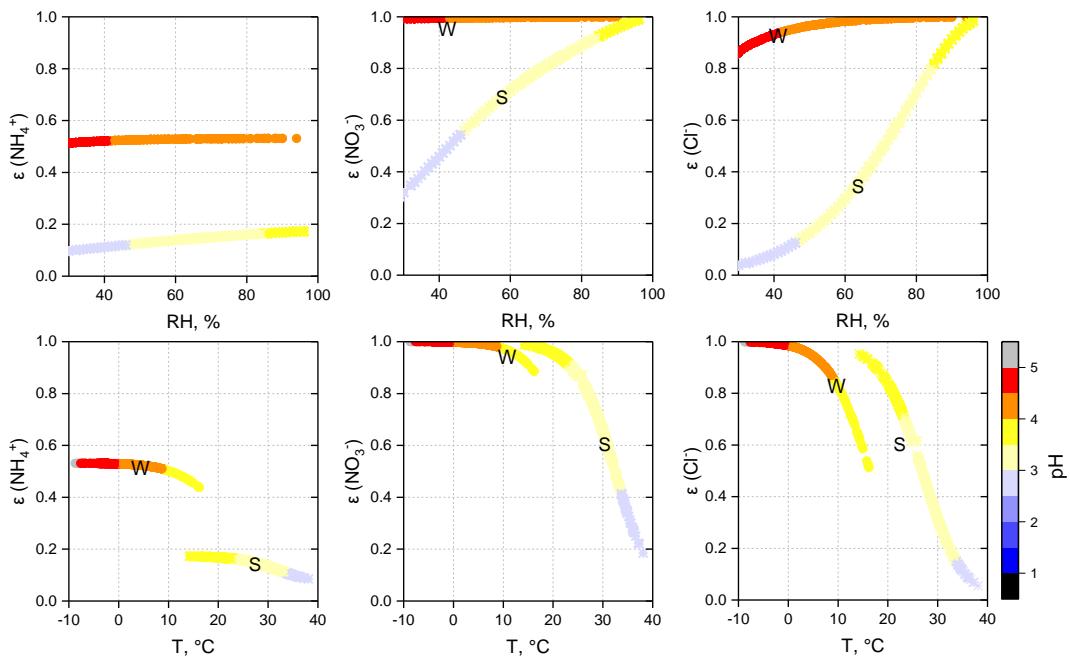


**Figure 10.** Sensitivities of  $\epsilon(\text{NH}_4^+)$ ,  $\epsilon(\text{NO}_3^-)$ ,  $\epsilon(\text{Cl}^-)$  to RH and T colored by aerosol pH in summer and winter.

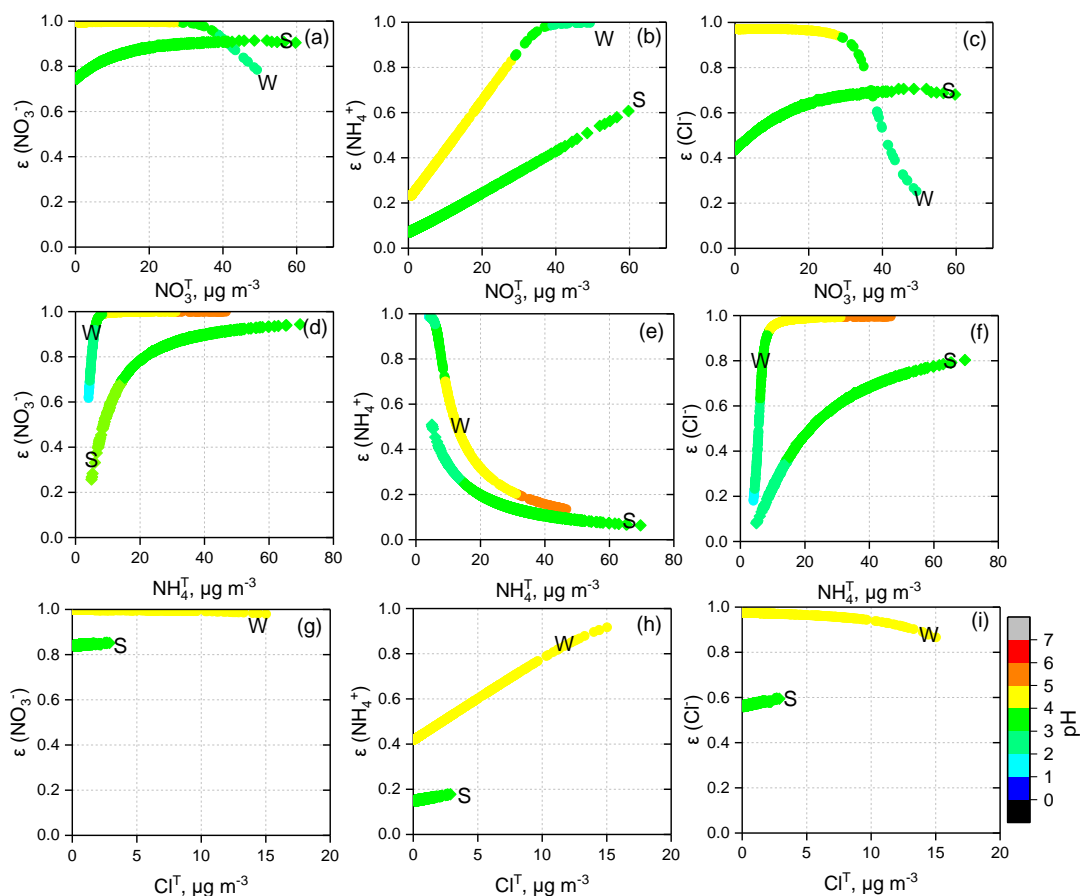


**Figure 11.** Sensitivities of  $\epsilon(\text{NH}_4^+)$ ,  $\epsilon(\text{NO}_3^-)$ ,  $\epsilon(\text{Cl}^-)$  to  $\text{NO}_3^{\text{T}}$ ,  $\text{NH}_4^{\text{T}}$ ,  $\text{Cl}^{\text{T}}$  colored by aerosol pH in summer and winter.

**Specific Comments:**

1. Line 37 change specials to species

**Response:** In the revised manuscript, the word “specials” has been changed to “species” (**Page 3, line 38, in the revised manuscript**)

2. Line 202 and following, it is not just lack of  $\text{NH}_3$  data that can affect predicted pH, what about  $\text{HNO}_3$ ,  $\text{HCl}$ , etc?

**Response:** Thank you for your important advice, the gaseous precursor  $\text{NH}_3$ ,  $\text{HNO}_3$ ,  $\text{HCl}$  were all important for predicting pH with the forward mode. Actually, the  $\text{NH}_3$ ,  $\text{HNO}_3$ ,  $\text{HCl}$  obtained from the iteration method were all used in predicting the size-resolved aerosol pH. Here we missed other gases’ names, in the revised manuscript, it has been corrected. (**Page 9, line 221-224, in the revised manuscript**)

3. Line 205, how much did the pH change when the iteration approach is used? Or, were the predicted gas species concentrations reasonable relative to what was measured during the MARGA study period.

**Response:** (1) As explained above, the MOUDI sampling was not synchronous with MARGA observation in time, hence the gas species concentrations were not available for MOUDI samples.

(2) The fine mode aerosol pH determined through the iteration procedure was higher than that with no gaseous species. In summer and autumn, the difference of fine mode aerosol pH was 0.1~1 between the predictions with and without gaseous species, while it was 0.1~2.9 in winter. The overall low RH in winter resulted in the low ALWC, hence in the gas-particle portioning procedure more  $\text{NH}_4^+$  was portioned into the gas phase and led to the low aerosol pH for fine mode particles.

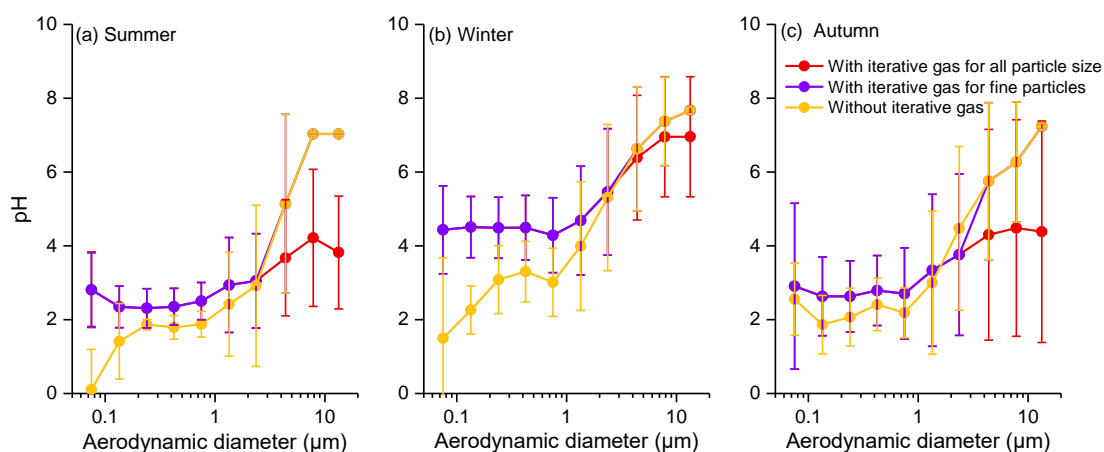


**Figure R1** The averaged size-resolved aerosol pH in three seasons predicted with three assumptions: (1) predicted with no iterative gases, (2) predicted assuming lack of equilibrium with gas phase for coarse mode particles, (3) predicted assuming all particles in equilibrium with the gas phase.

4. Line 229 is superfluous, it is well known that low pH means high acidity.

**Response:** The sentence “implying the higher aerosol acidity” has been deleted in the revised manuscript.

5. Line 235 to 238: this paragraph seems out of place.

**Response:** Thank you for your advice, this paragraph has been deleted from the revised manuscript.

6. Fig 3 caption, what does transverse direction mean on a polar plot?

**Response:** In the polar plot, the shaded contour indicates the average of variables for varying wind

speeds (radial direction) and wind directions (transverse direction). And this was explicated in Figure 5.

7. Line 246 change souther to southern.

**Response:** “souther” has been changed to “southwest” and “southeast” in the revised manuscript. **(Page 12, line 312 and 313, in the revised manuscript)**

8. Line 276-286. From Fig 4 it does not appear that pH and sulfate diurnal trends are always the same (actually inverse), as stated. Looks like a stronger inverse trend with liquid water. The more quantitative analysis is needed to support the statements made in this section.

**Response:** Thanks for your suggestion. In fact, we want to express that the diurnal variation of aerosol acidity (not aerosol pH) is consistent with the diurnal variation of  $\text{SO}_4^{2-}$  over four seasons.

In the revised manuscript, the diurnal variation of  $\text{NO}_3^-$  was added in Figure 6. The diurnal variation of  $\text{NO}_3^-$  in winter and spring agreed well with the aerosol acidity. But in summer and autumn, the agreement was not well. Figure S11 shows the relationship between mass concentrations of  $\text{SO}_4^{2-}$  and  $\text{NO}_3^-$  and aerosol pH at different ALWC levels for all four seasons. At the relatively low ALWC, the increasing  $\text{SO}_4^{2-}$  could decrease the aerosol pH obviously; at the relatively high ALWC, the negative correlation still existed between  $\text{SO}_4^{2-}$  mass concentration and aerosol pH. On the contrary, a weak positive correlation was found between  $\text{NO}_3^-$  and aerosol pH at the relatively low ALWC and the aerosol pH was almost invariable with the  $\text{NO}_3^-$  mass concentration at the relatively high ALWC. Compared with the  $\text{NO}_3^-$ , the  $\text{SO}_4^{2-}$  had a greater effect on aerosol pH. But when the ALWC was high enough (for example, higher than  $100 \mu\text{g m}^{-3}$ ), the impact of dilution of ALWC to the  $\text{H}_{\text{air}}^+$  was more significant. **(Page 13, line 337- 346, in the revised manuscript)**

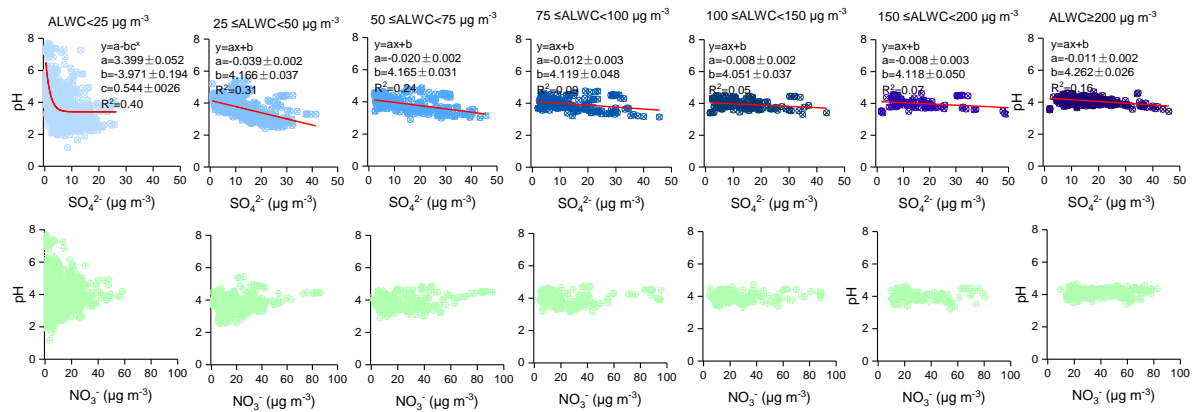


**Figure S10.** The relationship between  $SO_4^{2-}$  and  $NO_3^-$  mass concentration and aerosol pH at different ALWC levels.

9. Line 327, provide a physical explanation for the U shape dependency of  $H^+$  on  $NO_3^-$

**Response:** As mentioned above, we discussed the dependency of  $H^+_{air}$  on  $NO_3^T$  instead of the  $NO_3^-$ . In addition, we find that the shape of the curve for the dependency of  $H_{air}^+$  on total nitrate was also affected by the input average RH. In the revised manuscript, the data of RH lower than 30% were excluded. Similar with other seasons, the elevated  $NO_3^T$  could increase the  $H_{air}^+$  exponentially.

10. Line 330-331: Is it really true that there is a straightforward relationship between  $NH_3$  and  $H^+$  over broad  $NH_3$  concentration ranges? Ie, will increases in  $NH_3$  always lead to higher dissolved  $NH_3$ ? Technically it may be true, but the relationship may be highly nonlinear under certain conditions. This statement seems too broad.

**Response:** Thanks for your advice, the statement here is not rigorous. The relationship between the reduction of  $H_{air}^+$  and the increase of  $NH_3$  was indeed nonlinear, and the increasing  $NH_3$  could only promote  $NH_3$  dissolution to a certain extent. The purpose of the statement of Line 330-331 was to explain the decrease of aerosol pH resulting from the elevated  $NH_4^T$ . As you commented, the gas-particle partition ( $\epsilon(NH_4^+)$ ,  $\epsilon(NO_3^-)$ ,  $\epsilon(Cl^-)$ ) could help us understand fundamentally what is driving pH. We explain the decrease of aerosol pH resulting from the elevated  $NH_4^T$  in detail in your 13<sup>th</sup> comment.

11. Line 335, this is an obvious statement based on Eq (1). In fact much of the discussion throughout relating pH,  $H^+$  and LWC are obvious from Eq (1).

**Response:** The corresponding sentences in line 335 has been deleted in the revised manuscript.

12. Line 358 and on regarding changes in pH with  $\text{NO}_3^-$ . The authors discuss the trends they observe in the sensitivity analysis and  $\text{NO}_3^-/\text{SO}_4^{2-}$ , but never provide an explanation. By just reporting of results, the value of this work is greatly limited, despite the what could be done with this unique data set.

**Response:** During the thermodynamic process of aerosol, all the  $\text{SO}_4^{2-}$  would dissolve in the aerosol liquid water, the amount of sulfate can be considered stable and it would not be affected by the  $\text{NO}_3^-$ . From the point of the model, the concentrations of  $\text{NO}_3^-$  and  $\text{SO}_4^{2-}$  are both the output of ISO-II. Thus, the ratio of  $\text{NO}_3^- / \text{SO}_4^{2-}$  can only reflect the objective state of particles, it is not the cause or the indicator of aerosol pH. After careful consideration, we decide to remove this part of the discussion.

13. Lines 380 and on regarding TA and TS. Most of these statements are technically incorrect (although, from a broad perspective they may have a grain of truth to them). The authors data show that the pH is far from neutral despite it being  $\text{NH}_3$  rich. This analysis largely continues misconceptions of how aerosol composition depends on interactions between  $\text{SO}_4^{2-}$ ,  $\text{NH}_3$ ,  $\text{NH}_4^+$ ,  $\text{HNO}_3$ ,  $\text{NO}_3^-$  and LWC. Eg, is  $\text{HNO}_3$  only taken up once sulfate is so-called neutralized; maybe this can be tested with the data (there should be no  $\text{NO}_3^-$  and then a sudden jump in  $\text{NO}_3^-$  when  $[\text{TA}]/2[\text{TS}]$  is greater than 1. Another example, why does pH vary, even for this data set, if  $\text{NH}_3$  is always in great excess? It is suggested that the authors look at S curves (partitioning of say  $\text{NH}_3$  and/or  $\text{HNO}_3$  vs pH) instead of the analysis currently being used.

**Response:** Firstly, we think you are right, our statements here have some problems. Figure S21 showed that the elevated  $[\text{TA}]/2[\text{TS}]$  didn't increase the  $\text{NO}_3^-$  mass concentration, high  $\text{NO}_3^-$  mass concentration occurred when  $[\text{TA}]/2[\text{TS}]$  varies over a wide range (2~15). But in the NCP, the excess of ammonia in the atmosphere is indeed true, the ratio of  $[\text{TA}]/2[\text{TS}]$  is much higher than 1. The poor-ammonia cases were not observed in this work.

The relationship between aerosol pH and  $\text{NH}_4^+$  was nonlinear.  $\text{NH}_4^+$  in lower range had a significant impact on aerosol pH (Table S2), and higher  $\text{NH}_4^+$  generated limited pH change (Figure

9, S14, S17). Elevated  $\text{NH}_4^{\text{T}}$  could reduce  $\text{H}_{\text{air}}^+$  exponentially and slightly increase ALWC when the other input parameters were held constant. As the  $\text{NH}_4^{\text{T}}$  increases,  $\text{H}_{\text{air}}^+$  are consumed swiftly during the dissolution of  $\text{NH}_3$  and the further reaction with  $\text{SO}_4^{2-}$ ,  $\text{NO}_3^-$ , and  $\text{Cl}^-$ . And the elevated  $\text{NH}_4^{\text{T}}$  increased the  $\epsilon(\text{NO}_3^-)$  and  $\epsilon(\text{Cl}^-)$  when  $\text{NO}_3^{\text{T}}$  and  $\text{Cl}^{\text{T}}$  were fixed (Figure 11 and S20), which means the elevated  $\text{NH}_4^{\text{T}}$  alters the gas-particle partition and shifts more  $\text{NO}_3^{\text{T}}$  and  $\text{Cl}^{\text{T}}$  into particle phase, leading to the deliquescence of additional nitrate and chloride and increase of ALWC. **(Page 17, line 445- 453, in the revised manuscript)**

Although  $\text{NH}_3$  in the NCP is abundant, the aerosol pH is far from neutral, which may attribute to the limited ALWC. Compared to the liquid water content in clouds and precipitation, ALWC is much lower, hence the dilution of aerosol liquid water to  $\text{H}_{\text{air}}^+$  is weak. **(Page 17, line 462- 465, in the revised manuscript)**

The relationship between  $\epsilon(\text{NO}_3^-)$ ,  $\epsilon(\text{Cl}^-)$  and aerosol pH was analyzed by S curves proposed by Guo et al (2016, 2017), which were calculated based on the average temperature, aerosol liquid water, and activity coefficients. Their result showed that for a given ALWC and T, about 4 pH units increase are needed when the  $\epsilon(\text{NO}_3^-)$  and  $\epsilon(\text{Cl}^-)$  varies from 0 to 100%. In our opinion, the ALWC,  $\text{H}_{\text{air}}^+$ , aerosol pH,  $\epsilon(\text{NH}_4^+)$ ,  $\epsilon(\text{NO}_3^-)$ , and  $\epsilon(\text{Cl}^-)$  are all the output of ISO-II. They reflect an objective state of particles. Accordingly, it is reasonable to discuss the impact of input variables on output parameters with the results of ISO-II. On the basis of overall moderate aerosol acidity, the variation of aerosol pH is related to aerosol composition and meteorological conditions (RH and T). In the sensitivity analysis of this work, the influence of single variables on aerosol acidity is explicit. In the ambient atmosphere, multiple variables interact with each other, and aerosol acidity largely depends on the dominant factor.

14. Line 419 to 421. The loss of buffering capacity of the coarse mode mineral dust during winter pollution events is very interesting and has direct implications for predictions of  $\text{NO}_2 + \text{SO}_2$  oxidation pathways proposed by Wang et al 2016 and Cheng et al 2016. It is suggested that this finding be noted more prominently, maybe even included in the Abstract. However, this period does not seem to be shown in the plots?

**Response:** Wang et al (2016) and Cheng et al (2016) advocate that the aqueous oxidation of  $\text{SO}_2$  by

NO<sub>2</sub> is key to efficient sulfate formation but is only feasible under two atmospheric conditions: on fine aerosols with high relative humidity and NH<sub>3</sub> neutralization (aerosol pH ~7) or under cloud conditions. Their results focused on the fine particles, hence whether the loss of buffering capacity of the coarse mode mineral dust during winter pollution has a direct implication on their results remains to be discussed. But for fine particles, excessive NH<sub>3</sub> does not raise aerosol pH sufficiently.

15. The use of the word synthetically throughout the paper is confusing, it is suggested that it not be used since its meaning is unclear.

**Response:** The word “synthetically” has been deleted in the revised manuscript.

## References

- Guo, H., Sullivan, A. P., Campuzano-Jost, P., Schroder, J. C., Lopez-Hilfiker, F. D., Dibb, J. E., Jimenez, J. L., Thornton, J. A., Brown, S. S., Nenes, A., Weber, R. J.: Fine particle pH and the partitioning of nitric acid during winter in the northeastern United States, *J. Geophys. Res. Atmos.*, 121, 10355-10376, 2016.
- Guo, H., Liu, J., Froyd, K. D., Roberts, J. M., Veres, P. R., Hayes, P. L., Jimenez, J. L., Nenes, A., and Weber, R. J.: Fine particle pH and gas–particle phase partitioning of inorganic species in Pasadena, California, during the 2010 CalNex campaign, *Atmos. Chem. Phys.*, 17, 5703-5719, 2017.
- Guo, H., Otjes, R., Schlag, P., Scharr, A. K., Nenes, A., Weber, R. J.: Effectiveness of ammonia reduction on control of fine particle nitrate. *Atmos. Chem. Phys. Discuss.*, <https://doi.org/10.5194/acp-2018-378>, 2018.
- Huang, X. J., Liu, Z. R., Liu, J. Y., Hu, B., Wen, T. X., Tang, G. Q., Zhang, J. K., Wu, F. K., Ji, D. S., Wang, L. L., Wang, Y. S.: Chemical characterization and source identification of PM<sub>2.5</sub> at multiple sites in the Beijing–Tianjin–Hebei region, China, *Atmos. Chem. Phys.*, 17, 12941–12962, 2017.
- Ma, Q.X., Wu, Y.F., Zhang, D. Z., Wang, X.J., Xia, Y.J., Liu, X.Y., Tian, P., Han, Z.W., Xia, X.G., Wang, Y., Zhang, R.J.: Roles of regional transport and heterogeneous reactions in the PM<sub>2.5</sub> increase during winter haze episodes in Beijing, *Sci. Total Environ.*, 599-600, 246-253, 2017.
- Zhao, P. S., Chen, Y. N., Su, J.: Size-resolved carbonaceous components and water-soluble ions



measurements of ambient aerosol in Beijing. *J. Environ. Sci.*, 54, 298-313, 2017.

## **Anonymous Referee #2**

This paper presents observations and analysis of the inorganic aerosol system in Beijing for 2017. The pH values are realistic; however, more analysis to verify the methods would make for a stronger paper.

### **Response:**

Thanks for your important comments, which are very useful to make our paper more rigorous. Please see our point-by-point responses to the comments and the revised manuscript for details. The order of the Figures or Tables in Response is the same as the corresponding Figure or Table appears in the main text and supplemental materials.

Major comments:

**1. Clarify the methodology in terms of how pH was calculated. How was the pH in different size ranges modeled and combined? Even if that appears in other work (as indicated in the text), a quick summary of the method would be useful. Line 209 indicates pH (for the coarse mode?) was determined by ignoring the gas phase and running ISORROPIA in a forward mode with zero gas. How was this assumption verified? Figure 2 shows a comparison of total species modeled vs predicted, but that doesn't give a sense of how the size-dependent predictions worked. Line 438 indicates that NH<sub>3</sub>, HNO<sub>3</sub>, and HCl were determined through iteration when MOUDI data was used. Was that just for the fine mode particles?**

### **Response:**

The data set of MOUDI was obtained during 2013 and 2015, which was not synchronous with the online ion data (obtained in 2016 and 2017). There was no observation of gas precursors during the periods of MOUDI sampling, hence an iteration method used in Fang et al. (2017) and Guo et al. (2016) was applied in this work. As a brief summary, the predicted NH<sub>3</sub>, HNO<sub>3</sub>, and HCl concentrations from the *i*-1 run were applied to the *i*th iteration, until the gas concentrations converged. Based on these iterative gas phase concentrations, each MOUDI stage's measured aerosol ion concentrations and estimated gas concentrations, as well as the averaged RH and T during each group sampling time, were input the ISORROPIA-II to determine pH for each stage. The particles at each size bin were assumed to be internally mixed. **(Page 9, line 221- 230, in the revised manuscript)**

The comparisons of iterative and predicted  $\text{NH}_3$ ,  $\text{HNO}_3$ , and  $\text{HCl}$  as well as measured and predicted  $\text{NO}_3^-$ ,  $\text{NH}_4^+$ ,  $\text{Cl}^-$ ,  $\varepsilon(\text{NH}_4^+)$ ,  $\varepsilon(\text{NO}_3^-)$ , and  $\varepsilon(\text{Cl}^-)$  for data from MOUDI samples were showed in Figure 3. The previous study showed that coarse mode particles are very difficult to reach equilibrium with the gaseous precursors due to kinetic limitations (Dassios et al., 1999; Cruz et al., 2000). Assuming coarse mode particles in equilibrium with the gas phase could result in a large bias between measured and predicted  $\text{NO}_3^-$  and  $\text{NH}_4^+$  in coarse mode particles (Fang et al, 2017). We also find that in this work, it can be clearly seen that assuming coarse mode particles in equilibrium with the gas phase could overpredict  $\text{NO}_3^-$  and  $\text{Cl}^-$  and underestimate  $\text{NH}_4^+$  in the coarse mode (the blue scatters), which could subsequently underestimate the coarse mode aerosol pH. Compared with the coarse mode particles, the measured and predicted  $\text{NO}_3^-$ ,  $\text{NH}_4^+$ , and  $\text{Cl}^-$  agreed very well in fine mode particles. Considering the kinetic limitations and nonideal gas-particle partitioning in coarse mode particles, the aerosol pH in coarse mode was determined by ignoring the gas phase. **(Page 9-10, line 231- 242, in the revised manuscript)**

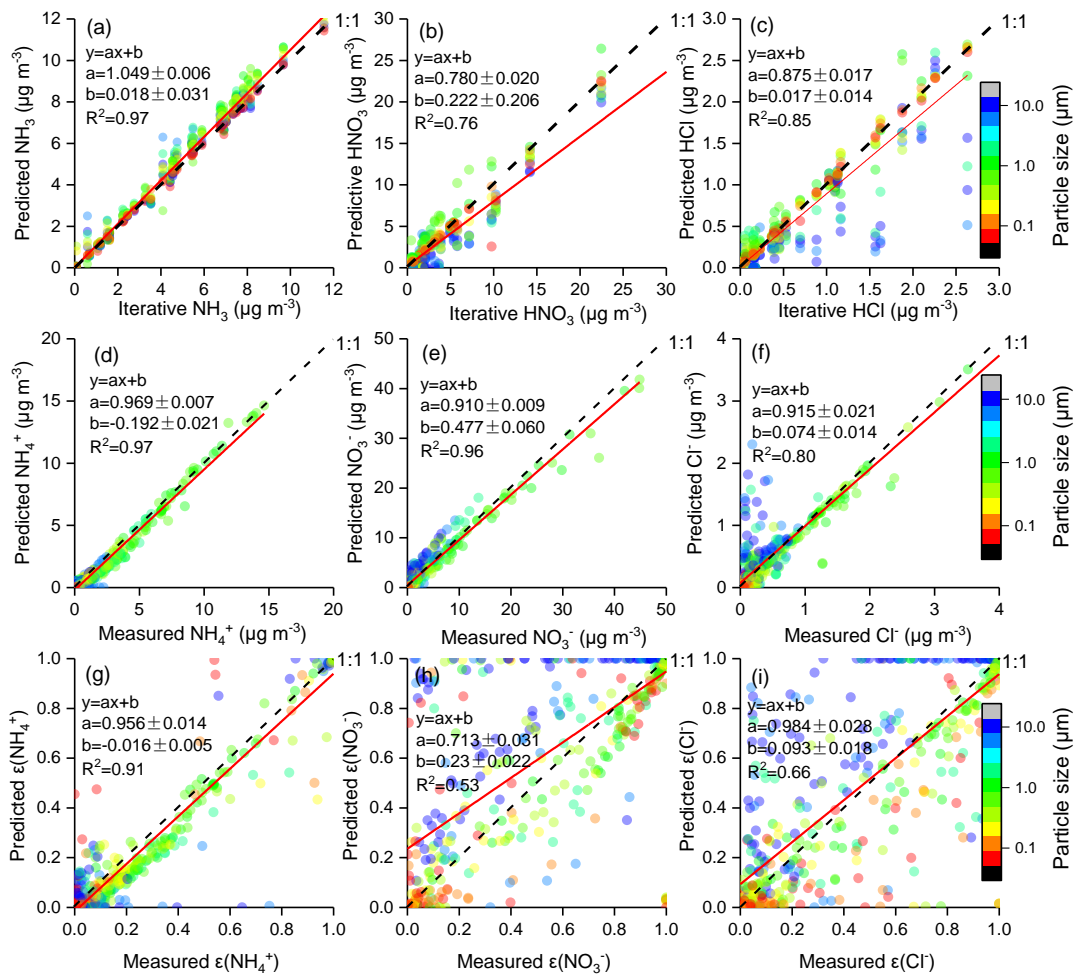


**Figure 3.** The comparisons of iterative and predicted  $\text{NH}_3$ ,  $\text{HNO}_3$ ,  $\text{HCl}$  as well as measured and predicted  $\text{NO}_3^-$ ,  $\text{NH}_4^+$ ,  $\text{Cl}^-$ ,  $\epsilon(\text{NH}_4^+)$ ,  $\epsilon(\text{NO}_3^-)$ ,  $\epsilon(\text{Cl}^-)$  for data from MOUDI samples, which all colored by particle size.

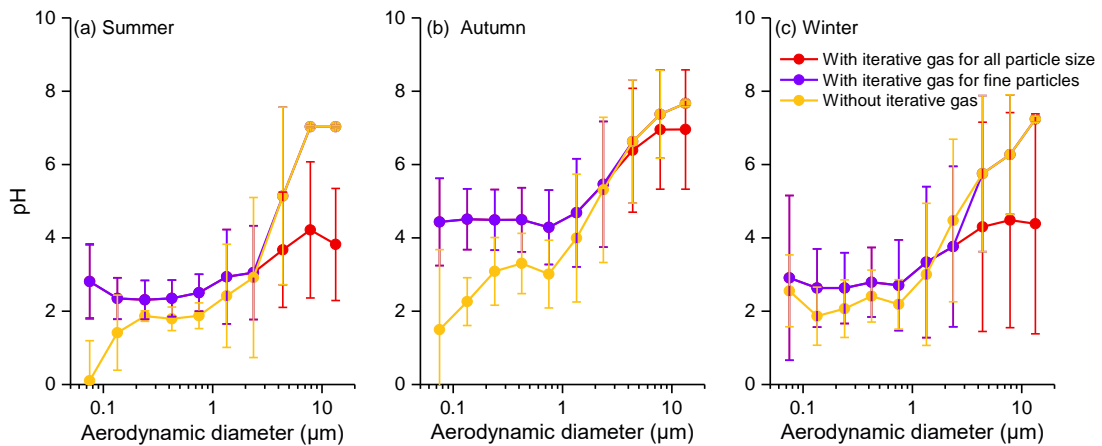


**Figure R1** The averaged size-resolved aerosol pH in three seasons predicted with three assumptions: (1) predicted with no iterative gases, (2) predicted assuming lack of equilibrium with gas phase for

coarse mode particles, (3) predicted assuming all particles in equilibrium with the gas phase.

**2. Driving factor analysis: The driving factors for pH were obtained by holding all composition, RH, and T parameters at average values and then varying one of the input values (line 291 and thereafter-consider putting some of this method in section 2). A larger change in ALWC, H+air, or pH due to varying one input was interpreted as that input having a major influence on pH. The authors do note that this method will not capture the effect of simultaneous changes in more than one factor.**

**Response:**

Thanks for your important advice. The detailed introduction of the method about aerosol pH driving factor analysis has been put in section 2.5. In the real ambient air, the thermodynamic process of the aerosol is complicated, it is not easy to tell the effect of one certain factor on the aerosol pH. The ALWC,  $H_{\text{air}^+}$ , and aerosol pH are all the output of ISORROPIA-II. They reflect an objective state of particles. Considering the relative independence between input parameters, it is reasonable to discuss the influence of input variables on output parameters with the results of ISORROPIA-II. Thus, in this paper, we focus on the sensitivity analysis of single-factor variation, which can reflect the variation tendency of aerosol pH caused by the change of each variable.

The detailed description of sensitivity analysis method was put in Section 2.5 (**Page 10-11, line 245- 270, in the revised manuscript**)

**a. Did the authors consider restricting the output values used to calculate sensitivities (e.g. Table 2) to space actually probed in the ambient? For example, ALWC output from the simulation varying RH spans 0-140  $\mu\text{g}/\text{m}^3$  while most other input parameters did not result in this range of ALWC values. Was 140  $\mu\text{g}/\text{m}^3$  ALWC predicted for any of the actual atmospheric conditions? What space is actually probed in the ambient atmosphere in terms of ALWC, H+air, and pH compared to what is probed in the simulated data holding all but one parameter constant?**

**Response:** All data used in the sensitivity analysis were based on the actual observation, not randomly generated simulation data, which helps us capture a more real impact. When the RH was considered as a variable, ALWC output spans 0-140  $\mu\text{g}/\text{m}^3$ , this mainly attributed to the vital impact

of RH on ALWC, especially when the RH was higher than 80% owing to the exponential increase of ALWC with the RH. Whereas in other simulated cases, the averaged RH was generally within 50% ~ 75%, hence the output ALWC was relatively low. In summer and autumn, the actual ALWC was even more than 140  $\mu\text{g}/\text{m}^3$  when both aerosol components and RH were high.

**b. How can the method be evaluated? Does using average inputs result in the same predicted pH that would be obtained by averaging all individual pH predictions from individual inputs? Could the average pH and input be indicated on each panel of Figure 5 to 7? How evenly distributed over the input range are the various inputs? Would it be more appropriate to focus on the interquartile range instead of a full range of inputs?**

**Response:** The average value and variation range for each variable in all four seasons were listed in Table S1 and Figure S7. The aerosol pH1 is the value by averaging all individual pH predictions from each input variable, for example, the average aerosol pH was  $3.74 \pm 0.47$  when the  $\text{SO}_4^{2-}$  was regarded as an input variable while other input parameters were fixed with the average value. The aerosol pH2 is the value by using average inputs for all input parameters. In theory, pH1 and pH2 cannot be the same, otherwise, the effect of the variables on aerosol pH will not be reflected.

Table S1 The average value and range for each variable in all four seasons, as well as the two average aerosol pH types. The aerosol pH1 is the value by averaging all individual pH predictions from each continuous input variable, for example, the average aerosol pH was  $3.74 \pm 0.47$  when the  $\text{SO}_4^{2-}$  was regarded as a continuous input variable while other input parameters were fixed with the average value. The aerosol pH2 is the value by using average inputs for all input parameters. The unit of chemical components is  $\mu\text{g m}^{-3}$ .

Spring	$\text{SO}_4^{2-}$	$\text{NH}_4^+$	$\text{NO}_3^+$	$\text{Cl}^+$	RH, %	T, °C	Ca	Na	K	Mg
Average input	8.4	25.7	13.5	1.1	52	20.9	1.29	0.20	0.34	0.3
Variable range	3.0~41.4	0.1~33.9	0.4~77.6	0.03~6.27	30~92	10.0~33.3	0.1~3.0			
pH1	$3.74 \pm 0.47$	$3.69 \pm 0.19$	$3.65 \pm 0.53$	$3.81 \pm 0.09$	$3.79 \pm 0.05$	$3.81 \pm 0.27$	$3.73 \pm 0.16$			
pH2	3.82									
Winter	$\text{SO}_4^{2-}$	$\text{NH}_4^+$	$\text{NO}_3^+$	$\text{Cl}^+$	RH, %	T, °C	Ca	Na	K	Mg
Averaged	7.3	12.2	14.3	3.0	52	2.7	0.2	0.40	1.0	0.2
Ranges	2.0~34.6	1.3~46.7	0.8~49.3*	0.02~25.2	30~94	-8.7~16.2	0.01~0.7			
pH1	$4.32 \pm 1.21$	$3.86 \pm 1.04$	$4.27 \pm 0.48$	$4.27 \pm 0.16$	$4.39 \pm 0.18$	$4.36 \pm 0.29$	$4.36 \pm 0.04$			
pH2	4.36									
Summer	$\text{SO}_4^{2-}$	$\text{NH}_4^+$	$\text{NO}_3^+$	$\text{Cl}^+$	RH, %	T, °C	Ca	Na	K	Mg

Averaged	8.6	26.8	10.2	0.6	74	26.1	0.5	0.60	0.2	0.1
Ranges	0.6~40.1	1.2~69.6	0.3~59.8	0.1~2.8	30~97	14.2~38.1	0.02~2.9			
pH1	3.43±0.27	3.31±0.32	3.31±0.12	4.38±0.03	3.40±0.27	3.37±0.20	3.38±0.06			
pH2					3.38					
Autumn	SO <sub>4</sub> <sup>2-</sup>	NH <sub>4</sub> <sup>+</sup>	NO <sub>3</sub> <sup>-</sup>	Cl <sup>-</sup>	RH, %	T, °C	Ca	Na	K	Mg
Averaged	9.3	27.8	20.3	1.0	72	16.4	0.4	0.3	0.2	0.1
Ranges	0.3~54.7	3.2~67.5	0.2~90.5	0.06~5.17	30~97	-1.1~33.3	0.02~2.3			
pH1	3.85±0.23	3.60±0.58	3.70±0.12	3.84±0.04	3.94±0.10	3.84±0.29	3.84±0.03			
pH2					3.84					

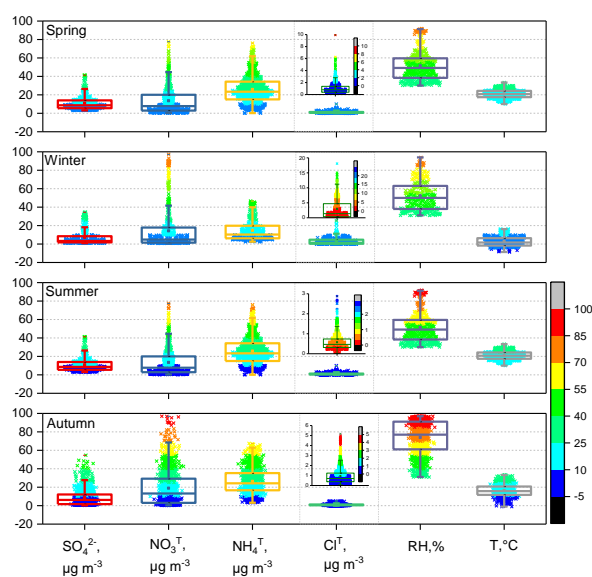


**Figure S7.** The distribution of each input variable for sensitivity analysis in four seasons

**c. Are there units to the quantities in table 2?**

**Response:** Units to the quantities in table 2 were missed in the manuscript, in the revised manuscript, we replace the deviation by relative standard deviation as the evaluation target, hence the unit is unified to %.

**d. How would a multiple linear regression analysis differ from the technique of varying one quantity at a time?**

**Response:** The relationships between input variables and aerosol pH are not simply linear. The method in this work based on the overall accurate relationship between variables rather than the permutation and combination in the mathematical sense, the latter may subversively change the

relationship between variables and does not conform to the actual physical laws. Moreover, the predicted aerosol pH in the sensitivity analysis was realistic, which confirms that the method we used was reasonable.

**e. Could a Monte Carlo method or other technique be used to make sure atmospherically relevant combinations of inputs are being used?**

**Response:** The Monte Carlo method is a good way to evaluate the uncertainty of the predicted aerosol pH and to determine if the input parameters are appropriate. However, as mentioned above, all input variables came from the actual observation to make sure the relationships between variables could conform to the actual physical laws. Moreover, the sensitivity analysis in this work focused on the variation tendency of aerosol pH rather the absolute aerosol pH value.

**3. Instead of classifying PM<sub>2.5</sub> into clean (0-75 ug/m<sup>3</sup>), polluted, and heavily polluted (>150 ug/m<sup>3</sup>), it may be illustrative to consider PM<sub>2.5</sub> in a continuum. 0-75 ug/m<sup>3</sup> on a daily average is not very clean as it includes concentrations that exceed air quality standards. In addition, by considering PM<sub>2.5</sub> concentrations as continuous, you may be able to better determine the association of pH with PM<sub>2.5</sub>. Consider that the pH for the three classifications is reported with a range/uncertainty that indicates the differences in pH between clean, polluted, and heavily polluted conditions are not statistically significant (values on line 262 overlap). However, if considered as a continuous variable, a regression with confidence interval could be provided and might provide a more robust analysis of the association.**

**Response:** Thanks for your suggestion. Firstly, three groups for PM<sub>2.5</sub> were classified by hourly PM<sub>2.5</sub> mass concentration, not daily average PM<sub>2.5</sub> mass concentration. Secondly, the differences in pH between clean, polluted, and heavily polluted conditions were indeed not significant, the conclusion in the manuscript was just taken from the average value of pH. More deep analysis has been added in the revised manuscript.

Table 1 showed that as the air quality deteriorates, all aerosol components, as well as ALWC and  $H_{\text{air}}^+$ , increased, but the differences in pH between clean, polluted, and heavily polluted conditions are not statistically significant. The relationship between PM<sub>2.5</sub> and aerosol pH was shown in Figure



S8, the aerosol pH under clean condition spanned 2~7 while the aerosol pH under polluted and heavily polluted conditions mostly concentrated in 3~5. Time series of mass fraction of  $\text{NO}_3^-$ ,  $\text{SO}_4^{2-}$ ,  $\text{NH}_4^+$ ,  $\text{Cl}^-$ , and crustal ions ( $\text{Mg}^{2+}$  and  $\text{Ca}^{2+}$ ) in total ions, as well as pH in all four seasons, were showed in Figure 4. It can be seen that on clean days, high aerosol pH ( $>6$ ) was generally companied by high mass fraction of crustal ions, while the relatively low aerosol pH ( $<3$ ) was companied by high mass fraction of  $\text{SO}_4^{2-}$  and low mass fraction of crustal ion, which was most obvious in summer (large part of aerosol pH with  $\text{RH} \leq 30\%$  were excluded in spring and winter). On polluted and heavily polluted days, the aerosol chemical composition was similar, mainly dominated by  $\text{NO}_3^-$ , hence the differences of aerosol pH on polluted and heavily polluted days were small. Compared with the mass concentration of  $\text{PM}_{2.5}$ , the different aerosol chemical compositions may be the essence that drives aerosol acidity. The impact of aerosol compositions on aerosol pH is discussed in Section 3.4. **(Page 11-12, line 291- 308, in the revised manuscript)**

**Table 1** Average mass concentrations of  $\text{NO}_3^-$ ,  $\text{SO}_4^{2-}$ ,  $\text{NH}_4^+$  and  $\text{PM}_{2.5}$  as well as RH, ALWC,  $\text{H}_{\text{air}}^+$ , and  $\text{PM}_{2.5}$  pH under clean, polluted, and heavily polluted conditions over four seasons.

Spring	$\text{PM}_{2.5}$	$\text{NO}_3^-$	$\text{SO}_4^{2-}$	$\text{NH}_4^+$	ALWC*	$\text{H}_{\text{air}}^+$ *	pH*
	$\mu\text{g m}^{-3}$	$\mu\text{g m}^{-3}$	$\mu\text{g m}^{-3}$	$\mu\text{g m}^{-3}$	$\mu\text{g m}^{-3}$	$\mu\text{g m}^{-3}$	
Averaged	62±36	14.9±14.6	9.7±7.9	7.9±7.3	23±35	6.8E-06±2.8E-05	4.0±1.0
Clean	44±17	7.9±6.6	6.2±3.7	4.8±3.2	14±26	3.2E-06±5.1E-06	4.1±1.1
Polluted	100±21	30.8±14.3	16.4±5.9	15.4±5.8	33±36	5.1E-06±4.3E-06	3.9±0.5
Heavily polluted	169±12	45.3±8.5	36.3±4.9	29.4±2.3	78±60	2.0E-05±6.5E-06	3.6±0.3
winter	$\text{PM}_{2.5}$	$\text{NO}_3^-$	$\text{SO}_4^{2-}$	$\text{NH}_4^+$	ALWC*	$\text{H}_{\text{air}}^+$ *	pH*
Averaged	60±69	13.7±21.0	7.3±8.7	7.3±10.0	35±46	2.2E-05±2.3E-04	4.5±0.7
Clean	22±20	3.6±3.9	2.8±1.8	2.2±2.0	10±16	3.2E-07±4.8E-07	4.5±0.6
Polluted	107±21	18.9±8.6	11.0±5.7	11.0±4.7	41±45	1.9E-05±9.1E-05	4.8±1.0
Heavily polluted	209±39	59.7±21.8	26.2±6.3	29.1±8.7	80±52	7.0E-05±4.7E-04	4.4±0.7
Summer	$\text{PM}_{2.5}$	$\text{NO}_3^-$	$\text{SO}_4^{2-}$	$\text{NH}_4^+$	ALWC*	$\text{H}_{\text{air}}^+$ *	pH*
Averaged	39±24	9.5±9.5	8.6±7.5	7.2±5.6	50±68	1.6E-05±1.8E-05	3.8±1.2
Clean	33±18	7.3±6.8	7.0±6.0	5.9±4.0	42±61	1.4E-05±1.6E-05	3.8±1.2
Polluted	87±13	26.5±10.5	20.7±7.0	17.6±4.8	100±88	3.1E-05±2.0E-05	3.5±0.4
Autumn	$\text{PM}_{2.5}$	$\text{NO}_3^-$	$\text{SO}_4^{2-}$	$\text{NH}_4^+$	ALWC*	$\text{H}_{\text{air}}^+$ *	pH*
Averaged	59±48	18.5±19.5	6.5±5.9	8.2±8.2	109±160	8.1E-06±1.1E-05	4.3±0.8
Clean	33±21	7.6±7.4	4.4±4.1	3.8±3.5	49±83	3.8E-06±6.6E-06	4.5±1.0
Polluted	105±21	33.8±11.6	14.3±6.3	16.0±4.6	225±189	1.7E-05±1.2E-05	4.1±0.3

Heavily polluted	174±18	63.4±15.4	25.0±15.9	29.0±5.1	317±236	2.2E-05±1.0E-05	4.1±0.2
------------------	--------	-----------	-----------	----------	---------	-----------------	---------

---

\* For data with RH>30%.

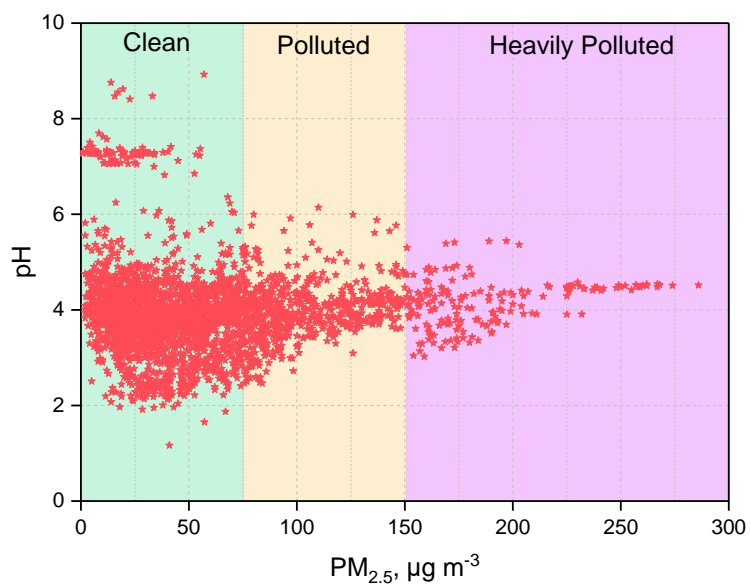


**Figure S8.** The relationship between PM<sub>2.5</sub> mass concentration and aerosol pH, the dots with RH≤30% were excluded.

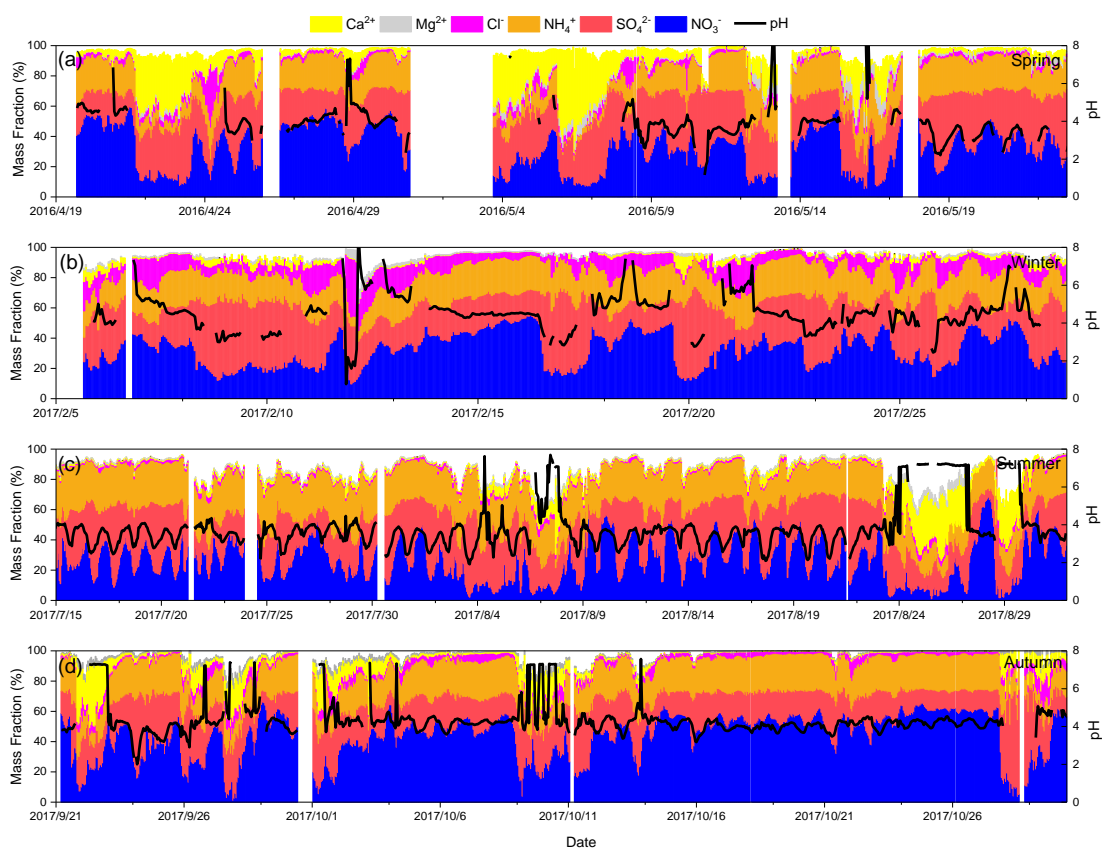


**Figure 4.** Time series of mass fraction of  $\text{NO}_3^-$ ,  $\text{SO}_4^{2-}$ ,  $\text{NH}_4^+$ ,  $\text{Cl}^-$ , crustal ions ( $\text{Mg}^{2+}$ ,  $\text{Ca}^{2+}$ ) in total ions as well as aerosol pH in all four seasons.

**4. Better connect the size-resolved measurements with the rest of the text. To what degree did the presence of coarse material drive ambient pH? Do figures 5-7 and the analysis regarding drives of pH only consider fine mode pH?**

**Response:** Thanks for your suggestion. The data set of MOUDI was obtained during 2013 and 2015, whereas the online ion data was obtained in 2016 and 2017. (1) The sensitivity analysis in this work aimed at the  $\text{PM}_{2.5}$  (*ie* fine particles) since the  $\text{PM}_{2.5}$  components in four seasons were available and has a high temporal resolution (1h). In addition, the data set has a wide range, covering different levels of haze events, making it suitable for sensitivity analysis. The MOUDI data were only utilized to determine the size-resolved aerosol pH. (2) In this work, the coarse mode aerosol acidity was generally neutral, which mainly attributed to the higher mass concentration of mineral materials in the coarse mode. The sensitivity analysis in this work showed that the aerosol pH increased approximately linearly with the elevated  $\text{Ca}^{2+}$  in  $\text{PM}_{2.5}$  (Figure S18). However, the impact of  $\text{Ca}^{2+}$

has a limited impact on fine mode aerosol pH due to its low mass concentration in PM<sub>2.5</sub>. Our previous paper showed that the mineral materials such as Ca<sup>2+</sup> and Mg<sup>2+</sup> mainly concentrated in the coarse mode (Figure R2, same data set with this work, Zhao et al, 2017; Su et al., 2018). We did some supplementary simulations under extreme cases that Ca<sup>2+</sup> and Mg<sup>2+</sup> are removed from the input files. The results showed that the presence of Ca<sup>2+</sup> and Mg<sup>2+</sup> in coarse mode has a crucial effect on aerosol pH (Figure S22), the difference of aerosol pH (with and without Ca<sup>2+</sup> and Mg<sup>2+</sup>) for particles larger than 1 μm increased with the increasing particle size. The aerosol pH in coarse mode decreased by 4~6.5 unit when the Ca<sup>2+</sup> and Mg<sup>2+</sup> are removed. (Page 19, line 508- 514, in the revised manuscript)

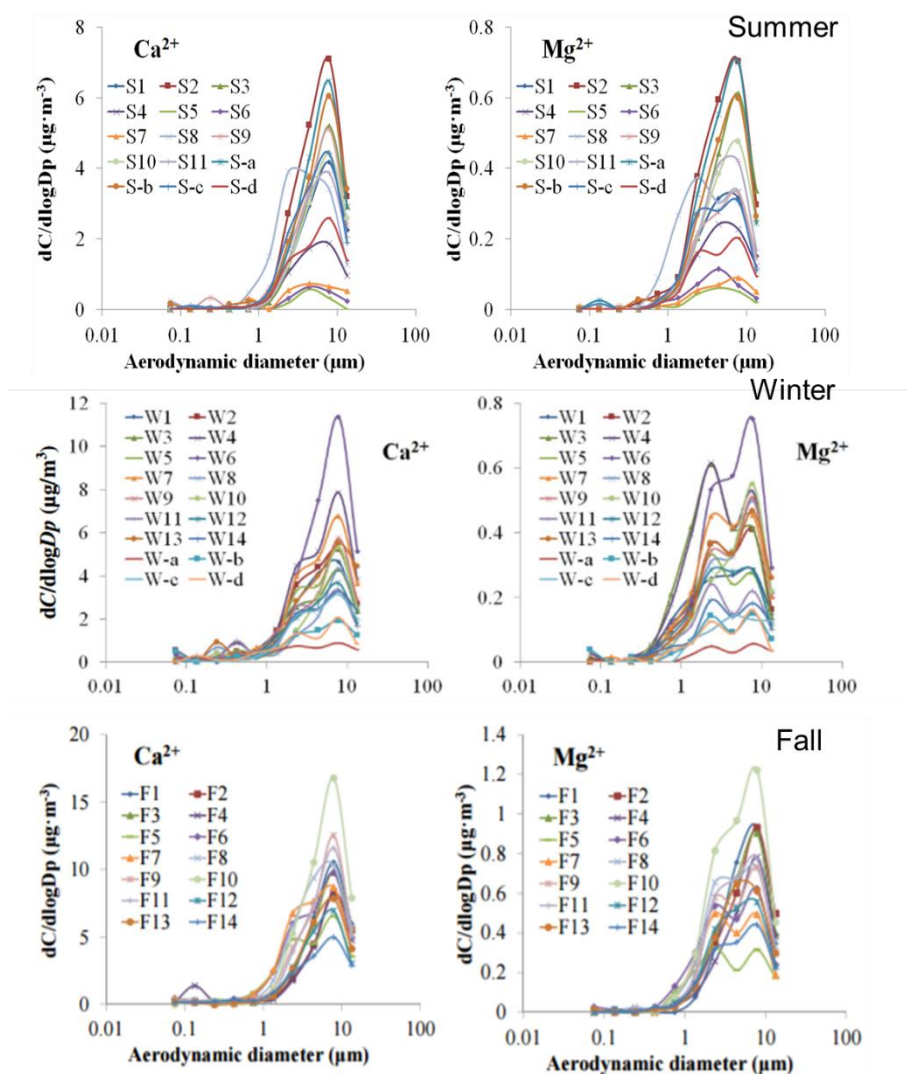


**Figure R2.** Size distributions of the mass concentration for Ca<sup>2+</sup> and Mg<sup>2+</sup> in summer, winter, and fall. (Zhao et al, 2017; Su et al., 2018)

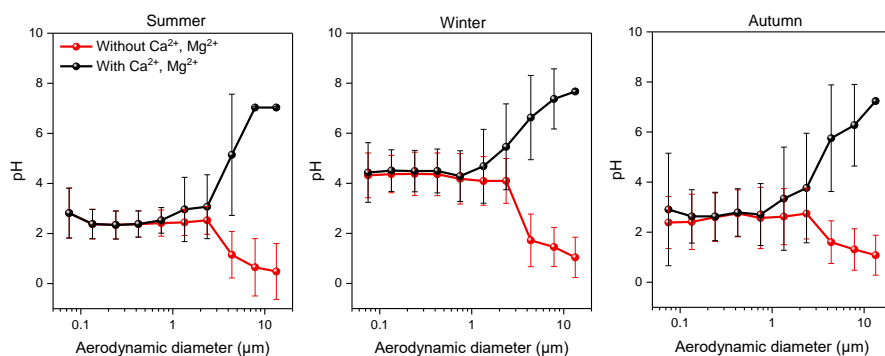


**Figure S22.** Size distributions of the aerosol pH with and without  $\text{Ca}^{2+}$  and  $\text{Mg}^{2+}$  in summer, winter, and autumn.

**Minor comments:**

1. Line 49. Instead of stating that aerosol acidity is “usually estimated” by the charge balance, I would indicate “sometimes” or “frequently,” but not usually as many studies do use a thermodynamic model.

**Response:** Thank you for your good advice, “usually” has been changed to “frequently” in the revised manuscript. (Page 3, line 50, in the revised manuscript)

2. Line 52-55 wording indicates ion balance fails because acidity is estimated by aerosol water extract. This doesn’t follow well as ion balance (e.g. difference between number of charge equivalent anions and cations) doesn’t require extraction.

**Response:** Thank you for your correction, here we want to express that the simple ion balance cannot predict the hydronium ion concentration in the aerosol liquid water accurately. In the revised manuscript, this statement has been reworded. (Page 3, line 53-55, in the revised manuscript)

3. Line 95: may want to indicate models “often” assume internal mixtures (but that is not a requirement).

**Response:** The sentences about this assumption were deleted in the revised manuscript.

4. Line 98-99: For this statement indicating nitrate is mainly in the fine mode, does that need to be qualified by indicating a location or time of year? Does fine mode nitrate generally exceed coarse nitrate?

**Response:** Thank you for your question. This statement about nitrate is mainly aimed at the aerosol composition in China. Many studies in China showed that the fine mode nitrate generally exceeds

coarse nitrate except for the dust days. In Beijing, the fine mode ( $\leq 2.5 \mu\text{m}$ ) nitrate concentration at different polluted level was 3~5 times higher than that in coarse mode (2.5~10  $\mu\text{m}$ ) (Meier et al., 2009; Tian et al., 2014; Sun et al., 2014), and the same size distribution was found in southern cities of China on non-dust days (Pan et al., 2009; Wang et al., 2015; Ding et al., 2017). However, in dust days, the  $\text{PM}_{10}$  concentration was much higher than that of  $\text{PM}_{2.5}$ , resulting in the elevated nitrates in coarse mode (Pan et al., 2009; Wang et al., 2015). In the revised manuscript, the statement was qualified. **(Page 5, line 91-92, in the revised manuscript)**

5. Near line 155 and Figure 1: Spring shows a fairly persistent difference in the concentration of  $\text{PM}_{10}$  vs  $\text{PM}_{2.5}$ . Two dust episodes are mentioned. With the exception of these two episodes, do you have a sense of what is contributing to the  $\text{PM}_{10}$ - $\text{PM}_{2.5}$  material? Late September also indicates an episode in which  $\text{PM}_{10}$  is elevated compared to  $\text{PM}_{2.5}$ .

**Response:** The  $\text{PM}_{2.5-10}$  was generally regarded as coarse particles. On clean days, the crustal materials could account for more than 30% of the total  $\text{PM}_{2.5-10}$ . During the dust events, crustal materials could account for more than 60% of the coarse particles (Xu, 2010). However, during the severe haze events,  $\text{SO}_4^{2-}$ ,  $\text{NO}_3^-$ ,  $\text{NH}_4^+$ , OM, and EC also substantially accumulated in the coarse mode (Pan et al., 2009; Tian et al., 2014).

6. Line 190 indicates water uptake onto hydrophilic organics can be ignored unless the fraction of particle water due to organics is near 1 (100%). Water due to uptake on organics is presumably important even when it is not the sole contributor to particulate water. The threshold of 1 should be removed and perhaps a statement about the potential error incurred by ignoring ALWCo should be added.

**Response:** Thank you for your good suggestion. Surely part of organic species in particles such as water-soluble secondary organic carbon is hygroscopic, especially in ultrafine particles. In the revised manuscript, the threshold of 1 has been removed and a statement about the potential error incurred by ignoring ALWCo has been added as below. **(Page 8, line 180-182, in the revised manuscript)**

7. Text on lines 235-238 seems misplaced or unnecessary.

**Response:** This paragraph has been deleted in the revised manuscript.

8. Line 277 highlights sulfate as a driving factor for pH. Sulfate peaked at night during the winter (Figure 4) when photochemical activity is lower. To what degree is the diurnal variation in sulfate driven by chemistry vs meteorology (e.g. planetary boundary layer depth)?

**Response:** The diurnal variation in sulfate was complex, especially during the severe haze episodes, where the rapid increase in mass concentration was mainly due to the accumulation induced by the unfavorable meteorological condition. Figure R2(a) and R2(b) showed that for most of the time, the mass fraction of  $\text{SO}_4^{2-}$  in total ions has little variation when  $\text{SO}_4^{2-}$  mass concentration increased largely, which could be regarded as the contribution of meteorology. However, at some moments in the nighttime (gray shadow in the figure), both mass concentration and mass fraction of  $\text{SO}_4^{2-}$  showed a significant increase, which mainly attributed to the secondary reaction of  $\text{SO}_2$ . Overall, the mean  $\text{SO}_4^{2-}$  fraction in total ions at night in winter was slightly higher than that in daytime (Figure R2(c)), but differences are not statistically significant. Hence the diurnal variation in sulfate was more driven by meteorology.

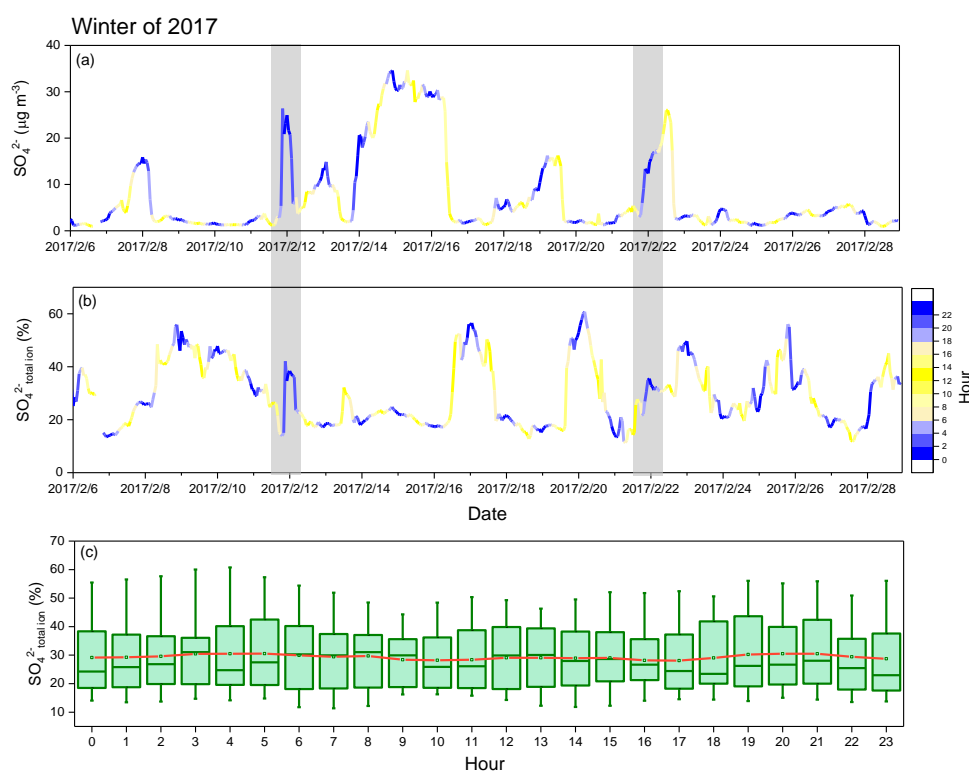


**Figure R2.** Time series of  $\text{SO}_4^{2-}$  mass concentration (a) and  $\text{SO}_4^{2-}$  mass fraction in total ions (b) as well as the diurnal variation of  $\text{SO}_4^{2-}$  mass fraction in total ions in winter.

9. Line 284: Is the key difference between the US and Beijing more driven by the higher concentrations or the greater variability in concentrations?

**Response:** Thank you for your question. According to the record of literature (Guo et al., 2015),  $H_{\text{air}}^+$  diurnal variation was less significant while the ALWC diurnal variation was significant, hence the diurnal pattern in pH was mainly driven by particle water dilution. However, in this work, we find that both  $H_{\text{air}}^+$  and ALWC had significant diurnal variation, and the aerosol acidity variation agreed well with sulfate. In the North China Plain, the  $PM_{2.5}$  mass concentration has a wide variation range and the average value was high. For example, in winter, the  $PM_{2.5}$  mass concentration in Beijing was several to dozens times higher than that in the US, which means there are more seeds in the limited water vapor, hence the dilution of aerosol liquid water to  $H_{\text{air}}^+$  doesn't work at all, the diurnal variation of aerosol components was more important. Therefore, we think both the higher concentrations and the greater variability in concentrations have important effects on the difference between the US and Beijing. (Page 13-14, line 348-355, in the revised manuscript)

10. Line 384:386 represents a simplified description of ammonia partitioning in which ammonia acts first to neutralize sulfate and then any leftover ammonia can react with nitrate to make ammonium nitrate. Perhaps the authors do not mean this so simply. Reword to reflect the semivolatile nature of ammonia and nitrate.

**Response:** The statements here indeed have some problems. In the revised manuscript, we try to give the impact of  $NH_4^T$  on aerosol pH with another explanation. Elevated  $NH_4^T$  could reduce  $H_{\text{air}}^+$  exponentially and slightly increase ALWC when the other input parameters were held constant, leading to the decrease of aerosol pH. As the  $NH_4^T$  increases,  $H_{\text{air}}^+$  are consumed swiftly during the dissolution of  $NH_3$  as well as the further reaction with  $SO_4^{2-}$ ,  $NO_3^-$ , and  $Cl^-$ . And the elevated  $NH_4^T$  increases the  $\epsilon(NO_3^-)$  and  $\epsilon(Cl^-)$  when  $NO_3^T$  and  $Cl^T$  were fixed (Figure 10), which means the elevated  $NH_4^T$  alter the gas-particle partition and shifts more  $NO_3^T$  and  $Cl^T$  into particle phase, and the deliquescence of additional nitrate and chloride increased ALWC slightly. (Page 17, line 447-453, in the revised manuscript)



11. Line 388: Do the authors mean that aerosol would be fully neutralized except for the fact that ammonia is taken up into clouds and precipitation? Reword to reflect the buffering nature of ammonia.

**Response:** We are afraid that the reviewer misunderstood what we meant. Here we want to deliver that although the ammonia in the atmosphere is excessive, the other conditions are limited, the ALWC is one of them. Compared to the liquid water content in clouds and precipitation, ALWC is much lower, hence the dilution of aerosol liquid water to  $H_{air}^+$  is much weaker. In the revised manuscript, we reword Line 376-388 to more clearly express our point. **(Page 17, line 462-465, in the revised manuscript)**

12. Caption to table 2: This table appears to be the sensitivity of acidity, ALWC, and  $H^+$  to chemical components (not the other way around). Please clarify caption.

**Response:** Thanks for your careful check, the caption to Table 2 (Table 3 in the revised manuscript) has been clarified as below:

**Table 3** Sensitivity of ALWC,  $H_{air}^+$ , and  $PM_{2.5}$  pH to  $SO_4^{2-}$ ,  $NH_4^T$ ,  $NO_3^T$ ,  $Cl^T$ ,  $Ca^{2+}$ , RH, and T. The larger magnitude of the relative standard deviation (RSD) represents the larger impact derived from the variation of variables. **(Page 29, line 776-778, in the revised manuscript)**

13. Figure 3: use a common color scale for all panels.

**Response:** Color scale in figures has been unified.

14. Figure 5, 6, 7, caption. These figures appear to be the sensitivity of ALWC,  $H^+$ , and pH to chemical components. Reword caption.

**Response:** Thanks for your careful check, captions to Figure 5, 6, 7 (7-9 in the revised manuscript) have been clarified as below: **(Page 33, line 818-823, in the revised manuscript)**

**Figure 7.** Sensitivities of  $H_{air}^+$  to  $SO_4^{2-}$ ,  $NO_3^T$ ,  $NH_4^T$ ,  $Cl^T$ , as well as meteorological parameters (RH, T) in summer and winter.

**Figure 8.** Sensitivities of ALWC to  $SO_4^{2-}$ ,  $NO_3^T$ ,  $NH_4^T$ ,  $Cl^T$ , as well as meteorological parameters (RH, T) in summer and winter.

**Figure 9.** Sensitivities of aerosol pH to  $SO_4^{2-}$ ,  $NO_3^T$ ,  $NH_4^T$ ,  $Cl^T$ , as well as meteorological parameters

(RH, T) in summer and winter.

15. Line 136: Have you looked at trends from 2013, 2015, and 2017 datasets you have collected?

**Response:** In this work, the water-soluble ions of PM<sub>2.5</sub> samples and MOUDI samples were not collected synchronously. Water-soluble ions (SO<sub>4</sub><sup>2-</sup>, NO<sub>3</sub><sup>-</sup>, Cl<sup>-</sup>, NH<sub>4</sub><sup>+</sup>, Na<sup>+</sup>, K<sup>+</sup>, Mg<sup>2+</sup>, Ca<sup>2+</sup>) of PM<sub>2.5</sub> and trace gases (HCl, HNO<sub>3</sub>, HNO<sub>2</sub>, SO<sub>2</sub>, NH<sub>3</sub>) in the ambient air were measured by an online analyzer (MARGA) at hourly temporal resolution during the spring (April and May in 2016), winter (February in 2017), summer (July and August in 2017) and autumn (September and October in 2017). While the size-resolved sampling was conducted during July 12-18, 2013; January 13-19, 2014; July 3-5, 2014; October 9-20, 2014; and January 26-28, 2015. Compared to the real-time PM<sub>2.5</sub> sampling, MOUDI sampling time is short, which is not conducive to analyze the variation tendency of aerosol composition and acidity in time. MOUDI samples were mainly used to analyze the change of aerosol composition and acidity in different particle size.

16. Additional improvements in terms of editing would be useful.

**Response:** The English in the manuscript has been improved by an English native speaker.

## References

- Cruz, C. N., Dassios, K. G., Pandis, S. N.: The effect of dioctyl phthalate films on the ammonium nitrate aerosol evaporation rate. *Atmos. Environ.*, 34, 3897-3905, 2000.
- Dassios, K. G., Pandis, S. N.: The mass accommodation coefficient of ammonium nitrate aerosol. *Atmos. Environ.*, 33 (18), 2993-3003, 1999.
- Dai, Q. L., Bi, X. H., Liu, B. S., Li, L. W., Ding, J., Song, W. B., Bi, S. Y., Schulze, B. C., Song, C.B., Wu, J. H., Zhang, Y. F., Feng, Y. C., Hopke, P. K.: Chemical nature of PM<sub>2.5</sub> and PM<sub>10</sub> in Xi'an, China: Insights into primary emissions and secondary particle formation. *Environ. Pollu.*, 240 155-166, 2018, doi:10.1016/j.envpol.2018.04.111.
- Ding, X. X., Kong, L. D., Du, C. T., Zhanzakova, A., Fu, H. B., Tang, X. F., Wang, L., Yang, X., Chen, J. M., Cheng, T. T.: Characteristics of size-resolved atmospheric inorganic and carbonaceous aerosols in urban Shanghai. *Atmos. Environ.*, 167, 625-641, 2017, doi: 10.1016/j.atmosenv.2017.08.043

- Fang, T., Guo, H. Y., Zeng, L. H., Verma, V., Nenes, A., Weber, R. J.: Highly acidic ambient particles, soluble metals, and oxidative potential: A link between sulfate and aerosol toxicity, *Environ. Sci. Technol.*, 51, 2611-2620, 2017.
- Gao, J. J., Tian, H. Z., Cheng, K., Lu, L., Zheng, M., Wang, S. X., Wang, K.: The variation of chemical characteristics of PM<sub>2.5</sub> and PM<sub>10</sub> and formation causes during two haze pollution events in urban Beijing, China. *Atmos. Environ.* 107,1-8, 2015.
- Guo, H., Xu, L., Bougiatioti, A., Cerully, K. M., Capps, S. L., Hite Jr., J. R., Carlton, A. G., Lee, S.-H., Bergin, M. H., Ng, N. L., Nenes, A., Weber, R. J.: Fine-particle water and pH in the southeastern United States, *Atmos. Chem. Phys.*, 15, 5211-5228, 2015.
- Guo, H., Sullivan, A. P., Campuzano-Jost, P., Schroder, J. C., Lopez-Hilfiker, F. D., Dibb, J. E., Jimenez, J. L., Thornton, J. A., Brown, S. S., Nenes, A., Weber, R. J.: Fine particle pH and the partitioning of nitric acid during winter in the northeastern United States, *J. Geophys. Res. Atmos.*, 121, 10355-10376, 2016.
- Meier, J., Wehner, B., Massling, A., Birmili, W., Nowak, A., Gnauk, T., Brüggemann, E., Herrmann, H., Min, H., Wiedensohler, A.: Hygroscopic growth of urban aerosol particles in Beijing (China) during wintertime: a comparison of three experimental methods, *Atmos. Chem. Phys.*, 9, 6865–6880, 2009.
- Pan, X. L., Yan, P., Tang, J., Ma, J. Z., Wang, Z. F., Gbaguidi, A., and Sun, Y. L.: Observational study of influence of aerosol hygroscopic growth on scattering coefficient over rural area near Beijing mega-city, *Atmos. Chem. Phys.*, 9, 7519-7530, 2009.
- Su, J., Zhao, P. S., Dong, Q.: Chemical Compositions and Liquid Water Content of Size-Resolved Aerosol in Beijing. *Aerosol Air Qual. Res.*, 18, 680-692, 2018.
- Sun, K., Qu, Y., Wu, Q., Han, T. T., Gu, J. W., Zhao, J. J., Sun, Y. L., Jiang, Q., Gao, Z. Q., Hu, M., Zhang, Y. H., Lu, K. D., Nordmann, S., Cheng, Y. F., Hou, L., Ge, H., Furuuchi, M., Hata, M., Liu X. G.: Chemical characteristics of size-resolved aerosols in winter in Beijing, *J. Environ. Sci.*, 26,1641-1650, 2014, [doi: 10.1016/j.jes.2014.06.004](https://doi.org/10.1016/j.jes.2014.06.004).
- Tian, S. L., Pan, Y. P., Liu, Z.R., Wen, T. X., Wang, Y. S.: Size-resolved aerosol chemical analysis of extreme haze pollution events during early 2013 in urban Beijing, China. *J. Hazard. Mater.*, 279, 452-460, 2014.

Wang, H.L., Zhu, B., Shen, L. J., Xu, H. H., An, J. L., Xue, G. Q., Cao, J. F.: Water-soluble ions in atmospheric aerosols measured in five sites in the Yangtze River Delta, China: Size-fractionated, seasonal variations and sources. *Atmos. Environ.*, 123, 370-379,2015, doi: 10.1016/j.atmosenv.2015.05.070

Xu, C.: Characteristics, source and the formation mechanism of aerosol in mega-city, China [D], Fudan University, Shanghai, 2010.

Zhao, P. S., Chen, Y. N., Su, J.: Size-resolved carbonaceous components and water-soluble ions measurements of ambient aerosol in Beijing. *J. Environ. Sci.*, 54, 298-313, 2017.

---

1 **Aerosol pH and its influencing factors in Beijing**

2 **Jing Ding<sup>2,1</sup>, Pusheng Zhao<sup>1,3\*</sup>, Jie Su<sup>1</sup>, Qun Dong<sup>1</sup>, ~~and~~ Xiang Du<sup>2,1</sup>, and Yufen**  
3 **Zhang<sup>2</sup>**

带格式的: 上标

4 <sup>1</sup> Institute of Urban Meteorology, China Meteorological Administration, Beijing 100089, China

5 <sup>2</sup> State Environmental Protection Key Laboratory of Urban Ambient Air Particulate Matter Pollution  
6 Prevention and Control, College of Environmental Science and Engineering, Nankai University,  
7 Tianjin 300071, China

8 <sup>3</sup> ~~Max Planck Institute for Chemistry, Mainz 55128, Germany~~

9 \* Correspondence to: Pusheng P. S. Zhao (pszhao@ium.cn)

---

## Abstract

Acidity (pH) plays a key role in the physical and chemical behavior of aerosol and cannot be measured directly. In this work, aerosol liquid water content (ALWC) and size-resolved pH are predicted by thermodynamic model (ISORROPIA II) in 2017 of Beijing. The mean aerosol pH over four seasons is  $4.3 \pm 1.6$  (spring),  $4.5 \pm 1.1$  (winter),  $3.9 \pm 1.3$  (summer),  $4.1 \pm 1.0$  (autumn), respectively, showing the moderate aerosol acidity. The aerosol pH in fine mode is in the range of 1.8–3.9, 2.4–6.3 and 3.5–6.5 for summer, autumn and winter, respectively. And coarse particles are generally neutral or alkaline. Diurnal variation of aerosol pH follows both aerosol components (especially the sulfate) and ALWC. For spring, summer and autumn, the averaged nighttime pH is 0.3–0.4 unit higher than that on daytime. Whereas in winter, the aerosol pH is relatively low at night and higher at sunset.  $\text{SO}_4^{2-}$  and RH are two crucial factors affecting aerosol pH. For spring, winter and autumn, the effect of  $\text{SO}_4^{2-}$  on aerosol pH is greater than RH, and it is comparable with RH in summer. The aerosol pH decreases with elevated  $\text{SO}_4^{2-}$  concentration. As the  $\text{NO}_3^-$  concentration increases, the aerosol pH firstly increases and then decreases. Sulfate dominant aerosols are more acidic with pH lower than 4, whereas nitrate-dominated aerosols are weak in acidity with pH ranges 3–5. In recent years, the dominance of  $\text{NO}_3^-$  in inorganic ions may be another reason responsible for the moderately acidic aerosol. ALWC has a different effect on aerosol pH in different seasons. In winter, the increasing RH could reduce the aerosol pH whereas it shows a totally reverse tendency in summer, and the elevated RH has little effect on aerosol pH in spring and autumn when the RH is between 30% and 80%. The dilution effect of ALWC on  $\text{H}_{\text{am}}^+$  is only obvious in summer. The elevated  $\text{NH}_3$  and  $\text{NH}_4^+$  could reduce aerosol acidity by decreasing  $\text{H}_{\text{am}}^+$  concentration exponentially.

The acidity or pH is an important feature of ambient aerosol. At present, the aerosol pH in the North China Plain, either seasonal variation or size-resolved characteristics, need to be further studied. In addition, it is also worthy of discussion about what factors have a greater impact on pH and how these factors affect pH. In view of these, the hourly water-soluble ions ( $\text{SO}_4^{2-}$ ,  $\text{NO}_3^-$ ,  $\text{Cl}^-$ ,  $\text{NH}_4^+$ ,  $\text{Na}^+$ ,  $\text{K}^+$ ,  $\text{Mg}^{2+}$ , and  $\text{Ca}^{2+}$ ) of  $\text{PM}_{2.5}$  and trace gases (HCl,  $\text{HNO}_3$ ,  $\text{HNO}_2$ ,  $\text{SO}_2$ , and  $\text{NH}_3$ ) were online measured by a MARGA system in four seasons during 2016 and 2017 in Beijing. Furthermore, the size-resolved aerosol was also sampled by a MOUDI sampler and analyzed for the chemical compositions of different sizes. On the basis of these data, the particle hydronium ion

39 concentration per volume air ( $H_{air}^+$ ), aerosol liquid water content (ALWC), and  $PM_{2.5}$  pH were  
40 calculated by using ISORROPIA-II. Moreover, the sensitivities of  $H_{air}^+$ , ALWC, aerosol pH to all  
41 the main influencing factors were discussed. In Beijing, the  $PM_{2.5}$  pH over four seasons showed  
42 moderately acid. The  $PM_{2.5}$  acidity in NCP was both driven by aerosol composition and particle  
43 water. The sensitivity analysis revealed that  $SO_4^{2-}$ , T,  $NH_4^+$ , and RH (only in summer) are crucial  
44 factors affecting the  $PM_{2.5}$  pH. The  $SO_4^{2-}$  had a key role for aerosol acidity, especially in winter and  
45 spring. The impact of  $NO_3^-$  on  $PM_{2.5}$  pH was different in four seasons. Although  $NH_3$  in the NCP  
46 was abundant, the  $PM_{2.5}$  pH was far from neutral, which mainly attributed to the limited ALWC.  
47 Elevated  $Ca^{2+}$  concentration could increase the aerosol pH because of the buffering capacity of  $Ca^{2+}$   
48 to the acid species and the weak water solubility of  $CaSO_4$ . The sensitivity analysis also implied  
49 that decreasing  $NO_3^+$  could reduce the  $\epsilon(NH_4^+)$  effectively. In contrast, the nitrate response to  $NH_4^+$   
50 control was highly nonlinear. According to the size-resolved results, the pH for coarse mode, which  
51 was near or even higher than 7, was much higher than that for fine mode. It must be noted that the  
52 aerosol pH in coarse mode showed a marked decrease when under heavily polluted condition.

53 **Key words:** Aerosol pH, ~~Size distribution, Influencing~~ISORROPIA-II, ~~Influencing~~ factors,  
54 Beijing–

55

---

## 56 1. Introduction

57 Acidity or pH, which drives many processes related to particle composition, gas-aerosol  
58 partitioning and aerosol secondary formation, is an important aerosol property (Jang et al., 2002;  
59 Eddingsaas et al., 2010; Surratt et al., 2010). The aerosol acidity has a significant effect on the  
60 aerosol secondary formation through the gas-aerosol partitioning of semi-volatile and volatile  
61 ~~special species~~ (Pathak et al., 2011a; Guo et al., 2016). Recent studies have shown that aerosol  
62 acidity could promote the generation of secondary organic aerosol by affecting the aerosol acid-  
63 catalyzed reactions (Rengarajan et al., 2011~~;-~~). Moreover, metals can become soluble by acid  
64 dissociation under lower ~~aerosol pH conditions~~ (Shi et al., 2011; Meskhidze et al., 2003) or by  
65 forming a ligand with ~~organic species~~, such as oxalate at higher pH (Schwertmann et al., 1991).  
66 In addition, higher aerosol acidity ~~could can~~ lower the acidification buffer capacity and ~~affected~~  
67 the formation of acid rain. The investigation ~~in of~~ aerosol acidity is conducive to better understand  
68 the important role of aerosols in acid deposition and atmospheric chemical reactions.

69 The hygroscopic components in the aerosols include water-soluble inorganic ions and part of  
70 organic acid (Peng, 2001; Wang et al., 2017). The deliquescence relative humidity (DRH) for the  
71 mixed-salt is lower than that of any ~~one single~~ component (Seinfeld and Pandis, 2016), hence the  
72 ambient aerosols are generally droplets containing liquid water. The aerosol pH actually is the pH  
73 of the aerosol liquid water. The aerosol acidity is ~~usually frequently~~ estimated by the charge balance  
74 of measurable cations and anions. A net negative balance correlated with an acidic aerosol and vice  
75 versa (Zhang et al., 2007; Pathak et al., 2011b; Zhao et al., 2017). Generally, a larger value of the  
76 ion balance implies a stronger acidity or stronger alkaline. Nevertheless, an ion balance or other  
77 similar proxies fail to represent the true aerosol pH because ~~the aerosol acidity estimated by this  
78 way is measured through the aerosol water extract, which poorly predicts the concentration of  
79 hydronium ion in the aerosol liquid water (Guo et al., 2015; Hennigan et al., 2015). Moreover,  
80 due to the large amounts of water is used for extraction, the results cannot reflect the characteristics  
81 of the in-situ aerosol acidity, and it cannot be applied to study the influence of aerosol acidity on  
82 gas-particle conversion. In-situ aerosol acidity, defined as the free predict H<sup>+</sup> concentration in the  
83 liquid phase accurately (Guo et al., 2015; Hennigan et al., 2015) of a particle, is an important  
84 parameter that actually affects the chemical behavior of the particle,~~ which could be calculated by



---

85 hydrogen ion concentration ~~per volume air ( $H_{air}^+$ )~~ and the aerosol liquid water content (ALWC).  
86 It is critical to obtain the ALWC in calculating aerosol acidity. One way to calculate the ALWC  
87 is based upon the assumption that the volume of ALWC is equal to subtracting the volume of dry  
88 aerosol particles from that of wet particles (Guo et al., 2015; Bian et al. 2014; Engelhart et al. 2011).  
89 Under this assumption, ALWC could be calculated by the size-resolved hygroscopic growth factors  
90 ( $g(D, RH)$ ) combining particle size distribution (PNSDs) or by the hygroscopic growth factor of  
91 aerosol scattering coefficient ( $f(RH)$ ) (Bian et al. 2014; Guo et al., 2015; Kuang et al., 2017a). The  
92  $g(D, RH)$ , defined as the ratio of the diameter of the wet particle at a certain relative humidity to the  
93 corresponding diameter at dry conditions, ~~could~~ be measured by a H-TDMA (Hygroscopic  
94 Tandem Differential Mobility Analyzer) (Liu et al., 1978; Swietlicki et al., 2008; Liu et al., 2011).  
95 ~~And the~~  $f(RH)$  ~~could~~ be observed by the wet & dry nephelometer system (Covert et al., 1972;  
96 Rood et al. 1985; Yan et al., 2009; Kuang et al., 2016, 2017b).

97 Another way to calculate the ALWC is based on the aerosol chemical components with  
98 thermodynamic models, such as ISORROPIA-II, AIM, ADDEM etc. (Nenes et al., 1998;  
99 Fountoukis and Nenes, 2007, Clegg et al., 1998, Topping et al., 2005a, b). Based on the aerosol  
100 chemical components as well as temperature and relative humidity, the aerosol thermodynamic  
101 models ~~could~~ output both ALWC and ~~concentration of the hydronium ion in air (moles  $H^+$  per~~  
102 ~~volume of air, denoted hereafter as  $H_{air}^+$ ),~~ which offers a more precise approach to acquire aerosol  
103 pH (Pye et al., 2013). Among these thermodynamic models, ISORROPIA and ISORROPIA-II are  
104 ~~most~~ widely used owing to its rigorous calculation and performance on computational speed.  
105 ISORROPIA simulates the gas-particle partitioning in the  $H_2SO_4$ ,  $NH_3$ ,  $HNO_3$ ,  $HCl$ ,  $Na^+$ ,  $H_2O$   
106 system, while its second version, ISORROPIA-II, adds  $Ca^{2+}$ ,  $K^+$ ,  $Mg^{2+}$  and the corresponding salts  
107 to the simulated particle components in thermodynamic equilibrium with water vapor and gas-phase  
108 precursors.

109 Comparisons were made in some studies to investigate the consistency of calculated ALWC  
110 derived from the above methods. In the North China Plain, ~~(NCP)~~, Bian et al. (2014) found that the  
111 ALWC calculated using size-resolved hygroscopic growth factors and the PNSD agreed well with  
112 that calculated using ISORROPIA II at higher relative humidity (>60%). Relatively good  
113 consistency was also found in the study of Engelhart et al. (2011) in ~~the~~ USA based on the similar

114 method. Guo et al. (2015) compared the ALWC calculated by  $f(\text{RH})$  with the total predicted water  
115 by organics and inorganics. The total predicted water was highly correlated and on average within  
116 10 % of the  $f(\text{RH})$  measured water. Though good consistencies in ALWC were found among these  
117 methods, the  $\text{H}_{\text{air}}^+$  could only be obtained by the thermodynamic models, which have had been  
118 applied to predict aerosol acidity in many studies (Nowak et al., 2006; Fountoukis et al., 2009;  
119 Weber et al., 2016; Fang et al., 2017).

120 ~~When calculating aerosol acidity with thermodynamic models, the aerosol is assumed internally~~  
121 ~~mixed and the bulk properties of aerosol are used, without considering variability of chemical~~  
122 ~~compositions with particle size. However, the size-resolved~~The characteristics of aerosol chemical  
123 components are ~~obviously~~ different ~~among multiple size ranges~~. Among inorganic ions,  $\text{SO}_4^{2-}$ ,  
124  $\text{NO}_3^-$ ,  $\text{Cl}^-$ ,  $\text{K}^+$ ,  $\text{NH}_4^+$  ~~are~~ mainly ~~eonecentrated~~concentrate in fine mode, ~~except for the dust days~~  
125 ~~(Meier et al., 2009; Pan et al., 2009; Tian et al., 2014)~~, whereas  $\text{Mg}^{2+}$ ,  $\text{Ca}^{2+}$  are abundant in coarse  
126 mode (Zhao et al., 2017). The aerosol acidity is affected by coupling among many variables.  
127 Therefore, it could be expected that the aerosol pH is the result of the balance between the soluble  
128 acidic ( $\text{SO}_4^{2-}$ ,  $\text{NO}_3^-$ ,  $\text{Cl}^-$  and some soluble organic acids) and alkaline ( $\text{NH}_4^+$ ,  $\text{Na}^+$ ,  $\text{K}^+$ ,  $\text{Mg}^{2+}$ ,  $\text{Ca}^{2+}$ )  
129 ~~component in the aerosol, also diverse under different particle size~~. The gas precursor ( $\text{NH}_3$ ,  $\text{HNO}_3$ ,  
130 and  $\text{HCl}$  ~~for~~) of main water-soluble ions, as well as ambient temperature and relative humidity, are  
131 also important factors affecting the aerosol acidity. In some countries where ~~PM~~particle matter  
132 concentration is very low, the pH diurnal variation was mainly driven by meteorological conditions  
133 (Guo et al., 2015, 2016; Bougiatioti et al., 2016). In China, however, the annual average  $\text{PM}_{2.5}$   
134 concentration in some ~~mega-cities~~megacities was  $\sim 2$  times higher than the national standard value  
135 ( $35 \mu\text{g m}^{-3}$ ) and the inorganic ions ~~aeount~~accounted for 40%~50% to  $\text{PM}_{2.5}$ , especially in the North  
136 China Plain (Zou et al., 2018; Huang et al., 2017; Gao et al., 2018). Hence it can be expected that  
137 the aerosol composition is also a crucial factor on pH, which cannot be ignored.

138 The North China Plain is the region with the most severe aerosol pollution in China. Nevertheless,  
139 only a few studies have focused on aerosol pH at in this region. ~~Cheng et al. (2016) estimated the~~  
140 ~~averaged pH by ISORROPIA-II, and Wang et al. (2016) derived the particle pH by using a molar~~  
141 ~~ratio approach in Beijing, their results show~~Some studies conducted in NCP showed that the aerosol  
142 acidity was close to neutral. ~~However, Liu et al. (2017) and Shi et al. (2017) found that, while in~~

带格式的: 英语(英国)

143 ~~some other studies the~~ fine particles in the North China Plain ~~were~~ showed moderately acidic based  
144 ~~on the hourly measured particulate water-soluble ions and precursor gases along with ISORROPIA-~~  
145 ~~II, with an average pH of 4.2 in winter of Beijing and 4.9 in Tianjin.~~ (Cheng et al., 2016; Wang et al.,  
146 2016; Liu et al., 2017; Shi et al., 2017). These results ~~are~~ were all significantly higher than that in  
147 the United States or Europe, where aerosols ~~are~~ were often highly acidic with a pH lower than 3.0  
148 (Guo et al., 2015, 2016; Bougiatioti et al., 2016; Weber et al., 2016; Young et al., 2013). The  
149 differences in aerosol pH in ~~the North China Plain~~ NCP mainly ~~resulted~~ resulted from the different  
150 ~~calculated~~ methods (ion balance & thermodynamic equilibrium models). ~~Several studies have~~  
151 ~~shown that the ion-balance and reverse-mode calculations of thermodynamic equilibrium models~~  
152 ~~are~~ or different data sets ~~not applicable to interpret the aerosol acidity~~ (Hennigan et al., 2015; Liu  
153 et al., 2017; Song et al., 2018). Moreover, the ~~change~~ variation of the ~~PM<sub>2.5</sub>~~ chemical composition of  
154 ~~PM<sub>2.5</sub>~~ in ~~the North China Plain~~ NCP in recent years also contributed to the differences in aerosol pH.  
155 The observations in previous studies exploring aerosol acidity in ~~the North China Plain~~ NCP were  
156 almost conducted before 2015. In the recent three years, the chemical composition of PM<sub>2.5</sub> in  
157 Beijing has undergone tremendous changes. Nitrate has replaced sulfate and is dominant in  
158 inorganic ions in most cases (Zhao et al., 2017; Huang et al., 2017; Ma et al., 2017). Moreover,  
159 studies about seasonal variation of aerosol pH and size-resolved aerosol pH are rare in ~~the North~~  
160 ~~China Plain~~ NCP, and the key factors affecting aerosol acidity are still not well understood.

161 In this work, thermodynamic model ISORROPIA-II with ~~the~~ forward mode ~~is~~ was utilized to  
162 predict ALWC and aerosol pH in Beijing. The hourly measured PM<sub>2.5</sub> inorganic ions and precursor  
163 gases in four seasons during 2016 to 2017 ~~are~~ were used to analyze the seasonal and diurnal variation  
164 of aerosol acidity, and the sensitivity analysis ~~is~~ was conducted to identify the key factors that  
165 affecting the aerosol pH. In our previous studies, the multi-stage cascade impactors (MOUDI-122)  
166 were used for size-resolved aerosol sampling ~~during~~ from 2013 to 2015. The actual relative humidity  
167 inside the impactors was calculated, and the size ~~distribution~~ distributions of water-soluble ions,  
168 organic carbon, and elemental carbon in three seasons were discussed (Zhao et al., 2017; Su et al.,  
169 2018). Based on these size-resolved results, the pH for aerosol in different size ranges could also be  
170 ~~modeled, which can help to evaluate whether it is appropriate to calculate the overall pH of PM<sub>2.5</sub>~~  
171 ~~ignoring the differences in particle size~~ predicted.

---

172 **2. Data Collection and Methods**

173 **2.1 Site**

174 The measurements were performed at the Institute of Urban Meteorology in Haidian district of  
175 Beijing (39°56'N, 116°17'E). The sampling site was located next to a high-density residential area,  
176 without significant air pollution emissions around the site. Therefore, the observation data could  
177 represent the air quality levels of the urban area of Beijing.

178 **2.2 Online data collection**

179 Water-soluble ions ( $\text{SO}_4^{2-}$ ,  $\text{NO}_3^-$ ,  $\text{Cl}^-$ ,  $\text{NH}_4^+$ ,  $\text{Na}^+$ ,  $\text{K}^+$ ,  $\text{Mg}^{2+}$ , and  $\text{Ca}^{2+}$ ) of  $\text{PM}_{2.5}$  and trace gases  
180 ( $\text{HCl}$ ,  $\text{HNO}_3$ ,  $\text{HNO}_2$ ,  $\text{SO}_2$ , and  $\text{NH}_3$ ) in the ambient air were measured by an online analyzer  
181 (MARGA) at hourly temporal resolution during the spring (April and May in 2016), winter  
182 (February in 2017), summer (July and August in 2017) and autumn (September and October in  
183 2017). The more details about MARGA can be found at ten Brink et al. (2007). The  $\text{PM}_{2.5}$  and  $\text{PM}_{10}$   
184 mass concentrations (TEOM 1405DF), the hourly ambient temperature and relative humidity were  
185 also synchronously attained.

186 Hourly concentrations of  $\text{PM}_{2.5}$ ,  $\text{PM}_{10}$ , and water-soluble ions in  $\text{PM}_{2.5}$ , as well as meteorological  
187 parameters during the observation, are shown in Figure 1. In the spring, two dust events occurred  
188 (21-22, April and 5-6, May). During the first dust event, the wind came predominantly from  
189 the north with mean wind speed  $3.5 \text{ m s}^{-1}$ . The  $\text{PM}_{10}$  concentration reached  $425 \mu\text{g m}^{-3}$   
190 while the  $\text{PM}_{2.5}$  concentration was only  $46 \mu\text{g m}^{-3}$  on the peak hour. Similarly, the second dust event  
191 was resulted from the strong wind coming from the northwest direction. In the following pH  
192 analysis based on MARGA data, it was assumed that the particles were internally mixed, and the  
193 chemical compositions were the same for particles of different sizes in  $\text{PM}_{2.5}$ . Hence, these two dust  
194 events were excluded from this analysis.

195 **Figure 1**

196 **2.3 size-resolved chemical compositions**

197 A Micro-Orifice Uniform Deposit Impactor (MOUDI-120) was used to collect size-resolved  
198 aerosol samples with the calibrated 50% cut sizes of 0.056, 0.10, 0.18, 0.32, 0.56, 1.0, 1.8, 3.1, 6.2,  
199 9.9 and  $18 \mu\text{m}$ . Size-resolved sampling was conducted during July 12-18, 2013; January 13-19,  
200 2014; July 3-5, 2014; October 9-20, 2014; and January 26-28, 2015. Fifteen, fourteen, and eighteen

sets of samples were obtained for the summer, autumn, and winter, respectively. Except for two sets of samples, all the samples were collected in daytime (from 08:00 to 19:00) and nighttime (from 20:00 to 7:00 the next day), respectively. One hour of preparation time was set for filter changing and nozzle plate washing with ethanol. The water-soluble ions were analyzed from the samples by using an ion chromatography (DIONEX ICS-1000). The detailed information about the features of MOUDI-120, and the procedures of sampling, pre-treatment, and laboratory chemical analysis (including the quality assurance & quality control) were described in our previous papers (Zhao et al., 2017; Su et al., 2018-2018). It should be noted that there was no observation of gas precursors during the periods of MOUDI sampling.

#### 2.4 Aerosol pH prediction

As mentioned in the Introduction, pH of ambient aerosols could be predicted by the thermodynamic model such as AIM and ISORROPIA. AIM is considered as an accurate benchmark model while ISORROPIA has been optimized for use in chemical transport models. Currently, ISORROPIA-II, adding  $K^+$ ,  $Mg^{2+}$ , and  $Ca^{2+}$  (Fountoukis and Nenes, 2007), could calculate the equilibrium  $H_{air}^+$  (particle hydronium ion concentration per volume air) and ALWC with reasonable accuracy by taking water-soluble ions mass concentration, temperature, and relative humidity as input. The  $H_{air}^+$  and ALWC were then used to predict aerosol pH by the Eq. (1).

$$pH = -\log_{10} H_{aq}^+ \cong -\log_{10} \frac{1000 H_{air}^+}{ALWC_i} \quad (1)$$

Where  $H_{aq}^+$  (mole  $L^{-1}$ ) is the hydronium ion concentration in the ambient particle liquid water.  $H_{aq}^+$  can also be deemed to be the  $H_{air}^+$  ( $\mu g m^{-3}$ ) divided by the concentration of ALWC associated with inorganic species,  $ALWC_i$  ( $\mu g m^{-3}$ ). Both inorganic and part of organic species in particles are hygroscopic. However, the pH prediction is not highly sensitive to the water uptake by organic species ( $ALWC_o$ ), unless the  $ALWC_o$  mass fraction to the total particle water is close to 1 (Guo et al., 2015, 2016). And the similar result was also found in Beijing in Liu et al. (2017). Hence the aerosol pH could be fairly predicted by ISORROPIA-II with just measurements of inorganic species in most cases. However, it should be noted that the potential error could be incurred by ignoring  $ALWC_o$  in regions where hygroscopic organic species has a relatively high contribution to fine particles.

带格式的: 两端对齐

229 In ISORROPIA-II, forward and reverse mode are provided to predict ALWC and  $H_{air}^+$ . In forward  
230 mode, ~~known quantities are~~ T, RH, and the total (i.e. gas+aerosol) concentrations of  $NH_3$ ,  $H_2SO_4$ ,  
231  $HCl$ , and  $HNO_3$ ; ~~need to be input~~. Reverse mode calculates the equilibrium partitioning given the  
232 ~~concentration~~ concentrations of only aerosol ~~composition~~ compositions together with RH and T as  
233 input. In this work, the online ion chromatography MARGA was used to measure both inorganic  
234 ions of  $PM_{2.5}$  and precursor gases. ~~Moreover, several studies had shown that the ion balance and~~  
235 ~~reverse-mode calculations of thermodynamic equilibrium models were not applicable to interpret~~  
236 ~~the aerosol acidity (Hennigan et al., 2015; Liu et al. 2017; Song et al., 2018), hence ISORROPIA-~~  
237 ~~II was run in the “forward mode” for aerosols in metastable condition. Moreover, the forward mode~~  
238 ~~was~~ The forward mode was also reported less sensitive to measurement error than the reverse mode  
239 (Hennigan et al., 2015; Song et al., 2018). ~~Hence, ISORROPIA-II was run in the “forward mode”~~  
240 ~~for aerosols in the metastable condition in this study.~~

241 When using ISORROPIA-II to calculate the  $PM_{2.5}$  acidity, all particles were assumed internally  
242 mixed and the bulk properties were used, without considering the variability of chemical  
243 compositions with particle size. In the ambient atmosphere, the aerosol chemical composition is  
244 complicated, hence the deliquescent relative humidity of aerosol is generally low (Seinfeld and  
245 Pandis, 2016) and the particles usually exist in the form of droplets, which makes the assumption  
246 that the particles are in a liquid state (metastable condition) reasonable. However, when the particles  
247 are exposed to a quite low RH, the state of particles may change. Figure 2 and Figure S1-S4 exhibit  
248 the comparisons between predicted and measured  $NH_3$ ,  $HNO_3$ ,  $HCl$ ,  $NH_4^+$ ,  $NO_3^-$ ,  $Cl^-$ ,  $\epsilon(NH_4^+)$   
249  $(NH_4^+/(NH_3+NH_4^+), \text{ mol/mol})$ ,  $\epsilon(NO_3^-)$  ( $NO_3^-/(HNO_3+NO_3^-), \text{ mol/mol}$ ), and  $\epsilon(Cl^-)$  ( $Cl^-/(HCl+Cl^-)$ ,  
250 mol/mol) based on real-time ion chromatography data, which are all colored by the corresponding  
251 RH. It can be seen that agreements between predicted and measured  $NH_3$ ,  $NH_4^+$ ,  $NO_3^-$ , and  $Cl^-$  are  
252 pretty well, the  $R^2$  of linear regressions are all higher than 0.94, and the slopes are around 1.  
253 Moreover, the agreement between predicted and measured  $\epsilon(NH_4^+)$  is better when compared with  
254  $\epsilon(NO_3^-)$  and  $\epsilon(Cl^-)$ . The slope of linear regression between predicted and measured  $\epsilon(NH_4^+)$  was  
255 0.93, 0.91, 0.95, and 0.96 and the  $R^2$  is 0.87, 0.93, 0.89, and 0.97 in spring, winter, summer, and  
256 autumn, respectively. However, measured and predicted partitioning of  $HNO_3$  and  $HCl$  show  
257 significant discrepancies ( $R^2$  of 0.28 and 0.18), which may attribute to the much lower gas

258 concentrations compared with the particle concentrations, as well as the gas denuder measurement  
259 uncertainties from particle collection artifacts (Guo et al., 2018). Obviously, more scatter points  
260 deviate from the 1:1 line when ISORROPIA-II runs at  $RH < 30\%$ , which is much evident in winter  
261 and spring. For data with  $RH \leq 30\%$ , the predictions are significantly improved when assuming  
262 aerosol in stable mode (solid + liquid) (Figure S5-S6). However, the aerosol liquid water was almost  
263 zero and cannot be used to predict aerosol pH. It reveals that it is not reasonable to predict the  
264 aerosol pH using the thermodynamic model when the RH is relatively low. Consequently, we only  
265 discussed the  $PM_{2.5}$  pH for data with RH higher than 30% in this work.

### 266 **Figure 2**

267 Running ISORROPIA-II in the forward mode with only aerosol concentrations as input may  
268 result in a bias in predicted pH due to repartitioning of ammonia in the model, leading to a lower  
269 predicted pH when gas-phase data are not available (Hennigan et al., 2015). In this work, since no  
270  $NH_3(g)$  gas phase was available for the size-resolved pH prediction. We determined aerosol pH in the  
271 fine mode through an iteration procedure that used the measured particulate species and  
272 ISORROPIA-II to predict gas species, the detailed information could be found in Fang et al. (2017)  
273 and Guo et al. (2017, 2016). As for coarse mode particles, equilibrium is not considered between the  
274 gas and particles a brief summary, due to kinetic limitations (Dassios et al., 1999; Cruz et al., 2000),  
275 the pH was determined by ignoring the gas phase and ISORROPIA-II was run in forward mode  
276 with zero gas predicted  $NH_3$ ,  $HNO_3$ , and  $HCl$  concentrations— from the  $i-1$  run were applied to the  
277  $i$ th iteration, until the gas concentrations converged. Based on these iterative gas phase  
278 concentrations, the ion concentrations from samples collected by the MOUDI as well as the  
279 averaged RH and T during each sampling period were used to determine aerosol pH for different  
280 size ranges. Just like calculating the pH of  $PM_{2.5}$ , it was also assumed that all the particles at each  
281 size bin were internally mixed and had the same pH.

282 The comparisons of iterative and predicted  $NH_3$ ,  $HNO_3$ , and  $HCl$  as well as measured and  
283 predicted  $NO_3^-$ ,  $NH_4^+$ ,  $Cl^-$ ,  $\epsilon(NH_4^+)$ ,  $\epsilon(NO_3^-)$ , and  $\epsilon(Cl^-)$  for data from MOUDI samples are  
284 showed in Figure 3. The previous study showed that coarse mode particles were very difficult to  
285 reach equilibrium with the gaseous precursors due to kinetic limitations (Dassios et al., 1999; Cruz  
286 et al., 2000). The accuracy of the aerosol pH prediction is primarily assessed by the reproduction of

semivolatile components partitioning between gas and particle phases. A comparison between predicted  $\text{NO}_3^-$ ,  $\text{NH}_4^+$  and measured values colored by RH is shown in Figure 2. Overall, the model captures the measured  $\text{NO}_3^-$ ,  $\text{NH}_4^+$ , and the predicted  $\text{NO}_3^-$ ,  $\text{NH}_4^+$  are on average within  $\pm 20\%$  of the measurements, with  $R^2 > 0.9$ , and best agreement is observed at RH above 60%.

). Assuming coarse mode particles in equilibrium with the gas phase could result in a large bias between measured and predicted  $\text{NO}_3^-$  and  $\text{NH}_4^+$  in coarse mode particles (Fang et al, 2017). We also find that in this work, it can be clearly seen that assuming coarse mode particles in equilibrium with the gas phase could overpredict  $\text{NO}_3^-$  and  $\text{Cl}^-$  and underestimate  $\text{NH}_4^+$  in the coarse mode (the blue scatters), which could subsequently underestimate the coarse mode aerosol pH. Compared with the coarse mode particles, the measured and predicted  $\text{NO}_3^-$ ,  $\text{NH}_4^+$ , and  $\text{Cl}^-$  agreed very well in fine mode particles. Considering the kinetic limitations and nonideal gas-particle partitioning in coarse mode particles, the aerosol pH in coarse mode was determined by ignoring the gas phase.

**Figure 4-3**

带格式的: 缩进: 首行缩进: 0 字符

## **2.5 Sensitivities of aerosol pH to $\text{SO}_4^{2-}$ , $\text{NO}_3^-$ , $\text{NH}_4^+$ , $\text{Cl}^-$ , RH, and T**

In the real ambient air, the thermodynamic process of the aerosol is complicated, it is not easy to tell the effect of one factor on the aerosol pH. The ALWC,  $H_{\text{air}}^+$ , aerosol pH,  $\epsilon(\text{NH}_4^+)$ ,  $\epsilon(\text{NO}_3^-)$ , and  $\epsilon(\text{Cl}^-)$  are all the output of ISORROPIA-II. Together, they reflect an objective state of particles. Considering the relative independence between input parameters, it is reasonable to discuss the influence of input variables on output parameters with the results of ISORROPIA-II. Thus, in this paper, we focus on the sensitivity analysis of single-factor variation, which can reflect the variation tendency of aerosol pH caused by the change of each variable.

In the ISORROPIA-II, the input parameters include  $\text{SO}_4^{\text{T}}$  (total sulfate (gas+aerosol) expressed as equivalent  $\text{H}_2\text{SO}_4$ ),  $\text{NO}_3^{\text{T}}$  (total nitrate (gas+aerosol) expressed as equivalent  $\text{HNO}_3$ ),  $\text{NH}_4^{\text{T}}$  (total ammonium (gas+aerosol) expressed as equivalent  $\text{NH}_3$ ),  $\text{Cl}^{\text{T}}$  (total chloride (gas+aerosol) expressed as equivalent  $\text{HCl}$ ),  $\text{Na}^+$ ,  $\text{Ca}^{2+}$ ,  $\text{K}^+$ ,  $\text{Mg}^{2+}$ , RH, and T. After running, the gas and aerosol phase of  $\text{NO}_3^{\text{T}}$ ,  $\text{NH}_4^{\text{T}}$ , and  $\text{Cl}^{\text{T}}$  would be reappportioned and output. In view of this, it is more reasonable to analyze the impact of  $\text{NO}_3^{\text{T}}$ ,  $\text{NH}_4^{\text{T}}$ , and  $\text{Cl}^{\text{T}}$  on aerosol pH, rather than the impact of a single gas or



316 aerosol phase of  $\text{NO}_3^-$ ,  $\text{NH}_4^+$ , and  $\text{Cl}^-$  on aerosol pH. In addition, the mass concentration of  $\text{K}^+$  and  
317  $\text{Mg}^{2+}$  was low, so the variables in the sensitivity analysis were determined as  $\text{SO}_4^{2-}$ ,  $\text{NO}_3^-$ ,  $\text{NH}_4^+$ ,  
318  $\text{Cl}^-$ ,  $\text{Ca}^{2+}$ , RH, and T. When assessing how a variable affects ALWC,  $\text{H}_{\text{air}}^+$ , and aerosol pH, the real-  
319 time measured values of this variable and the averaged values of other variables in each season were  
320 input ISORROPIA-II. The magnitude of the relative standard deviation (RSD) of calculated aerosol  
321 pH can reflect the impact of one variable on the aerosol acidity. The higher the RSD, the greater the  
322 impact, vice versa. The average value and variation range for each variable in all four seasons are  
323 listed in Table S1 and Figure S7.

324 The sensitivity analysis in this work aimed at the  $\text{PM}_{2.5}$  (*ie* fine particles) because the  $\text{PM}_{2.5}$   
325 components in four seasons were available and had a high temporal resolution (1h). In addition, the  
326 data set had a wide range, covering different levels of haze events. Noted that the sensitivity analysis  
327 in this work only reflected the characteristics during the observation periods, further work is needed  
328 to determine whether the sensitivity analysis is valid in other environments.

### 329 3. Results and Discussion

#### 330 3.1 Overall summary of aerosol $\text{PM}_{2.5}$ pH over four seasons

331 The averaged  $\text{PM}_{2.5}$  concentration is concentrations were  $62 \pm 36$ ,  $60 \pm 69$ ,  $39 \pm 24$ , and  $59 \pm 48$   $\mu\text{g m}^{-3}$   
332 in for observation periods of spring, winter, summer, and autumn observation, respectively. (Table  
333 1). Among all ions measured,  $\text{NO}_3^-$ ,  $\text{SO}_4^{2-}$ , and  $\text{NH}_4^+$  were three dominant species, accounting  
334 for 83% ~ 87% of total ions. Compared with other seasons, the averaged concentration of primary  
335 inorganic ions ( $\text{Cl}^-$ ,  $\text{Na}^+$ ,  $\text{K}^+$ ,  $\text{Mg}^{2+}$ ,  $\text{Ca}^{2+}$ ) was higher in spring. The aerosol in Beijing showed the  
336 moderate acidity with aerosol  $\text{PM}_{2.5}$  pH was of  $4.30 \pm 1.60$ ,  $4.5 \pm 0.7$ ,  $3.8 \pm 1.1$ ,  $3.9 \pm 1.32$ , and  $4.1 \pm 1.3 \pm 0$   
337 in 8 for spring, winter, summer, and autumn observation, respectively. (data at RH  $\leq 30\%$  were  
338 excluded). The overall winter aerosol  $\text{PM}_{2.5}$  pH is was comparable to the result found in Beijing ( $4.2$ ,  
339 winter) from Liu et al. (2017) and  $4.5$  from Guo et al. (2017), but lower than that ( $4.9$ , winter  
340 and spring) in Tianjin (Shi et al., 2017), another mega city about 120 km away from Beijing. The  
341 summer aerosol  $\text{PM}_{2.5}$  pH was lowest among all four seasons, implying the higher aerosol acidity.  
342 The seasonal variation of aerosol  $\text{PM}_{2.5}$  pH in this work was similar to the result from Tan et al.  
343 (2018) except for spring, which was winter ( $4.11 \pm 1.37$ ) > autumn ( $3.13 \pm 1.20$ ) > spring ( $2.12 \pm$   
344  $0.72$ ) > summer ( $1.82 \pm 0.53$ ). Noted that the observation in Tan et al. (2018) was conducted in 2014

345 of Beijing in 2014, the distinction in the aerosol composition may be compositions was probably  
346 responsible for the lower aerosol  $PM_{2.5}$  pH in their work.

347 The acid-liquid surface has a catalytic effect on the gas-liquid reaction process, and the presence  
348 of the oxidant can significantly increase the reaction rate and promote the formation of secondary  
349 aerosols (Liu et al., 2012). How the moderate acidity of aerosol in the North China Plain affect the  
350 formation of secondary aerosols needs to be further investigated.

### 351 **Figure 2**

352 Wind dependence of  $PM_{2.5}$ ,  $NO_3^-$ ,  $SO_4^{2-}$ ,  $NH_4^+$ ,  $Ca^{2+}$  concentration and the averaged pH are shown  
353 in Figure 3 and Fig. S1. In spring and summer, the high aerosol pH occurs with both NW and SW  
354 strong winds (wind speed  $>3 \text{ m s}^{-1}$ ) while the low aerosol pH occurs with calm winds (wind speed  
355  $<2 \text{ m s}^{-1}$ ) and SW winds with wind speed lower than  $3 \text{ m s}^{-1}$ . For winter, we surprisingly found that  
356 the high aerosol pH is mainly concentrated in the SSW direction, while the aerosol pH in northerly  
357 winds is as low as 3–4. In autumn, the aerosol pH accompanied by NW winds is much higher than  
358 that accompanied by souther winds. Generally, the northerly winds usually occur with cold front  
359 systems and high wind speeds, which could sweep away air pollutants but raise dust in which the  
360 crustal species ( $Ca^{2+}$ ,  $Mg^{2+}$ ) content are higher.

361 Haze episodes usually occur with SW and SE winds and calm winds in Beijing, the air pollutants  
362 are transported to Beijing from other cities located in SW and SE directions, leading to the  
363 accumulation of pollutants. Beijing is surrounded by mountains on three sides, and south Beijing  
364 is plain. The industry is mainly concentrated in the south of Beijing, and there are plenty of  
365 emission sources in these two major transport pathways from southwest and southeast directions,  
366 leading to the higher  $PM_{2.5}$  concentration. We find that the aerosol pH is negatively correlated  
367 with  $PM_{2.5}$  concentration in spring, summer, and autumn whereas it shows the positive  
368 relationship in winter. **Table 1**,

369 To further investigate the aerosol  $PM_{2.5}$  pH performance under different pollution level levels over  
370 four seasons, the  $PM_{2.5}$  concentration is concentrations were classified into three groups with  $0\sim75$   
371  $\mu\text{g m}^{-3}$ ,  $75\sim150 \mu\text{g m}^{-3}$ , and  $>150 \mu\text{g m}^{-3}$ , representing the clean, polluted, and heavily polluted  
372 days conditions, respectively. Overall, as the air quality deteriorates, ALWC and  $H_{\text{mic}}^+$  all increased,  
373 but the aerosol acidity performs differently. In spring, summer, and autumn, the pH on The

带格式的: 居中, 缩进: 首行缩进: 0 字符

带格式的: 字体: 加粗

374 relationship between  $PM_{2.5}$  and its pH is shown in Figure S8. The  $PM_{2.5}$  pH under clean days  
375 is condition spanned 2~7 while the  $PM_{2.5}$  pH under polluted and heavily polluted conditions mostly  
376 concentrated in 3~5. Table 1 shows that as the air quality deteriorated, aerosol components, as well  
377 as ALWC and  $H_{air}^+$ , all increased for each season, but the differences in  $PM_{2.5}$  pH for three pollution  
378 levels were not statistically significant. In terms of the averaged values, the  $PM_{2.5}$  pH under the  
379 clean condition was the highest (Table 1), then followed by polluted days and heavily polluted  
380 days conditions in spring, summer, and autumn. In winter, however, the averaged pH on under  
381 polluted days (5 condition) ( $4.8 \pm 1.0$ ) is was the highest, then followed by clean ( $4.5 \pm 0.6$ ) and heavily  
382 polluted days conditions ( $4.4 \pm 0.9$ ) and clean days (7).

383 Time series of mass fraction of  $NO_3^-$ ,  $SO_4^{2-}$ ,  $NH_4^+$ ,  $Cl^-$ , and crustal ions ( $Mg^{2+}$  and  $Ca^{2+}$ ) in total  
384 ions, as well as pH in all four seasons, are showed in Figure 4.3 ( $\pm 1.1$ ). It can be seen that on clean  
385 days, high  $PM_{2.5}$  pH ( $>6$ ) was generally companied by high mass fraction of crustal ions, while the  
386 relatively low  $PM_{2.5}$  pH ( $<3$ ) was companied by high mass fraction of  $SO_4^{2-}$  and low mass fraction  
387 of crustal ion, which was most obvious in summer (large part of  $PM_{2.5}$  pH with  $RH < 30\%$  were  
388 excluded in spring and winter). On polluted and heavily polluted days, the aerosol chemical  
389 composition was similar, mainly dominated by  $NO_3^-$ , hence the differences of  $PM_{2.5}$  pH on polluted  
390 and heavily polluted days were small. Compared with the mass concentration of  $PM_{2.5}$ , the different  
391 aerosol chemical compositions might be the essence that drove aerosol acidity. The impact of  
392 aerosol compositions on  $PM_{2.5}$  pH is discussed in Section 3.4.

393  
394 **Figure 34**

395 **Table 1**

396  
397  
398 Beijing is surrounded by mountains on three sides. Haze episodes usually occur with southwest  
399 and southeast winds as well as calm winds in Beijing. The industry is mainly concentrated in the  
400 south of Beijing, leading to the higher  $PM_{2.5}$  concentration in Beijing by the regional transport and  
401 accumulation. Wind dependence of  $PM_{2.5}$ ,  $NO_3^-$ ,  $SO_4^{2-}$ ,  $NH_4^+$  and the averaged  $PM_{2.5}$  pH are shown  
402 in Figure 5 and Figure S9. In spring, summer, and autumn, the  $PM_{2.5}$  pH in northern direction were

带格式的

带格式的: 无孤行控制

带格式的

generally higher than that in the southwest direction, but the high pH in summer also occurred with southwest strong winds (wind speed  $>3 \text{ m s}^{-1}$ ). Generally, the northerly winds usually occur with cold front systems, which could sweep away air pollutants but raised dust in which the crustal ion species ( $\text{Ca}^{2+}$ ,  $\text{Mg}^{2+}$ ) were higher. In winter, the  $\text{PM}_{2.5}$  pH distributed relatively evenly in each wind direction, but we surprisingly found that the pH in northerly winds is as low as 3–4, which was consistent with the high mass fraction of  $\text{SO}_4^{2-}$  on the clean days caused by the northerly winds.

Figure 5

### 3.2 Diurnal variation of aerosol pH, ALWC, and $\text{H}_{\text{air}}^{+}$ , and $\text{PM}_{2.5}$ pH

The diurnal variation for variations of  $\text{NO}_3^-$ ,  $\text{SO}_4^{2-}$ , ALWC is similar over four seasons, but distinctions are found in  $\text{H}_{\text{air}}^{+}$  and  $\text{pH-PM}_{2.5}$  pH are exhibited in Figure 6. The diurnal variations (Figure 4) for ALWC,  $\text{H}_{\text{air}}^{+}$ , and pH was similar over four seasons. Generally, nighttime mean ALWC is higher than daytime and reached a peak at near 04:00 ~ 06:00 (local time). After sunrise, the increasing temperatures resulted in a rapid drop in RH, leading to the obvious loss of particle water, ALWC reached the lowest level in the afternoon. For spring, summer, and autumn, the significant  $\text{H}_{\text{air}}^{+}$  peak starting at roughly 12:00 and reaching a maximum between 16:00 and 18:00, the  $\text{H}_{\text{air}}^{+}$  was highest in the afternoon and then followed by nighttime, and  $\text{H}_{\text{air}}^{+}$  was relatively low in the forenoon. The low ALWC and high  $\text{H}_{\text{air}}^{+}$  resulted in the minimum pH in the afternoon. The averaged nighttime pH is 0.3–0.4 unit higher than that on daytime for spring, summer, and autumn, respectively. However, for winter,  $\text{H}_{\text{air}}^{+}$  in the nighttime is slightly higher than that in the daytime, and the aerosol pH is relatively low at night and higher at sunset. Noted that the diurnal variation variations of aerosol  $\text{PM}_{2.5}$  pH is all consistent there were for the cases with RH higher than 30%. If the data at  $\text{RH} < 30\%$  were included, the diurnal variation variations of  $\text{H}_{\text{air}}^{+}$ , pH, and  $\text{SO}_4^{2-}$  over four seasons, it seems that the in winter were changed (Figure S10).  $\text{H}_{\text{air}}^{+}$  and  $\text{SO}_4^{2-}$  is were both higher at nighttime since the nocturnal boundary layer height was generally low in winter and easily resulted in the accumulation of  $\text{SO}_4^{2-}$ , hence leading to a key factor affecting aerosol lower pH at the night.

Figure 4

The distinguishing diurnal patterns of aerosol pH over four seasons indicate that aerosol

带格式的: 字体: Times New Roman

带格式的: 字体: Times New Roman

带格式的: 字体: Times-Roman

带格式的: 字体: Times-Roman

带格式的: 字体: Times-Roman

带格式的: 上标

带格式的: 字体: Times New Roman

带格式的: 字体: Times New Roman

带格式的: 字体: Times New Roman

composition is a key factor for the diurnal variation of aerosol pH, which is very different from what Guo et al. (2015) found in the southeastern United States: the pH diurnal variation is largely driven by meteorological conditions due to the dilution of ALWC to  $H_{\text{air}}^+$ , not aerosol composition. The biggest reason for the discrepancy is that the hygroscopic components in particles such as  $(\text{NH}_4)_2\text{SO}_4$  and  $\text{NH}_4\text{NO}_3$  in Beijing are much higher than that in the southeastern United States (lower than  $5 \mu\text{g m}^{-3}$ ) while the mean RH is lower. Thus the influence of aerosol composition on pH cannot be ignored in Beijing.

**3.3** The diurnal variation of  $\text{NO}_3^-$  in winter and spring agreed well with the aerosol acidity. Nevertheless, in summer and autumn, the agreement was not well. Figure S11 shows the relationship between mass concentrations of  $\text{SO}_4^{2-}$  and  $\text{NO}_3^-$  and  $\text{PM}_{2.5}$  pH at different ALWC levels for all four seasons. At the relatively low ALWC, the increasing  $\text{SO}_4^{2-}$  could decrease the pH obviously; at the relatively high ALWC, the negative correlation still existed between  $\text{SO}_4^{2-}$  mass concentration and  $\text{PM}_{2.5}$  pH. On the contrary, a weak positive correlation was found between  $\text{NO}_3^-$  and pH at the relatively low ALWC and the  $\text{PM}_{2.5}$  pH was almost invariable with the  $\text{NO}_3^-$  mass concentration at the relatively high ALWC. Compared with the  $\text{NO}_3^-$ , the  $\text{SO}_4^{2-}$  had a greater effect on  $\text{PM}_{2.5}$  pH. When the ALWC was high enough (for example, higher than  $100 \mu\text{g m}^{-3}$ ), the impact of dilution of ALWC to the  $H_{\text{air}}^+$  was more significant.

### Figure 6

Guo et al. (2015) found that the ALWC diurnal variation was significant, and the diurnal pattern in pH was mainly driven by particle water dilution. However, in this work, both  $H_{\text{air}}^+$  and ALWC had significant diurnal variations, and the aerosol acidity variation agreed well with sulfate, indicating the aerosol acidity in NCP was both driven by aerosol composition and particle water. For example, in the winter of NCP, the  $\text{PM}_{2.5}$  mass concentration in Beijing was several to dozens times higher than that in the US, which means there are more seeds in the limited particle water, and the RH was generally low, hence the dilution of aerosol liquid water to  $H_{\text{air}}^+$  doesn't work at all, the diurnal variation of aerosol components was more important.

### 3.3 Gas-particle separation

Table 2 exhibits the measured  $\epsilon(\text{NH}_4^+)$ ,  $\epsilon(\text{NO}_3^-)$ , and  $\epsilon(\text{Cl}^-)$  at different RH levels. The measured

460  $\epsilon(\text{NH}_4^+)$ ,  $\epsilon(\text{NO}_3^-)$ , and  $\epsilon(\text{Cl}^-)$  increased with the elevated RH in all four seasons, indicating more  
461  $\text{NH}_4^+$ ,  $\text{NO}_3^-$ , and  $\text{Cl}^-$  were partitioned into particle phase at higher RH. In winter and spring,  $\text{NO}_3^-$   
462 and  $\text{Cl}^-$  were dominated by particle phases,  $\epsilon(\text{NO}_3^-)$  and  $\epsilon(\text{Cl}^-)$  was higher than 65%. Whereas in  
463 summer and autumn, the lower RH generally accompanied by higher ambient temperature, more than  
464 half of the  $\text{NO}_3^-$  and  $\text{Cl}^-$  were partitioned into the gaseous phase. When the RH reached above 60%,  
465 more than 90% of  $\text{NO}_3^-$  and 70% of  $\text{Cl}^-$  were in the particle phase for all four seasons. Compared  
466 with  $\epsilon(\text{NO}_3^-)$  and  $\epsilon(\text{Cl}^-)$ , the  $\epsilon(\text{NH}_4^+)$  was pretty lower. In spring, summer, and autumn, the average  
467  $\epsilon(\text{NH}_4^+)$  was still lower than 0.3 even when the RH >60%, which might attribute to the higher  $\text{NH}_3$   
468 mass concentration in the atmosphere. The averaged  $\text{NH}_3$  was  $21.5 \pm 8.7 \mu\text{g m}^{-3}$ ,  $19.6 \pm 6.4 \mu\text{g m}^{-3}$ ,  
469 and  $16.8 \pm 8.0 \mu\text{g m}^{-3}$  in spring, summer, and autumn, respectively. In winter, the average  $\epsilon(\text{NH}_4^+)$   
470 were much higher than that in other seasons with the relatively lower  $\text{NH}_3$  mass concentration  
471 ( $4.9 \pm 2.8 \mu\text{g m}^{-3}$ ).

472 **Table 2.**

473 **3.4 Factors affecting ALWC,  $\text{H}_{\text{air}}^+$  and aerosol pH<sup>+</sup>,  $\text{PM}_{2.5}$  pH, and gas-particle partitioning**

474 As mentioned above, the aerosol chemical composition has a non-negligible effect on  
475 aerosol  $\text{PM}_{2.5}$  pH. In this work, the effects of aerosol chemical components ( $\text{NO}_3^-$ ,  $\text{SO}_4^{2-}$ ,  $\text{NH}_4^+$ ,  $\text{SO}_4^{2-}$ ,  
476  $\text{NO}_3^-$ ,  $\text{NH}_4^+$ ,  $\text{Cl}^-$ ,  $\text{Ca}^{2+}$ ) and precursor gases ( $\text{NH}_3$ ,  $\text{HNO}_3$ ), as well as meteorological parameters  
477 ( $\text{RH}$ ,  $T$ ), RH, and T on aerosol  $\text{PM}_{2.5}$  pH were performed through a sensitivity analysis over four  
478 seasons. When assessing how a factor affects aerosol acidity, ALWC, or  $\text{H}_{\text{air}}^+$ , the real-time  
479 measured values of an evaluated factor and the averaged values for other factors in

带格式的: 默认段落字体, 字体: +西文正文 (等线)

480 As shown in Table 3, for ALWC, the largest relative standard deviation (RSD) was observed  
481 when RH was taken as the evaluated factor, then followed by  $\text{SO}_4^{2-}$  or  $\text{NO}_3^-$ , which means the RH  
482 had the greatest influence on ALWC, and  $\text{SO}_4^{2-}$  and  $\text{NO}_3^-$  were major hygroscopic components in  
483 the aerosol. The  $\text{SO}_4^{2-}$ , RH,  $\text{NO}_3^-$ , and  $\text{NH}_4^+$  were all important influential factors for  $\text{H}_{\text{air}}^+$ ,  
484 especially  $\text{SO}_4^{2-}$ . The  $\text{SO}_4^{2-}$  and T were two crucial factors affecting the  $\text{PM}_{2.5}$  pH variation. The  
485  $\text{PM}_{2.5}$  pH was also sensitive to  $\text{NH}_4^+$  when it was in a lower range and sensitive to RH only in  
486 summer. The relationship between pH and  $\text{NH}_4^+$  was nonlinear, the impact of  $\text{NH}_4^+$  on pH weakened  
487 as  $\text{NH}_4^+$  increased. In spring, the crucial factor for the  $\text{PM}_{2.5}$  pH variation was  $\text{SO}_4^{2-}$  while it was  
488  $\text{SO}_4^{2-}$  and  $\text{NH}_4^+$  in winter. In summer, the most important factor affecting  $\text{PM}_{2.5}$  pH was RH, then

带格式的: 字体: Times-Roman

489 followed by  $\text{NH}_4^+$  and  $\text{SO}_4^{2-}$ . In autumn, the effect of  $\text{NH}_4^+$  on  $\text{PM}_{2.5}$  pH was considerable,  $\text{SO}_4^{2-}$   
490 and T were also important. Figure 7-9 and S12-S17 show how these factors affecting the ALWC,  
491  $\text{H}_{\text{air}}^+$ , and aerosol acidity over four seasons. The sensitivity analysis for ALWC and  $\text{H}_{\text{air}}^+$  were  
492 similar over four seasons, while the sensitivity of  $\text{PM}_{2.5}$  pH to RH and  $\text{NO}_3^-$  in four seasons were  
493 different from each season are input in ISORROPIA-II. For example, the magnitude of the deviation  
494 for calculated aerosol pH can reflect the effect of an evaluated factor on the aerosol acidity. The  
495 higher the deviation, the greater the effect, vice versa. Noted other. In this study, winter and summer  
496 were chosen for a detailed discussion of sensitivity analysis because more heavy pollution episodes  
497 happened in winter while the photochemical reaction was relatively strong in summer.

498 **Table 3**

499 **Figure 7**

500 **Figure 8**

501 **Figure 9**

502  
503 **RH:** RH had a different impact on  $\text{PM}_{2.5}$  pH in different seasons. In winter, the  $\text{PM}_{2.5}$  pH  
504 decreased with the increasing RH, whereas the  $\text{PM}_{2.5}$  pH increased with the increasing RH in  
505 summer. In spring and autumn, the RH between 30~83% had little impact on  $\text{PM}_{2.5}$  pH. The  
506 explanation for this is that the sensitivity analysis in this work only reflects the  
507 characteristics; increased RH actually diluted the solution and promoted ionization, releasing  $\text{H}_{\text{air}}^+$   
508 and increasing ALWC as well, but the gradient was different. In winter, variation in  $\text{H}_{\text{air}}^+$  caused by  
509 RH changes was much larger than variation in ALWC, whereas it showed an opposite tendency in  
510 summer. In autumn and spring, variation in  $\text{H}_{\text{air}}^+$  caused by RH changes was slightly higher than the  
511 variation in ALWC. The different impact of RH on  $\text{PM}_{2.5}$  pH indicated that the dilution effect of  
512 ALWC on  $\text{H}_{\text{air}}^+$  was obvious only in summer, the high RH during the observation period, severe haze  
513 in winter could increase the aerosol acidity.

514 **T:** At high ambient temperature,  $\epsilon(\text{NH}_4^+)$ ,  $\epsilon(\text{NO}_3^-)$ , and  $\epsilon(\text{Cl}^-)$  all showed a decreased tendency  
515 (Figure 10 and S19). The procedure of  $\text{NH}_4^+ \rightarrow \text{NH}_3$  releases one  $\text{H}^+$  to particle phase, whereas the  
516 procedure of  $\text{NO}_3^- \rightarrow \text{HNO}_3$  or  $\text{Cl}^- \rightarrow \text{HCl}$  both need one  $\text{H}^+$  from the particle phase. Compared with  
517 the loss of  $\text{NO}_3^-$  from  $\text{NH}_4\text{NO}_3$  as well as  $\text{Cl}^-$  from  $\text{NH}_4\text{Cl}$ , greater loss of  $\text{NH}_4^+$  from  $\text{NH}_4\text{NO}_3$ ,

518  $\text{NH}_4\text{Cl}$ , and  $(\text{NH}_4)_2\text{SO}_4$  resulted in a net increase in particle  $\text{H}^+$  and lower pH. In addition, the  
519 molality-based equilibrium constant ( $K^*$ ) of  $\text{NH}_3\text{-NH}_4^+$  partitioning decreased faster with  
520 increasing temperature when compared with that of  $\text{HNO}_3\text{-NO}_3^-$  partitioning, resulting in a net  
521 increase in particle  $\text{H}^+$  (Guo et al., 2018). Moreover, higher ambient temperature tends to lower  
522 ALWC, which further work is needed to determine whether the sensitivity analysis is valid in other  
523 environments. And decreases the  $\text{PM}_{2.5}$  pH. The wide range of ambient temperature in autumn made  
524 a significant impact on  $\text{PM}_{2.5}$  pH in the sensitivity analysis in this paper only focused on single  
525 factor variations, however, in reality, changes in one factor could alter other factors and made it  
526 more complicated.

#### 527 **Figure 10**

528 As show in Table 2, for ALWC, the largest deviation is observed when RH is taken as the  
529 evaluated factor, then followed by  $\text{SO}_4^{2-}$  and  $\text{NO}_3^-$  ( $\text{NO}_3^-$  and  $\text{SO}_4^{2-}$  in autumn), which means that the  
530 RH affect ALWC most and  $\text{SO}_4^{2-}$  and  $\text{NO}_3^-$  are major hygroscopic components in the aerosol.  $\text{SO}_4^{2-}$   
531 is the most influential factor for  $\text{H}_{\text{aif}}^+$ , and RH,  $\text{NO}_3^-$ , and  $\text{NH}_3$  are also important factors affecting  
532  $\text{H}_{\text{aif}}^+$ . Synthetically,  $\text{SO}_4^{2-}$  and RH are two crucial factors affecting aerosol pH. For spring, winter  
533 and autumn, the effect of  $\text{SO}_4^{2-}$  on aerosol pH is greater than the RH, and it is comparable with RH  
534 in summer. Figure 4-6 and S2-S7 show how these factors affecting the aerosol acidity, ALWC and  
535  $\text{H}_{\text{aif}}^+$  in detail over four seasons. The sensitivity analysis for ALWC and  $\text{H}_{\text{aif}}^+$  are similar over four  
536 seasons, while the sensitivity analysis of RH on aerosol pH in summer is different from the other  
537 three seasons. In this study, the sensitivity analysis in winter and summer are chosen for detailed  
538 description since winter is of a lot of concern due to the poor air quality while the photochemical  
539 reactions are strongest in summer.

#### 540 **Table 2**

541 The positive linear relationships between  $\text{SO}_4^{2-}$ ,  $\text{NO}_3^-$ ,  $\text{HNO}_3$  concentration and ALWC as well  
542 as negative linear relationship between  $\text{Ca}^{2+}$  concentration and ALWC are observed in the sensitive  
543 analysis. Exponential relationships between RH and ALWC are observed, and the ALWC increased  
544 rapidly with increasing RH, especially when the RH higher than 80%. Elevated  $\text{NH}_4^+$  and  $\text{NH}_3$   
545 concentration could increase ALWC slightly. As for temperature, ALWC decreased with the  
546 increasing temperature nonlinearly. High temperature could affect gas-aerosol partitioning, shifts the

带格式的: 段落间距段前: 0 磅, 段后: 0 磅



547 equilibrium from  $\text{NO}_3^-$  to  $\text{HNO}_3$ , underpredicted the  $\text{NO}_3^-$  and  $\text{NH}_4^+$  concentration, thus decreasing  
548 the ALWC. In addition, the higher temperature could also decrease RH and results in low ALWC in  
549 the real atmosphere.

#### 550 **Figure 5**

551 As mentioned above,  $\text{SO}_4^{2-}$  and RH are the most important factors on  $\text{H}_{\text{air}}^+$ . An exponential  
552 growth of  $\text{H}_{\text{air}}^+$  with elevated  $\text{SO}_4^{2-}$ , RH,  $\text{NO}_3^-$ , and T are found, whereas an exponential decrease  
553 of  $\text{H}_{\text{air}}^+$  with elevated  $\text{NH}_3$  and  $\text{NH}_4^+$  are found. Though  $\text{H}_{\text{air}}^+$  concentration decreased linearly with  
554 the augment of  $\text{Ca}^{2+}$  concentration,  $\text{Ca}^{2+}$  concentration is generally lower than  $3 \mu\text{g m}^{-3}$  and generates  
555 a little variation in  $\text{H}_{\text{air}}^+$  compared to other factors. It should be noted that a “U” shape between  $\text{NO}_3^-$   
556 and  $\text{H}_{\text{air}}^+$  are found in spring (Fig.S2),  $\text{H}_{\text{air}}^+$  drops with the increasing  $\text{NO}_3^-$  concentration within  $20$   
557  $\mu\text{g m}^{-3}$  and then starts to grow with the increasing  $\text{NO}_3^-$  concentration. The addition of  $\text{NH}_3$  or  $\text{NH}_4^+$   
558 has a much more obvious effect on  $\text{H}_{\text{air}}^+$  than ALWC. The higher the  $\text{NH}_3$  concentration in the  
559 atmosphere, the more  $\text{NH}_3$  will dissolve in the aerosol liquid water and balance the  $\text{H}_{\text{air}}^+$  partially.  
560 Increasing temperature or RH alone will increase  $\text{H}_{\text{air}}^+$  when other influencing factors were fixed,  
561 which is consistent over four seasons.

#### 562 **Figure 6**

563 The effects of all these factors on aerosol pH is actually a superposition of the effects on ALWC  
564 and  $\text{H}_{\text{air}}^+$ . Synthetically, the effect of chemical components ( $\text{NO}_3^-$ ,  $\text{SO}_4^{2-}$ ,  $\text{NH}_4^+$ ,  $\text{Ca}^{2+}$ ) and precursor  
565 gases ( $\text{NH}_3$ ,  $\text{HNO}_3$ ), as well as meteorological parameters (RH, T) on aerosol pH is shown in Figure  
566 7. The most important influencing factor on aerosol acidity is  $\text{SO}_4^{2-}$ . The aerosol pH decreases about  
567 2.8 (5 to 2.2), 6.0 (6 to 0), 1.0 (3.8 to 2.8), and 1.1 (4 to 2.9) unit with  $\text{SO}_4^{2-}$  concentration goes  $\text{SO}_4^{2-}$ ;  
568  $\text{SO}_4^{2-}$  had a key role in aerosol acidity, especially in winter and spring (Figure 9, S14, S17). In the  
569 sensitivity test, the  $\text{PM}_{2.5}$  pH decreased by about 1.6 (4.1 to 2.5), 4.9 (5.1 to 0.2), 1.0 (3.6 to 2.6),  
570 and 0.9 (4.0 to 3.1) unit with  $\text{SO}_4^{2-}$  concentration went up from 0 to  $40 \mu\text{g m}^{-3}$  in spring, winter,  
571 summer, and autumn, respectively. In spring and winter, the ALWC is was low, the variation of  $\text{SO}_4^{2-}$   
572 mass concentration could generate dramatic changes in aerosol pH.  $\text{H}_{\text{air}}^+$ . In section 3.1, the aerosol  
573 pH shows an obvious seasonal variation, the aerosol pH is generally low  $\text{PM}_{2.5}$  pH was lowest in

574 summer whereas highest in winter, which ~~iswas~~ consistent with the  $\text{SO}_4^{2-}$  mass fraction in total ions.  
575 The  $\text{SO}_4^{2-}$  mass fraction in total ions in summer ~~iswas~~ highest among four seasons with  
576  $32.4\% \pm 11.1\%$ , whereas it ~~iswas~~ lowest in winter with  $20.9\% \pm 4.4\%$ . ~~Similarly, the low aerosol pH~~  
577 ~~on clean days in winter also relates to the leading position of  $\text{SO}_4^{2-}$  (Table 1).~~

578  ~~$\text{NO}_3^-$ : The second important factor on aerosol acidity is RH. In the North China Plain, the severe~~  
579 ~~haze episodes usually occur with very high RH at a stable whether condition, resulting in the~~  
580 ~~considerable ALWC. In this work, except for summer, the increasing RH could reduce the aerosol~~  
581 ~~pH significantly when RH lower than  $\sim 30\%$ , and then the aerosol pH decreases slowly or keeps~~  
582 ~~almost a constant at  $\sim 4$  when the RH is between  $30\text{--}80\%$ , and the aerosol pH starts to increase with~~  
583 ~~the further increasing RH. However, the aerosol pH increases continuously  $\sim 1.5$  unit ( $2.5$  to  $4$ ) when~~  
584 ~~RH goes up from  $20\%$  to  $96\%$  in summer. The  $\text{PM}_{2.5}$  concentration is lowest in summer, while the~~  
585 ~~RH is relatively high, the high ALWC tends to dilute  $\text{H}_{\text{air}}^+$  and increase aerosol pH. The sensitivity~~  
586 ~~analysis suggests that ALWC has a different effect on aerosol pH. Impact of  $\text{NO}_3^-$  on  $\text{PM}_{2.5}$  pH was~~  
587 ~~also different, which was related to the averages of input  $\text{NH}_4^+$  in different seasons. In winter, the~~  
588 ~~dilution effect of ALWC on  $\text{H}_{\text{air}}^+$  is obvious only  $\text{PM}_{2.5}$  pH decreased with increasing  $\text{NO}_3^-$~~   
589 ~~concentration, whereas little impact was found in summer.~~

590 ~~(Figure 7~~

591 ~~Different from  $\text{SO}_4^{2-}$ , the effect of  $\text{NO}_3^-$  on aerosol pH is not always same. In winter, summer9).~~  
592 ~~In spring and autumn, the aerosol  $\text{PM}_{2.5}$  pH increases first and then starts to decrease when~~  
593  ~~$\text{NO}_3^-$  dropped with the increasing  $\text{NO}_3^-$  concentration is larger than  $\sim 30 \mu\text{g m}^{-3}$ . There seems to be~~  
594 ~~a threshold for the effect of  $\text{NO}_3^-$  on aerosol acidity. From a mathematical point of view, the (Figure~~  
595 ~~S14, S17). In winter, the  $\text{NH}_4^+$  mass concentration was relatively low. As  $\text{NO}_3^-$  increases, all  $\text{NH}_3$~~   
596 ~~could be converted into  $\text{NH}_4^+$  ( $\epsilon(\text{NH}_4^+) \approx 1$ ). However, if  $\text{HNO}_3$  continued to dissolve and released~~  
597  ~~$\text{H}_{\text{air}}^+$ , it would result in the decrease of  $\text{PM}_{2.5}$  pH. In summer, the averages of  $\text{NO}_3^-$  and  $\text{Cl}^-$  was~~  
598 ~~relatively low but the  $\text{NH}_4^+$  was excessive, the highest  $\epsilon(\text{NH}_4^+)$  was only  $0.6$  with the corresponding~~  
599 ~~highest  $\text{NO}_3^-$ . The excessive  $\text{NH}_3$  could provide continuous buffering to the increasing  $\text{NO}_3^-$ ,~~  
600 ~~together with a significant dilution of ALWC on  $\text{H}_{\text{air}}^+$ , leading to the little changes in  $\text{PM}_{2.5}$  pH. In~~  
601 ~~spring and autumn, the increasing pH with elevated  $\text{NO}_3^-$  in lower range attributed to the dilution~~

带格式的: 字体: Times New Roman

带格式的: 字体: 非加粗

带格式的: 字体: Times New Roman

602 of ALWC to  $H_{\text{air}}^+$ .  $H_{\text{air}}^+$  concentration increased exponentially with elevated  $\text{NO}_3^-/\text{NO}_3^{\text{T}}$   
603 concentration, especially at higher  $\text{NO}_3^-/\text{NO}_3^{\text{T}}$  concentrations, whereas the ALWC increase increased  
604 linearly with elevated  $\text{NO}_3^-$  concentration. When  $\text{NO}_3^-/\text{NO}_3^{\text{T}}$  concentration is less than the  
605 threshold, (Figure S12-S17), hence ALWC played a dominant role, while when the  $\text{NO}_3^-/\text{NO}_3^{\text{T}}$   
606 concentration is greater than the threshold, the  $H_{\text{air}}^+$  has a greater effect and the aerosol acidity begins  
607 to increase.

608 Moreover, was low. With the further increase of  $\text{NO}_3^{\text{T}}$ , the variation in spring, the aerosol pH  
609 increases continuously with the  $H_{\text{air}}^+$  caused by  $\text{NO}_3^{\text{T}}$  addition of  $\text{NO}_3^-$ , which is not consistent with  
610 the previous thought that addition of anion could reduce the aerosol pH. Same results are found in  
611 Guo et al. (2017): at a constant ALWC, more  $\text{NO}_3^-$  is measured at higher pH. Based on the measured  
612  $\text{NO}_3^-/2\text{SO}_4^{2-}$  ratio (mole mole<sup>-1</sup>) of this work, we find that aerosol pH is generally between 3~5  
613 when the aerosol anionic composition is dominated by nitrate ( $\text{NO}_3^-/2\text{SO}_4^{2-}>1$ ), whereas when  
614  $\text{NO}_3^-/2\text{SO}_4^{2-}<1$ , about 86% was larger than the variation in ALWC, leading to the decrease of aerosol  
615 pH is lower than 4 (Figure 8). In recent years, the average annual concentration of  $\text{SO}_4^{2-}/\text{PM}_{2.5}$  pH.  
616 Besides, the relationship between  $\text{NO}_3^{\text{T}}$  and  $\epsilon(\text{NH}_4^+)$  in Beijing decreased significantly due to the  
617 strict emission control measures for industries and power plants, in most cases  $\text{NO}_3^-$  dominates  
618 inorganic ions (Zhao et al., 2017; Huang et al., 2017; Ma et al., 2017), which may be another reason  
619 responsible for the moderately acidic aerosol.

620 Elevated  $\text{NH}_3$  and  $\text{NH}_4^+$  could reduce aerosol acidity by the sensitivity analysis showed that  
621 decreasing  $H_{\text{air}}^+$  concentration exponentially. In this work,  $\text{NH}_3$  is rich in spring ( $21.5 \pm 8.7 \mu\text{g m}^{-3}$ ),  
622 summer ( $19.6 \pm 6.4 \mu\text{g m}^{-3}$ ) and autumn ( $16.8 \pm 8.0 \mu\text{g m}^{-3}$ ), and poor in winter ( $4.9 \pm 2.8 \mu\text{g m}^{-3}$ ). The  
623 ratio of  $[\text{TA}]/2[\text{TS}]$  provides  $\text{NO}_3^{\text{T}}$  could lower the  $\epsilon(\text{NH}_4^+)$  effectively (Figure 11 and S20), which  
624 helped  $\text{NH}_3$  maintain in the gas phase.

#### 625 **Figure 11**

626  **$\text{NH}_4^{\text{T}}$ :** The relationship between  $\text{PM}_{2.5}$  pH and  $\text{NH}_4^{\text{T}}$  was nonlinear.  $\text{NH}_4^{\text{T}}$  in lower range had a  
627 significant impact on the  $\text{PM}_{2.5}$  pH (Table S2), and higher  $\text{NH}_4^{\text{T}}$  generated limited pH change  
628 (Figure 9, S14, S17). Elevated  $\text{NH}_4^{\text{T}}$  could reduce  $H_{\text{air}}^+$  exponentially and slightly increase ALWC  
629 when the other input parameters were held constant. As the  $\text{NH}_4^{\text{T}}$  increased,  $H_{\text{air}}^+$  was consumed  
630 swiftly during the dissolution of  $\text{NH}_3$  and the further reaction with  $\text{SO}_4^{2-}$ ,  $\text{NO}_3^-$ , and  $\text{Cl}^-$ . The elevated

631  $\text{NH}_4^{\text{T}}$  increased the  $\epsilon(\text{NO}_3^-)$  and  $\epsilon(\text{Cl}^-)$  when  $\text{NO}_3^{\text{T}}$  and  $\text{Cl}^{\text{T}}$  were fixed (Figure 11 and S20), which  
632 means the elevated  $\text{NH}_4^{\text{T}}$  altered the gas-particle partition and shifted more  $\text{NO}_3^{\text{T}}$  and  $\text{Cl}^{\text{T}}$  into  
633 particle phase, leading to the deliquescence of additional nitrate and chloride and an increase of  
634 ALWC. It seems that  $\text{NH}_3$  emission control is a good way to reduce  $\text{NO}_3^-$ . However, the relationship  
635 between  $\text{NH}_4^{\text{T}}$  and  $\epsilon(\text{NO}_3^-)$  in the sensitivity analysis (Figure 11 and S20) showed that the  $\epsilon(\text{NO}_3^-)$   
636 response to  $\text{NH}_4^{\text{T}}$  control was highly nonlinear, which means the decrease of nitrate would happen  
637 only when the  $\text{NH}_4^{\text{T}}$  was greatly reduced. The same result was also obtained from a study of Guo et  
638 al (2018).

639 The ratio of  $[\text{TA}]/2[\text{TS}]$  provides a qualitative description for the ammonia abundance, where  
640  $[\text{TA}]$  and  $[\text{TS}]$  are the total (gas + aqueous + solid) molar concentrations of ammonia and sulfate.  
641 The rich-ammonia is defined as  $[\text{TA}] > 2[\text{TS}]$ , while if the  $[\text{TA}] \leq 2[\text{TS}]$ , then it is defined as poor-  
642 ammonia (Seinfeld and Pandis, 2016). In this work, the ratio of  $[\text{TA}]/2[\text{TS}]$  is/was much higher than  
643 1 and belongs/belonged to rich-ammonia (Fig. S8). In the poor-ammonia case, there is  
644 insufficient/insufficient (Figure. S21). Although  $\text{NH}_3$  to neutralize the available sulfate, hence the aerosol will be  
645 acidic. Whereas in the rich-ammonia case there is excess ammonia, the remaining ammonia after  
646 reaction with sulfuric acid will be available to react with nitric acid to produce  $\text{NH}_4\text{NO}_3$ , so that the  
647 aerosol phase will be neutralized to a large extent. However, the moderate aerosol acidity suggests  
648 that though there is excess ammonia in the atmosphere, due NCP was abundant, the  $\text{PM}_{2.5}$  pH was  
649 far from neutral, which might attribute to the limited ALWC compared with. Compared to the cloud  
650 liquid water content in clouds and precipitation, in most cases ALWC was much lower, hence the  
651 dilution of aerosol will not be alkaline/liquid water to  $\text{H}_{\text{air}}^+$  was weak.

652 Furthermore, elevated  $\text{Ca}^{2+}$  concentration could increase the aerosol pH and the change of  $\text{HNO}_3$   
653 concentration has little effect on pH. Elevated temperature in favor of enhancement the aerosol  
654 acidity by reducing ALWC and increasing  $\text{H}_{\text{air}}^+$ .

### 655 Figure 8

656 **3.4  $\text{Cl}^{\text{T}}$ :**  $\text{Cl}^{\text{T}}$  had a relatively larger impact on the  $\text{PM}_{2.5}$  pH in winter and spring compared to  
657 summer and autumn. Except for winter, the  $\text{Cl}^{\text{T}}$  mass concentration was generally lower than  $10 \mu\text{g}$   
658  $\text{m}^{-3}$ , which accounted for the little impact on  $\text{PM}_{2.5}$  pH. On account of the low level of  $\text{Cl}^{\text{T}}$ , the

带格式的: 缩进: 首行缩进: 1 字符

带格式的: 字体: Times New Roman

带格式的: 字体: Times-Roman

659 dilution of ALWC on  $H_{air}^+$  played a dominant role, generating the  $PM_{2.5}$  pH increase with elevated  
660  $Cl^-$ . However, similar to  $NO_3^-$ , higher  $Cl^-$  could decrease the  $PM_{2.5}$  pH.  
661  $Ca^{2+}$ : In fine particles,  $Ca^{2+}$  mass concentration was generally low. In the output of ISORROPIA-  
662 II, Ca existed as  $CaSO_4$  (slightly soluble). Elevated  $Ca^{2+}$  concentration could increase the  $PM_{2.5}$  pH  
663 by decreasing  $H_{air}^+$  and ALWC (Figure S18), the decreased  $H_{air}^+$  resulted from the buffering capacity  
664 of  $Ca^{2+}$  to the acid species, while the decreased ALWC resulted from the weak water solubility of  
665  $CaSO_4$ . As discussed in Section 3.1, on clean conditions, the  $PM_{2.5}$  pH could reach 6~7 when the  
666 mass fraction of  $Ca^{2+}$  was high, hence the role of mineral ions on  $PM_{2.5}$  pH could not be ignored in  
667 seasons (such as spring) or regions where mineral dust was an important source of fine particles.  
668 Due to the strict control measures for road dust, construction sites, and other bare ground, the  
669 nonvolatile cations in  $PM_{2.5}$  decreased significantly in NCP.

670

### 671 **3.5 Size distribution of aerosol components and pH**

672 According to the average  $PM_{2.5}$  concentration during every sampling ~~period~~periods, all the  
673 samples ~~are~~were also classified into three groups (clean, polluted, heavily polluted) with the same  
674 rule described in Section 3.2.1. A severe haze episode occurred during the autumn sampling, hence  
675 there were more heavily polluted samples for autumn than that in other seasons. Figure 9.12 shows  
676 the averaged size distributions of PM components and pH on clean, polluted, and heavily polluted  
677 ~~days~~conditions in summer, autumn, and winter, respectively. The  $NO_3^-$ ,  $SO_4^{2-}$ ,  $NH_4^+$ ,  $Cl^-$ ,  $K^+$ , OC,  
678 and EC ~~were~~ mainly concentrated in the size range with aerodynamic diameters between  
679 0.32~3.1  $\mu m$ , while  $Mg^{2+}$  and  $Ca^{2+}$  ~~were~~ predominantly distributed in the coarse mode. As shown in  
680 Figure 9.12, the concentration levels for all chemical components increased with the increasing  
681 pollution. During the haze episodes, the sulfate and nitrate in the accumulated mode increased  
682 significantly. However, the increase of  $Mg^{2+}$  and  $Ca^{2+}$  in the coarse mode were not as obvious as  
683 secondary ions, mainly due to the low wind speed and calm atmosphere which ~~make~~made it more  
684 difficult to raise dust during the heavy pollution. More detailed information about size distributions  
685 of mass concentration for all analyzed species during three seasons is shown in Zhao et al. (2017)  
686 and Su et al. (2018). As mentioned in section 2.4, assuming coarse mode particles in equilibrium  
687 with the gas phase could overpredict  $NO_3^-$  and  $Cl^-$  and underestimate  $NH_4^+$  in the coarse mode

688 (Figure 3), which subsequently underestimated the coarse mode aerosol pH. Thus, the gas phase  
689 was ignored for pH calculation of the coarse particles (>3.1 μm).

#### 690 **Figure 912**

带格式的: 段落间距段前: 0 磅, 段后: 0 磅

691 The aerosol pH for both ~~accumulation~~ fine mode and coarse mode in summer ~~were~~ lowest  
692 among three seasons, then followed by autumn and winter. The seasonal variation of aerosol pH  
693 derived from MOUDI data was consistent with that derived from real-time PM<sub>2.5</sub> chemical  
694 components measurement. In summer, the predominance of sulfate in the fine mode and high  
695 ambient temperature resulted in a low pH, ranging between 1.8 and 3.9. The sensitivity analysis of  
696 this work shows sulfate plays a key role in predicting pH, its high hygroscopicity leads to the  
697 formation of the aqueous drops and provides H<sub>air</sub><sup>+</sup> (Fang et al., 2017). Aerosol pH for fine particles  
698 in autumn and winter ~~are~~ in the range of 2.4 ~ 6.3 and 3.5 ~ 6.5, respectively. The difference of  
699 aerosol pH between size bins in fine mode was not significant, probably owing to the excessive NH<sub>3</sub>  
700 (Guo et al., 2017).

701 As for coarse particles, the predicted pH ~~is~~ approximately near or even higher than 7 for all of  
702 the three seasons in this work. ~~It should be noted that assuming~~, which mainly attributed to the  
703 buffering capacity of the coarse mode mineral dust. Simulations with extreme cases that Ca<sup>2+</sup> and  
704 Mg<sup>2+</sup> were removed from the input files were conducted. The results showed that the presence of  
705 Ca<sup>2+</sup> and Mg<sup>2+</sup> had a crucial effect on coarse mode aerosol pH (Figure S22), the difference of aerosol  
706 pH (with and without Ca<sup>2+</sup> and Mg<sup>2+</sup>) for particles larger than 1 μm increased with the increasing  
707 particle size. For particles smaller than 1 μm, the removal of Ca<sup>2+</sup> and Mg<sup>2+</sup> had little effect on  
708 aerosol pH.

带格式的: 字体颜色: 黑色

709 The aerosol pH in equilibrium with the gas phase generally overestimates acidity (pH<4) (Fang  
710 et al., 2017).

711 ~~On~~ coarse mode decreased significantly when under the heavily polluted days, the aerosol pH in  
712 coarse mode showed a marked fall condition, especially in autumn and winter. For example, the pH  
713 in stage 3 (3.1-6.2 μm) declined from 7.8 ~~on~~ under the clean days condition to 4.5 ~~on~~ under the heavily  
714 polluted days condition in winter, implying that the aerosols in coarse mode during severe hazy days  
715 would become weak acid from neutral. The obvious increase of nitrate in coarse mode ~~may~~ might  
716 responsible for this. Moreover, the significant decrease of mass ratios of Ca<sup>2+</sup> and Mg<sup>2+</sup> ~~also~~

weakened resulted in the alkaline loss of coarse mode buffering capacity.

The size distributions of aerosol pH and all analyzed chemical components in the daytime and nighttime are illustrated in Figure 10. For summer and autumn, the pH in the nighttime is higher than that in the daytime. Whereas, in winter, the pH is higher in the daytime. The diurnal variation for aerosol pH based on MOUDI data is consistent with the online data. In the daytime of summer and autumn, the solar radiation is strong and photochemical reaction is active as well as the RH is lower, leading to a lower aerosol pH than nighttime. Whereas in winter, the pH was higher in the daytime. In winter, the averaged RH during the sampling period is 43%, was relatively low, leading to a low ALWC, but the  $\text{SO}_4^{2-}$  and  $\text{NO}_3^-$  in the nighttime are obviously higher due to the lower boundary layer height. Therefore,  $\text{H}_{\text{air}}^+$  is more abundant in nighttime while the low ALWC had little effect on pH.

Figure 10

带格式的: 段落间距段前: 0 磅, 段后: 0 磅

## 5. Summary and conclusions

Aerosol acidity is important for the formation of secondary aerosols. Online measurements, the measured and predicted  $\text{NH}_3$ ,  $\text{NH}_4^+$ ,  $\text{NO}_3^-$ ,  $\text{Cl}^-$ , and  $\epsilon(\text{NH}_4^+)$  by using ISORROPIA-II agreed pretty well when RH was higher than 30%. It is not reasonable to assume aerosol is of many challenges to be measured directly. In a liquid state (metastable) and the aerosol pH could not be accurately predicted by a thermodynamic model where the RH is relatively low. Thus, we only discussed the  $\text{PM}_{2.5}$  pH for data with RH higher than 30% in this work. ISORROPIA-II with forward mode is applied to calculate the  $\text{H}_{\text{air}}^+$  and ALWC based on the 1-h  $\text{PM}_{2.5}$  inorganic ions, precursor gases ( $\text{HCl}$ ,  $\text{HNO}_3$ ,  $\text{NH}_3$ ) and RH, T. Moreover, the size distribution of pH is predicted based on the MOUDI samples with the same way, the gas phase  $\text{NH}_3$ ,  $\text{HNO}_3$  and  $\text{HCl}$  are determined through an iteration procedure. In

In Beijing, the mean aerosol  $\text{PM}_{2.5}$  pH over four seasons is (RH>30%) was  $4.30 \pm 1.60$  (spring),  $4.5 \pm 1.10$  (winter),  $3.98 \pm 1.32$  (summer),  $4.1 \pm 1.3 \pm 0.8$  (autumn), respectively, showing the moderate acidity. In this work, both  $\text{H}_{\text{air}}^+$  and ALWC had significant diurnal variation, and the  $\text{PM}_{2.5}$  acidity variation agreed well with sulfate, indicating the aerosol acidity. The seasonal variation of in NCP was both driven by aerosol pH is closely related to the  $\text{SO}_4^{2-}$ . Overall, the aerosol is more acidic on hazy days than clean days. The aerosol pH in fine mode is in the range of 1.8–3.9, 2.4–6.3 and

746 3.5—6.5 for summer, autumn composition and winter, respectively. As for coarse particles, the  
747 predicted pH is approximately near or even higher than 7.

748 Due to the significantly high level of hygroscopic components in particulate matter in Beijing,  
749 pH has a diurnal trend that follows both aerosol components (especially the sulfate) and ALWC. For  
750 spring, summer and autumn, the particle water. The averaged nighttime pH is 0.3–0.4 unit higher  
751 than that on daytime. However, in winter,  $H_{air}^+$  in nighttime is slightly. The  $PM_{2.5}$  pH in the northerly  
752 direction was higher than that in daytime and the aerosol pH is relatively low at night and higher at  
753 sunset. This result is very different from that found in southeastern United States: the pH diurnal  
754 variation is largely driven by meteorological conditions the southwest direction.

755 A sensitivity analysis was performed in this work to investigate how aerosol components,  
756 precursor gases  $SO_4^{2-}$ ,  $NO_3^-$ ,  $NH_4^+$ ,  $Cl^-$ ,  $Ca^{2+}$ ,  $RH$ , and meteorological conditions affect aerosol  
757 ALWC,  $H_{air}^+$ , and  $PM_{2.5}$  acidity. The RH affects ALWC most, then followed by  $SO_4^{2-}$  and  $NO_3^-$ . For  
758  $H_{air}^+$ ,  $SO_4^{2-}$  is the most or  $NO_3^-$ . The  $SO_4^{2-}$ ,  $RH$ ,  $NO_3^-$ , and  $NH_4^+$ , especially  $SO_4^{2-}$ , were all  
759 important influential factor, and  $RH$ ,  $NO_3^-$ ,  $NH_3$  are also important factors affecting for  $H_{air}^+$ .  
760 Synthetically as for  $PM_{2.5}$  pH,  $SO_4^{2-}$ ,  $T$ ,  $NH_4^+$ , and  $RH$  are two (only in summer) were crucial  
761 factors affecting aerosol pH. For spring,

762 In winter,  $PM_{2.5}$  pH decreased slightly with the increasing RH, whereas the  $PM_{2.5}$  pH increased  
763 with the increasing RH in summer. The dilution effect of ALWC on  $H_{air}^+$  was obvious only in  
764 summer. In spring and autumn, the effect of  $SO_4^{2-}$  RH had little impact on aerosol  $PM_{2.5}$  pH is greater  
765 than RH, and it is due to the comparable with RH in summer. The aerosol pH decreases with  
766 variations of  $H_{air}^+$  and ALWC. The measured  $\epsilon(NH_4^+)$ ,  $\epsilon(NO_3^-)$ , and  $\epsilon(Cl^-)$  increased with the  
767 elevated  $SO_4^{2-}$  concentration RH in all four seasons. In addition, the higher ambient temperature  
768 tended to lower  $PM_{2.5}$  pH due to the volatilization of  $NH_4^+$ ,  $NO_3^-$ ,  $Cl^-$  and the decrease of ALWC.

769  $SO_4^{2-}$  had a key role for aerosol acidity, especially in winter and spring. In spring and winter, the  
770 ALWC was relatively low, the variation of  $SO_4^{2-}$  concentration could generate dramatic changes in  
771 aerosol pH in spring and winter. As the  $NO_3^-$  concentration increases, the aerosol pH firstly increases  
772 and then decrease at a inflection point with  $30 \mu g m^{-3}$ . In this work, sulfate-dominant aerosols are  
773 more acidic with pH lower than 4, whereas nitrate-dominated aerosols are weak in acidity with pH  
774 ranges 3–5. In recent years, the  $SO_4^{2-}$  concentration of  $PM_{2.5}$  in Beijing  $H_{air}^+$ . The impact of  $NO_3^-$  on

带格式的: 字体: Times New Roman

带格式的: 字体: Times New Roman

带格式的: 字体: Times New Roman

带格式的: 字体: Times New Roman, 字体颜色: 红色

带格式的: 字体: Times New Roman

带格式的: 字体: Times New Roman

带格式的: 字体: Times New Roman



775 PM<sub>2.5</sub> pH was different in four seasons. In winter, the PM<sub>2.5</sub> pH decreased with increasing NO<sub>3</sub><sup>-</sup>  
776 concentration due to the low NH<sub>4</sub><sup>T</sup> mass concentration. In summer, the excessive NH<sub>3</sub> could provide  
777 continuous buffering to the increasing NO<sub>3</sub><sup>T</sup> and lead to little change in PM<sub>2.5</sub> pH.

778 The relationship between pH and NH<sub>4</sub><sup>T</sup> was nonlinear, the impact of NH<sub>4</sub><sup>T</sup> on PM<sub>2.5</sub> pH gradually  
779 weakened as NH<sub>4</sub><sup>T</sup> increased. Elevated NH<sub>4</sub><sup>T</sup> consumed H<sub>air</sub><sup>+</sup> swiftly and shifted more NO<sub>3</sub><sup>T</sup> and Cl<sup>T</sup>  
780 into particle phase. In NCP, NH<sub>3</sub> was much rich in spring, summer, and autumn, while less rich in  
781 winter. Although NH<sub>3</sub> in the NCP was abundant, the PM<sub>2.5</sub> pH was far from neutral, which mainly  
782 attributed to the limited ALWC.

783 Cl<sup>T</sup> and Ca<sup>2+</sup> had little impact on the PM<sub>2.5</sub> pH due to the low mass concentration. Elevated Ca<sup>2+</sup>  
784 concentration could increase the PM<sub>2.5</sub> pH because of the buffering capacity of Ca<sup>2+</sup> to the acid  
785 species and the weak water solubility of CaSO<sub>4</sub>.

786 The sensitivity analysis of the relationship between NO<sub>3</sub><sup>T</sup> and ε(NH<sub>4</sub><sup>+</sup>) imply that decreasing  
787 NO<sub>3</sub><sup>T</sup> could reduce the ε(NH<sub>4</sub><sup>+</sup>) effectively, which helped keep NH<sub>3</sub> in the gas phase. In contrast,  
788 the nitrate response to NH<sub>4</sub><sup>T</sup> control was highly nonlinear, the decrease of nitrate would happen only  
789 when the NH<sub>4</sub><sup>T</sup> was greatly reduced.

790 The size-resolved results showed that the pH of coarse particles was approximately near or even  
791 higher than 7 for all three seasons, which was quite higher than that of fine particles. The difference  
792 of aerosol pH between size bins in fine mode was not significant. The aerosol pH in coarse mode  
793 decreased significantly due to the strict emission control measures, in most cases NO<sub>3</sub><sup>-</sup> dominates  
794 inorganic ions, which may be another reason responsible for the moderately acidic aerosol, ~~and~~  
795 becoming weak acid from neutral, when under heavily polluted condition. For summer and autumn,  
796 the pH in the nighttime was higher than that in the daytime. Whereas in winter, the pH was higher  
797 in the daytime.

798 ALWC has a different effect on aerosol pH in different seasons. In winter, the increasing RH  
799 could reduce the aerosol pH whereas it shows a totally reverse tendency in summer, and the elevated  
800 RH has little effect on aerosol pH in spring and autumn when the RH is between 30% and 80%. The  
801 sensitivity analysis of this work highlights the diverse influence of ALWC on aerosol pH, the  
802 dilution effect of ALWC on H<sub>air</sub><sup>+</sup> is only obvious in summer. The elevated NH<sub>3</sub> and NH<sub>4</sub><sup>+</sup> could  
803 reduce aerosol acidity by decreasing H<sub>air</sub><sup>+</sup> concentration exponentially. In the North China Plain, the

804 ammonia is rich, the remaining ammonia after reaction with sulfuric acid will be available to react  
805 with nitric acid to produce  $\text{NH}_4\text{NO}_3$ , so that the aerosol phase will be neutralized to a large extent.  
806 However, the moderate aerosol acidity suggests that though there are excess ammonia in the  
807 atmosphere, in most cases the aerosol will not be alkaline due to the limited ALWC.

808  
809 Data availability. All data in this work are available by contacting the corresponding author P. S.  
810 Zhao (pszhao@ium.cn).

811  
812 Author contributions. P Z designed and led this study. J D and P Z interpreted the data and discussed  
813 the results. J S and X D analyzed the chemical compositions from size-resolved aerosol samples. J  
814 D and P Z wrote the manuscript.

815  
816 Competing interests. The authors declare that they have no conflict of interest.

#### 817 Acknowledgments

818  
819 This work was supported by the National Natural Science Foundation of China (41675131), the  
820 Beijing Talents Fund (2014000021223ZK49), and the Beijing Natural Science Foundation  
821 (8131003). Special thanks to the Max Planck Institute for Chemistry and Leibniz Institute for  
822 Tropospheric Research where Dr. Zhao visited as a guest scientist in 2018.

#### 823 **References**

- 824 Bian, Y. X., Zhao, C. S., Ma, N., Chen, J., Xu, W. Y.: A study of aerosol liquid water content based  
825 on hygroscopicity measurements at high relative humidity in the North China Plain. Atmos. Chem.  
826 Phys. 14, 6417-6426, 2014.
- 827 Bougiatioti, A., Nikolaou, P., Stavroulas, I., Kouvarakis, G., Weber, R., Nenes, A., Kanakidou, M.,  
828 Mihalopoulos, N.: Particle water and pH in the eastern Mediterranean: Source variability and  
829 implications for nutrient availability, Atmos. Chem. Phys., 16(7), 4579-4591, 2016.
- 830 Cheng, Y. F., Zheng, G. J., Wei C., Mu, Q., Zheng, B., Wang, Z. B., Gao, M., Zhang, Q., He, K. B.,  
831 Carmichael, G., Pöschl, U., Su, H.: Reactive nitrogen chemistry in aerosol water as a source of  
832 sulfate during haze events in China, Sci. Adv., 2:e1601530, 2016.
- 833 Clegg, S. L., et al.: A thermodynamic model of the system  $\text{H}^+$ ,  $\text{NH}_4^+$ ,  $\text{SO}_4^{2-}$ ,  $\text{NO}_3^-$ ,  $\text{H}_2\text{O}$  at  
834 tropospheric temperatures, J. Phys. Chem. 102A, 2137-2154, 1998.
- 835 Covert, D.S., Charlson, R.J., Ahlquist, N.C.: A study of the relationship of chemical composition  
836 and humidity to light scattering by aerosol. J. Appl. Meteorol. 11, 968-976, 1972.

带格式的: 行距: 单倍行距, 孤行控制

带格式的: 字体: 五号, 非加粗

带格式的: 字体: 五号, 非加粗, 倾斜

带格式的: 缩进: 首行缩进: 0 字符

---

837 Cruz, C. N., Dassios, K. G., Pandis, S. N.: The effect of dioctyl phthalate films on the ammonium  
838 nitrate aerosol evaporation rate. *Atmos. Environ.*, 34, 3897-3905, 2000.

839 Dassios, K. G., Pandis, S. N.: The mass accommodation coefficient of ammonium nitrate aerosol.  
840 *Atmos. Environ.*, 33 (18), 2993-3003, 1999.

841 Eddingsaas, N. C., VanderVelde, D. G., and Wennberg, P. O.: Kinetics and products of the acid-  
842 catalyzed ring-opening of atmospherically relevant butyl epoxy alcohols, *J. Phys. Chem. A*, 114,  
843 8106-8113, 2010.

844 Fang, T., Guo, H. Y., Zeng, L. H., Verma, V., Nenes, A., Weber, R. J.: Highly acidic ambient particles,  
845 soluble metals, and oxidative potential: A link between sulfate and aerosol toxicity, *Environ. Sci.*  
846 *Technol.*, 51, 2611-2620, 2017.

847 Fountoukis, C., and Nenes, A.: ISORROPIA II A computationally efficient aerosol thermodynamic  
848 equilibrium model for  $K^+$ ,  $Ca^{2+}$ ,  $Mg^{2+}$ ,  $NH_4^+$ ,  $Na^+$ ,  $SO_4^{2-}$ ,  $NO_3^-$ ,  $Cl^-$ ,  $H_2O$  aerosols, *Atmos. Chem.*  
849 *Phys.* 7, 4639-4659, 2007.

850 Fountoukis, C., Nenes, A., Sullivan, A., Weber, R., Van Reken, T., Fischer, M., Matías, E., Moya,  
851 M., Farmer, D., and Cohen, R. C.: Thermodynamic characterization of Mexico City aerosol  
852 during MILAGRO 2006, *Atmos. Chem. Phys.*, 9, 2141-2156, 2009.

853 Gao, J. J., Wang, K., Wang, Y., Liu, S. H., Zhu, C. Y., Hao, J. M., Liu, H. J., Hua, S. B., Tian, H. Z.:  
854 Temporal-spatial characteristics and source apportionment of  $PM_{2.5}$  as well as its associated  
855 chemical species in the Beijing-Tianjin-Hebei region of China. *Environ. Pollut.*, 233, 714-724,  
856 2018.

857 Guo, H., Sullivan, A. P., Campuzano-Jost, P., Schroder, J. C., Lopez-Hilfiker, F. D., Dibb, J. E.,  
858 Jimenez, J. L., Thornton, J. A., Brown, S. S., Nenes, A., Weber, R. J.: Fine particle pH and the  
859 partitioning of nitric acid during winter in the northeastern United States, *J. Geophys. Res. Atmos.*,  
860 121, 10355-10376, 2016.

861 Guo, H., Xu, L., Bougiatioti, A., Cerully, K. M., Capps, S. L., Hite Jr., J. R., Carlton, A. G., Lee, S.-  
862 H., Bergin, M. H., Ng, N. L., Nenes, A., Weber, R. J.: Fine-particle water and pH in the  
863 southeastern United States, *Atmos. Chem. Phys.*, 15, 5211-5228, 2015.

864 Guo, [H., Weber, R. J., and Nenes, A.: High levels of ammonia do not raise fine particle pH](#)  
865 [sufficiently to yield nitrogen oxide-dominated sulfate production, \*Sci. Rep.\*, 7, doi:](#)

---

866 [10.1038/s41598-017-11704-0](https://doi.org/10.1038/s41598-017-11704-0).

867 [Guo, H., Otjes, R., Schlag, P., Scharr, A. K., Nenes, A., Weber, R. J.: Effectiveness of ammonia](#)  
868 [reduction on control of fine particle nitrate. Atmos. Chem. Phys. Discuss.](#)  
869 <https://doi.org/10.5194/acp-2018-378>.

870 [Guo, S., Hu, M., Zamor, M. L., Peng, J. F., Shang, D. J., Zheng, J., Du, Z. F., Wu, Z. J., Shao, M.,](#)  
871 [Zeng, L. M., Molinac, M. J., Zhang R. Y.: Elucidating severe urban haze formation in China.](#)  
872 [PNAS, 111\(49\): 17373-17378, 2014.](#)

873 [Hennigan, C. J., Izumi, J., Sullivan, A. P., Weber, R. J., and Nenes, A.: A critical evaluation of proxy](#)  
874 [methods used to estimate the acidity of atmospheric particles, Atmos. Chem. Phys., 15, 2775-](#)  
875 [2790, 2015.](#)

876 [Huang, X. J., Liu, Z. R., Liu, J. Y., Hu, B., Wen, T. X., Tang, G. Q., Zhang, J. K., Wu, F. K., Ji, D.](#)  
877 [S., Wang, L. L., Wang, Y. S.: Chemical characterization and source identification of PM<sub>2.5</sub> at](#)  
878 [multiple sites in the Beijing–Tianjin–Hebei region, China, Atmos. Chem. Phys., 17, 12941–12962,](#)  
879 [2017.](#)

880 [Jang, M., Czoschke, N. M., Lee, S., and Kamens, R. M.: Heterogeneous atmospheric aerosol](#)  
881 [production by acidcatalyzed particle-phase reactions, Science, 298, 814-817, 2002.](#)

882 [Kuang, Y., Zhao, C. S., Ma, N., Liu, H. J., Bian, Y. X., Tao, J. C., and Hu, M.: Deliquescent](#)  
883 [phenomena of ambient aerosols on the North China Plain. Geophys. Res. Lett., 43, doi:](#)  
884 [10.1002/2016GL070273](https://doi.org/10.1002/2016GL070273), 2016.

885 [Kuang, Y., Zhao, C. S., Zhao, G., Tao, J. C., Ma, N., and Bian, Y. X.: A novel method for calculating](#)  
886 [ambient aerosol liquid water contents based on measurements of a humidified nephelometer](#)  
887 [system. Atmos. Meas. Tech. Discuss., doi.org/10.5194/amt-2017-330, 2017a.](#)

888 [Kuang, Y., Zhao, C. S., Tao, J. C., Bian, Y. X., Ma, N., and Zhao, G.: A novel method for deriving](#)  
889 [the aerosol hygroscopicity parameter based only on measurements from a humidified](#)  
890 [nephelometer system. Atmos. Chem. Phys., 17, 6651–6662, 2017b.](#)

891 [Liu, B. Y. H., Pui, D. Y. H., Whitby, K. T., et al.: The aerosol mobility chromatograph - new detector](#)  
892 [for sulfuric-acid aerosols. Atmos. Environ., 12\(1-3\), 99-104, 1978.](#)

893 [Liu, P. F., Zhao, C. S., Göbel, T., Hallbauer, E., Nowak, A., Ran, L., Xu, W. Y., Deng, Z. Z., Ma, N.,](#)  
894 [Mildenberger, K., Henning, S., Stratmann, F., and Wiedensohler, A.: Hygroscopic properties of](#)  
895 [aerosol particles at high relative humidity and their diurnal variations in the North China Plain,](#)  
896 [Atmos. Chem. Phys., 11, 3479-3494, 2011.](#)

---

897 Liu, H. J., Zhao, C. S., Nekat, B., et al.: Aerosol hygroscopicity derived from size-segregated  
898 chemical composition and its parameterization in the North China Plain. *Atmos. Chem. Phys.*,  
899 14 :2525-2539, 2014.

900 Liu, Z., Wu, L. Y., Wang, T. H., et al.: Uptake of methacrolein into aqueous solutions of sulfuric  
901 acid and hydrogen peroxide. *J. Phys. Chem. A*, 116, 437-442, 2012.

902 Ma, Q.X., Wu, Y.F., Zhang, D. Z., Wang, X.J., Xia, Y.J., Liu, X.Y., Tian, P., Han, Z.W., Xia, X.G.,  
903 Wang, Y., Zhang, R.J.: Roles of regional transport and heterogeneous reactions in the PM<sub>2.5</sub>  
904 increase during winter haze episodes in Beijing. *Sci. Total Environ.*, 599-600, 246-253, 2017.

905 [Meier, J., Wehner, B., Massling, A., Birmili, W., Nowak, A., Gnauk, T., Brüggemann, E., Herrmann,](#)  
906 [H., Min, H., Wiedensohler, A.: Hygroscopic growth of urban aerosol particles in Beijing \(China\)](#)  
907 [during wintertime: a comparison of three experimental methods. \*Atmos. Chem. Phys.\*, 9, 6865–](#)  
908 [6880, 2009.](#)

909 Meskhidze, N., Chameides, W. L., Nenes, A., and Chen, G.: Iron mobilization in mineral dust: Can  
910 anthropogenic SO<sub>2</sub> emissions affect ocean productivity? *Geophys. Res. Lett.*, 30, 2085,  
911 doi:10.1029/2003gl018035, 2003.

912 Nenes, A., et al.: ISORROPIA: A new thermodynamic model for multiphase multicomponent  
913 inorganic aerosols, *Aquatic Geochem.* 4, 123-152, 1998.

914 Nowak, J. B., Huey, L. G., Russell, A. G., Tian, D., Neuman, J. A., Orsini, D., Sjostedt, S. J., Sullivan,  
915 A. P., Tanner, D. J., Weber, R. J., Nenes, A., Edgerton, E., Fehsenfeld, F. C.: Analysis of urban  
916 gas phase ammonia measurements from the 2002 Atlanta Aerosol Nucleation and Real-Time  
917 Characterization Experiment (ANARChE), *J. Geophys. Res.*, 111, D17308,  
918 doi:10.1029/2006jd007113, 2006.

919 [Pan, X. L., Yan, P., Tang, J., Ma, J. Z., Wang, Z. F., Gbaguidi, A., and Sun, Y. L.: Observational](#)  
920 [study of influence of aerosol hygroscopic growth on scattering coefficient over rural area near](#)  
921 [Beijing mega-city. \*Atmos. Chem. Phys.\*, 9, 7519-7530, 2009.](#)

922 Pathak, R. K., Wang, T., Ho, K. F., Lee, S. C.: Characteristics of summertime PM<sub>2.5</sub> organic and  
923 elemental carbon in four major Chinese cities: Implications of high acidity for water soluble  
924 organic carbon (WSOC), *Atmos. Environ.*, 45, 318-325, 2011a.

925 Pathak, R. K., Wang, T. and Wu, W.S.: Nighttime enhancement of PM<sub>2.5</sub> nitrate in ammonia-poor

---

926 atmospheric conditions in Beijing and Shanghai: Plausible contributions of heterogeneous  
927 hydrolysis of N<sub>2</sub>O<sub>5</sub> and HNO<sub>3</sub> partitioning. *Atmos. Environ.*, 45: 1183-1191, 2011b.

928 Peng, C. G., Chan, M. N., and Chan, C. K.: The hygroscopic properties of dicarboxylic and  
929 multifunctional acids: Measurements and UNIFAC predictions, *Environ. Sci. Technol.*, 35, 4495-  
930 4501, 2001.

931 Pye, H. O., Pinder, R. W., Piletic, I. R., Xie, Y., Capps, S. L., Lin, Y. H., Surratt, J. D., Zhang, Z.,  
932 Gold, A., Luecken, D. J., Hutzell, W. T., Jaoui, M., Offenberg, J. H., Kleindienst, T. E.,  
933 Lewandowski, M., and Edney, E. O.: Epoxide pathways improve model predictions of isoprene  
934 markers and reveal key role of acidity in aerosol formation, *Environ. Sci. Technol.*, 47, 11056-  
935 11064, 2013.

936 Rengarajan, R., Sudheer, A.K., Sarin, M.M.: Aerosol acidity and secondary formation during  
937 wintertime over urban environment in western India. *Atmos. Environ.*, 45: 1940-1945, 2011.

938 Rood, M.J., Larson, T.V., Covert, D.S., Ahlquist, N.C.: Measurement of laboratory and ambient  
939 aerosols with temperature and humidity controlled nephelometry. *Atmos. Environ.* 19, 1181-1190,  
940 1985.

941 Schwertmann, U., Cornell, R. M.: *Iron Oxides In the Laboratory: Preparation and Characterization*,  
942 Weinheim, WCH Publisher, 1991.

943 Seinfeld, J. H., Pandis, S. N.: *Atmospheric Chemistry and Physics: From Air Pollution to Climate*  
944 *Change*, John Wiley & Sons, Inc., Hoboken, New Jersey, USA, 2016.

945 Shi, G. L., Xu, J., Peng, X., Xiao, Z. M., Chen, K., Tian, Y. Z., Guan, X. P., Feng, Y. C., Yu, H. F.,  
946 Nenes, A., Russell, A. G.: pH of aerosols in a polluted atmosphere: source contributions to highly  
947 acidic aerosol, *Environ. Sci. Technol.*, DOI: 10.1021/acs.est.6b05736, 2017.

948 Shi, Z., Bonneville, S., Krom, M. D., Carslaw, K. S., Jickells, T. D., Baker, A. R., Benning, L. G.:  
949 Iron dissolution kinetics of mineral dust at low pH during simulated atmospheric processing.  
950 *Atmos. Chem. Phys.*, 11, 995-1007, 2011.

951 Song, S. J., Gao, M., Xu, W. Q., Shao, J. Y., Shi, G. L., Wang, S. X., Wang, Y. X., Sun, Y. L., McElroy,  
952 M. B.: Fine particle pH for Beijing winter haze as inferred from different thermodynamic  
953 equilibrium models. *Atmos. Chem. Phys. Discuss.*, [doi.org/10.5194/acp-2018-6](https://doi.org/10.5194/acp-2018-6), 18, 7423-7438,  
954 2018.

955 Su, J., Zhao, P. S., Dong, Q.: Chemical Compositions and Liquid Water Content of Size-Resolved

带格式的: 超链接, 字体: +西文正文 (等线)

---

956 Aerosol in Beijing. *Aerosol Air Qual. Res.*, 18, 680-692, 2018.

957 Surratt, J. D., Chan, A. W., Eddingsaas, N. C., Chan, M., Loza, C. L., Kwan, A. J., Hersey, S. P.,  
958 Flagan, R. C., Wennberg, P. O., and Seinfeld, J. H.: Reactive intermediates revealed in secondary  
959 organic aerosol formation from isoprene, *P. Natl. Acad. Sci. USA*, 107, 6640-6645, 2010.

960 Swietlicki, E., Hansson, H.-C., Hämeri, K., Svenningsson, B., Massling, A., McFiggans, G.,  
961 McMurry, P.H., Petäjä, T., Tunved, P., Gysel, M., Topping, D., Weingartner, E., Baltensperger, U.,  
962 Rissler, J., Wiedensohler, A., Kulmala, M.: Hygroscopic properties of submicrometer  
963 atmospheric aerosol particles measured with H-TDMA instruments in various environments: a  
964 review. *Tellus Ser. B Chem. Phys. Meteorol.* 60, 432-469, 2008.

965 Tan, T. Y., Hu, M., Li, M. R., Guo, Q. F., Wu, Y. S., Fang, X., Gu, F. T., Wang, Y., Wu, Z. J.: New  
966 insight into PM<sub>2.5</sub> pollution patterns in Beijing based on one-year measurement of chemical  
967 compositions. *Sci. Total Environ.*, 621, 734-743, 2018.

968 ten Brink, H., Otjes, R., Jongejan, P., Slanina, S.: An instrument for semicontinuous monitoring of  
969 the size-distribution of nitrate, ammonium, sulphate and chloride in aerosol. *Atmos. Environ.* 41,  
970 2768-2779, 2007.

971 [Tian, S. L., Pan, Y. P., Liu, Z.R., Wen, T. X., Wang, Y. S.: Size-resolved aerosol chemical](#)  
972 [analysis of extreme haze pollution events during early 2013 in urban Beijing, China. \*J.\*](#)  
973 [Hazard. Mater.](#), 279, 452-460, 2014.

974 Topping, D. O., McFiggans, G. B., and Coe, H.: A curved multicomponent aerosol hygroscopicity  
975 model framework: Part 1– Inorganic compounds, *Atmos. Chem. Phys.*, 5, 1205-1222, 2005a.

976 Topping, D. O., McFiggans, G. B., and Coe, H.: A curved multicomponent aerosol hygroscopicity  
977 model framework: Part 2 – Including organic compounds, *Atmos. Chem. Phys.*, 5, 1223-1242,  
978 2005b

979 Wang, G., Zhang, R., Gomez, M. E., Yang, L., Levy Zamora, M., Hu, M., Lin, Y., Peng, J., Guo, S.,  
980 Meng, J., Li, J., Cheng, C., Hu, T., Ren, Y., Wang, Y., Gao, J., Cao, J., An, Z., Zhou, W., Li, G.,  
981 Wang, J., Tian, P., Marrero-Ortiz, W., Secret, J., Du, Z., Zheng, J., Shang, D., Zeng, L., Shao,  
982 M., Wang, W., Huang, Y., Wang, Y., Zhu, Y., Li, Y., Hu, J., Pan, B., Cai, L., Cheng, Y., Ji, Y.,  
983 Zhang, F., Rosenfeld, D., Liss, P. S., Duce, R. A., Kolb, C. E., and Molina, M. J.: Persistent sulfate  
984 formation from London Fog to Chinese haze, *Proc. Natl. Acad. Sci. U.S.A.*, 113, 13630-13635,  
985 2016.

---

986 Wang, X. W., Jing, B., Tan, F., Ma, J.B., Zhang, Y. H., Ge, M.F.: Hygroscopic behavior and chemical  
987 composition evolution of internally mixed aerosols composed of oxalic acid and ammonium  
988 sulfate, *Atmos. Chem. Phys.*, 17, 12797-12812, 2017.

989 Weber, R. J., Guo, H., Russell, A. G., Nenes, A.: High aerosol acidity despite declining atmospheric  
990 sulfate concentrations over the past 15 years. *Nat. Geosci.*, 9, 282-285, 2016.

991 Yan, P., Pan, X., Tang, J., et al.: Hygroscopic growth of aerosol scattering coefficient: A comparative  
992 analysis between urban and suburban sites at winter in Beijing. *Particuology*, 7, 52-60, 2009.

993 Young, A. H., Keene, W. C., Pszenny, A. A. P., Sander, R., Thornton, J. A., Riedel, T. P., Maben, J.  
994 R.: Phase partitioning of soluble trace gases with size-resolved aerosols in near-surface  
995 continental air over northern Colorado, USA, during winter, *J. Geophys. Res. Atmos.*, 118, 9414-  
996 9427, doi:10.1002/jgrd.50655, 2013.

997 Zhang, Q., Jimenez, J. L., Worsnop, D. R., Canagaratna, M.: A case study of urban particle acidity  
998 and its influence on secondary organic aerosol. *Environ. Sci. Technol.*, 41, 3213-3219, 2007.

999 Zhao, P. S., Chen, Y. N., Su, J.: Size-resolved carbonaceous components and water-soluble ions  
1000 measurements of ambient aerosol in Beijing. *J. Environ. Sci.*, 54, 298-313, 2017.

1001 Zhao, P. S., Dong, F., He, D., Zhao, X.J., Zhang, X.L., Zhang, W.Z., Yao, Q., Liu, H. Y.:  
1002 Characteristics of concentrations and chemical compositions for PM<sub>2.5</sub> in the region of Beijing,  
1003 Tianjin, and Hebei, China. *Atmos. Chem. Phys.*, 13, 4631-4644, 2013.

1004 Zou, J. N., Liu, Z. R., Hu, B., Huang, X. J., Wen, T. X., Ji, D. S., Liu, J. Y., Yang, Y., Yao, Q., Wang,  
1005 Y. S.: Aerosol chemical compositions in the North China Plain and the impact on the visibility in  
1006 Beijing and Tianjin. *Atmos. Res.* 201, 235-246, 2018. [\\_\\_\\_\\_\\_](#)



1007



1008  
1009  
1010  
1011  
1012  
1013  
1014  
1015  
1016  
1017  
1018  
1019  
1020

**Table captions**

**Table 1.** ~~The averaged  $PM_{2.5}$  and Average mass concentrations of  $NO_3^-$ ,  $SO_4^{2-}$ ,  $NH_4^+$  mass concentration and  $PM_{2.5}$~~  as well as RH, ALWC,  $H_{air}^+$ , ~~and  $PM_{2.5}$  pH~~ ~~on~~under clean, polluted, and heavily polluted ~~days~~conditions over four seasons.

**Table 2.** Average  $\epsilon(NH_4^+)$ ,  $\epsilon(NO_3^-)$ ,  $\epsilon(Cl^-)$ , and ambient temperature at different ambient RH levels in four seasons.

**Table 3.** Sensitivity of aerosol chemical components ( $NO_3^-$ , ALWC,  $H_{air}^+$ , and  $PM_{2.5}$  pH to  $SO_4^{2-}$ ,  $NH_4^+$ ,  $Ca^{2+}$ ), precursor gases ( $NH_3$ ,  $HNO_3$ ) and meteorological parameters (RH,  $NH_4^+$ ,  $NO_3^-$ ,  $Cl^-$ ,  $Ca^{2+}$ , RH, and T) to aerosol acidity, ALWC and  $H_{air}^+$ . The larger magnitude of the relative standard deviation (RSD) represents the larger impact derived from the variation of variables.

带格式的: 两端对齐

带格式的: 字体: Times New Roman

带格式的: 字体颜色: 黑色

带格式的: 字体: Times-Roman, 五号



Clean	33±21	7.6±7.4	4.4±4.1	3.8±3.5	<del>37±72</del> 49±83	<del>5.1E3.8E</del> 06±9.4E6.6E	4.25±1.20
Polluted	105±21	33.8±11.6	14.3±6.3	16.0±4.6	<del>182±172</del> 225±1	<del>1.8E7E</del> 05±1.3E2E	3.94.1±0.4
Heavily polluted	174±1	63.4±15.4	25.0±15.9	29.0±5.1	<del>315±212</del> 317±2	<del>3.6E2.2E</del> 05±2.6E1.0E	3.94.1±0.3

\* For data with RH>30%.

- 带格式的: 字体颜色: 自定义颜色( RGB(13,13,13) )
- 带格式的: 字体颜色: 自定义颜色( RGB(13,13,13) )
- 带格式的: 字体颜色: 自定义颜色( RGB(13,13,13) )
- 带格式的: 两端对齐
- 带格式的: 字体颜色: 自定义颜色( RGB(13,13,13) )
- 带格式的: 字体颜色: 自定义颜色( RGB(13,13,13) )
- 带格式的: 字体颜色: 自定义颜色( RGB(13,13,13) )
- 带格式的: 字体颜色: 自定义颜色( RGB(13,13,13) )
- 带格式的: 字体颜色: 自定义颜色( RGB(13,13,13) )
- 带格式的: 字体颜色: 自定义颜色( RGB(13,13,13) )
- 带格式的: 两端对齐
- 带格式的: 两端对齐
- 带格式的: 字体颜色: 自定义颜色( RGB(13,13,13) )
- 带格式的: 字体颜色: 自定义颜色( RGB(13,13,13) )
- 带格式的: 字体颜色: 自定义颜色( RGB(13,13,13) )
- 带格式的: 字体颜色: 自定义颜色( RGB(13,13,13) )

1024  
1025  
1026  
1027  
1028  
1029

1030

1031

**Table 2**

带格式的: 两端对齐

1032

	<u>RH</u>	<u>T, °C</u>	<u>ε(NH<sub>4</sub><sup>+</sup>)</u>	<u>ε(NO<sub>3</sub><sup>-</sup>)</u>	<u>ε(Cl<sup>-</sup>)</u>
	<u>≤ 30 %</u>	<u>24.8 ± 3.7</u>	<u>0.17±0.14</u>	<u>0.84±0.12</u>	<u>0.67±0.24</u>
<u>Spring</u>	<u>30~60 %</u>	<u>20.6 ± 3.8</u>	<u>0.25±0.14</u>	<u>0.91±0.06</u>	<u>0.82±0.16</u>
	<u>&gt;60 %</u>	<u>15.8 ± 2.7</u>	<u>0.28±0.12</u>	<u>0.96±0.03</u>	<u>0.96±0.06</u>
	<u>≤ 30 %</u>	<u>5.4 ± 5.3</u>	<u>0.31±0.13</u>	<u>0.78±0.12</u>	<u>0.89±0.14</u>
<u>Winter</u>	<u>30~60 %</u>	<u>1.0 ± 3.6</u>	<u>0.50±0.21</u>	<u>0.89±0.10</u>	<u>0.97±0.03</u>
	<u>&gt;60 %</u>	<u>-1.9 ± 2.1</u>	<u>0.60±0.20</u>	<u>0.96±0.03</u>	<u>0.99±0.01</u>
	<u>≤ 30 %</u>	<u>35.6± 0.4</u>	<u>0.06±0.02</u>	<u>0.35±0.20</u>	<u>0.39±0.17</u>
<u>Summer</u>	<u>30~60 %</u>	<u>29.6 ± 4.2</u>	<u>0.17±0.11</u>	<u>0.65±0.23</u>	<u>0.43±0.16</u>
	<u>&gt;60 %</u>	<u>25.2 ± 3.8</u>	<u>0.26±0.12</u>	<u>0.90±0.12</u>	<u>0.71±0.15</u>
	<u>≤ 30 %</u>	<u>21.7± 7.5</u>	<u>0.07±0.06</u>	<u>0.49±0.25</u>	<u>0.45±0.21</u>
<u>Autumn</u>	<u>30~60 %</u>	<u>20.8± 6.3</u>	<u>0.21±0.14</u>	<u>0.82±0.19</u>	<u>0.67±0.21</u>
	<u>&gt;60 %</u>	<u>14.9 ± 5.7</u>	<u>0.30±0.19</u>	<u>0.92±0.10</u>	<u>0.86±0.13</u>

1033

1034

1035

**Table 3**

<u>Impact Factor</u>	<u>SO<sub>4</sub><sup>2-</sup></u>	<u>NO<sub>3</sub><sup>T</sup></u>	<u>NH<sub>4</sub><sup>T</sup></u>	<u>Cl<sup>T</sup></u>	<u>Ca<sup>2+</sup></u>	<u>RH</u>	<u>T</u>	
<u>Spring</u>	<u>RSD-ALWC</u>	<u>50.5%</u>	<u>53.4%</u>	<u>2.9%</u>	<u>7.5%</u>	<u>21.2%</u>	<u>122%</u>	<u>13.1%</u>
	<u>RSD-H<sub>air</sub><sup>±</sup></u>	<u>223%</u>	<u>34.4%</u>	<u>26.8%</u>	<u>12.4%</u>	<u>49.8%</u>	<u>115%</u>	<u>49.5%</u>
	<u>RSD-pH</u>	<b><u>12.4%</u></b>	<u>5.2%</u>	<u>3.9%</u>	<u>2.4%</u>	<u>5.5%</u>	<u>1.3%</u>	<u>7.0%</u>
<u>Winter</u>	<u>RSD-ALWC</u>	<u>33.8%</u>	<u>28.7%</u>	<u>14.2%</u>	<b><u>30.7%</u></b>	<u>1.9%</u>	<u>103%</u>	<u>3.5%</u>
	<u>RSD-H<sub>air</sub><sup>±</sup></u>	<u>431%</u>	<u>431%</u>	<u>187.4%</u>	<b><u>52.3%</u></b>	<u>11.3%</u>	<u>136%</u>	<u>74.1%</u>
	<u>RSD-pH</u>	<b><u>28.1%</u></b>	<u>8.4%</u>	<b><u>27.0%</u></b>	<u>3.8%</u>	<u>1.0%</u>	<u>4.1%</u>	<u>6.7%</u>
<u>Summer</u>	<u>RSD-ALWC</u>	<u>49.4%</u>	<u>46.0%</u>	<u>6.9%</u>	<u>3.6%</u>	<u>9.0%</u>	<u>104%</u>	<u>10.8%</u>
	<u>RSD-H<sub>air</sub><sup>±</sup></u>	<u>131%</u>	<u>29.9%</u>	<u>78.1%</u>	<u>3.4%</u>	<u>18.1%</u>	<u>44.6%</u>	<u>33.9%</u>
	<u>RSD-pH</u>	<b><u>7.9%</u></b>	<u>3.6%</u>	<b><u>8.1%</u></b>	<u>0.8%</u>	<u>1.9%</u>	<b><u>8.6%</u></b>	<u>5.8%</u>
<u>Autumn</u>	<u>RSD-ALWC</u>	<u>32.8%</u>	<u>58.1%</u>	<u>9.9%</u>	<u>6.9%</u>	<u>3.3%</u>	<u>77.6%</u>	<u>5.5%</u>
	<u>RSD-H<sub>air</sub><sup>±</sup></u>	<u>171%</u>	<u>126.7%</u>	<u>333.1%</u>	<u>2.0%</u>	<u>9.3%</u>	<u>106%</u>	<u>59.6%</u>
	<u>RSD-pH</u>	<b><u>6.0%</u></b>	<u>3.3%</u>	<b><u>16.1%</u></b>	<u>1.0%</u>	<u>0.8%</u>	<u>2.4%</u>	<b><u>7.5%</u></b>

1036

1037

## Figure captions

**Figure 1.** Time series of relative humidity (RH), temperature (T) (a, e, i, m); PM<sub>2.5</sub>, PM<sub>10</sub>, and NH<sub>3</sub> (b, f, g, n); dominant water-soluble ion species: NO<sub>3</sub><sup>-</sup>, SO<sub>4</sub><sup>2-</sup>, and NH<sub>4</sub><sup>+</sup> (c, g, k, o); aerosol and PM<sub>2.5</sub> pH colored by PM<sub>2.5</sub> concentration (d, h, l, p) over four seasons.

**Figure 2.** Comparisons of predicted NO<sub>3</sub><sup>-</sup>, NH<sub>4</sub><sup>+</sup> to and measured values based on (a, b) online ion chromatography, NH<sub>3</sub>, HNO<sub>3</sub>, HCl, NH<sub>4</sub><sup>+</sup>, NO<sub>3</sub><sup>-</sup>, Cl<sup>-</sup>, ε(NH<sub>4</sub><sup>+</sup>), ε(NO<sub>3</sub><sup>-</sup>), and ε(Cl<sup>-</sup>) colored by RH. In this Figure, the data and (c, d) of four seasons were put together, and the comparisons for each season were shown in Figure S1-S4.

**Figure 3.** Comparisons of predicted and iterative NH<sub>3</sub>, HNO<sub>3</sub>, and HCl, as well as the predicted and measured NH<sub>4</sub><sup>+</sup>, NO<sub>3</sub><sup>-</sup>, Cl<sup>-</sup>, ε(NH<sub>4</sub><sup>+</sup>), ε(NO<sub>3</sub><sup>-</sup>), and ε(Cl<sup>-</sup>) colored by particle size. In this Figure, all MOUDI data— were put together.

**Figure 3-Figure 4.** Time series of mass fraction of NO<sub>3</sub><sup>-</sup>, SO<sub>4</sub><sup>2-</sup>, NH<sub>4</sub><sup>+</sup>, Cl<sup>-</sup>, and crustal ions (Mg<sup>2+</sup>, Ca<sup>2+</sup>) in total ions as well as PM<sub>2.5</sub> pH in all four seasons.

**Figure 5.** Wind dependence map of aerosol PM<sub>2.5</sub> pH over four seasons. In each picture, the shaded contour indicates the average of variables for varying wind speeds (radial direction) and wind directions (transverse direction).

**Figure 46.** Diurnal patterns of mass concentrations of NO<sub>3</sub><sup>-</sup> and SO<sub>4</sub><sup>2-</sup> in PM<sub>2.5</sub>, predicted aerosol liquid water content (ALWC) (a-d); H<sub>air</sub><sup>+</sup> predicted by ISORROPIAII (i-l); predicted aerosol<sup>+</sup>, and PM<sub>2.5</sub> pH (m-p) over four seasons. Mean and median values are shown, together with 25% and 75 % quantiles. Data with RH<30% were excluded, the shadow represents the time period when the RH lower than 30% mostly occurred.

**Figure 57.** Sensitivities of chemical components (NO<sub>3</sub><sup>-</sup>, H<sub>air</sub><sup>+</sup> to SO<sub>4</sub><sup>2-</sup>, NO<sub>3</sub><sup>T</sup>, NH<sub>4</sub><sup>+</sup>, Ca<sup>2+</sup>), precursor gases (NH<sub>3</sub>, HNO<sub>3</sub>)<sub>4</sub><sup>T</sup>, and Cl<sup>T</sup>, as well as meteorological parameters (RH, T) to ALWC in summer and winter.

**Figure 68.** Sensitivities of chemical components (NO<sub>3</sub><sup>-</sup>, ALWC to SO<sub>4</sub><sup>2-</sup>, NO<sub>3</sub><sup>T</sup>, NH<sub>4</sub><sup>+</sup>, Ca<sup>2+</sup>), precursor gases (NH<sub>3</sub>, HNO<sub>3</sub>)<sub>4</sub><sup>T</sup>, and Cl<sup>T</sup>, as well as meteorological parameters (RH, T) to H<sub>air</sub><sup>+</sup> in summer and winter.

**Figure 79.** Sensitivities of chemical components (NO<sub>3</sub><sup>-</sup>, PM<sub>2.5</sub> pH to SO<sub>4</sub><sup>2-</sup>, NO<sub>3</sub><sup>T</sup>, NH<sub>4</sub><sup>+</sup>, Ca<sup>2+</sup>), precursor gases (NH<sub>3</sub>, HNO<sub>3</sub>)<sub>4</sub><sup>T</sup>, and Cl<sup>T</sup>, as well as meteorological parameters (RH, T) to pH in

带格式的: 字体颜色: 黑色

带格式的: 字体颜色: 黑色

带格式的: 字体颜色: 黑色

带格式的: 字体颜色: 黑色

带格式的: 字体颜色: 黑色

带格式的: 无孤行控制

带格式的: 字体颜色: 文字 1

带格式的: 两端对齐

带格式的: 字体: 五号

带格式的: 字体: 五号

带格式的: 字体: 五号

带格式的: 字体: 五号

1067 summer and winter.

1068 **Figure 8.** Measured  $\text{NO}_3^-/2\text{SO}_4^{2-}$  ratio (mole mole<sup>-1</sup>) versus predicted pH colored by ambient RH.  
1069  $\text{NO}_3^-$ ,  $\text{SO}_4^{2-}$  dominant zone denotes  $\text{NO}_3^-/2\text{SO}_4^{2-} > 1$  or  $< 1$ .

1070 **Figure 9. Figure 10.** Sensitivities of  $\epsilon(\text{NH}_4^+)$ ,  $\epsilon(\text{NO}_3^-)$ , and  $\epsilon(\text{Cl}^-)$  to  $\text{NO}_3^-$ ,  $\text{NH}_4^+$ , and  $\text{Cl}^-$  colored by  
1071  $\text{PM}_{2.5}$  pH in summer and winter.

1072 **Figure 11.** Sensitivities of  $\epsilon(\text{NH}_4^+)$ ,  $\epsilon(\text{NO}_3^-)$ , and  $\epsilon(\text{Cl}^-)$  to RH and T colored by  $\text{PM}_{2.5}$  pH in summer  
1073 and winter.

1074 **Figure 12.** The size ~~distribution~~distributions of aerosol pH and all analyzed chemical components  
1075 ~~on~~under clean (a, d, g), polluted (b, e, h), and heavily polluted ~~days~~conditions (c, f, i) in summer,  
1076 autumn, and winter.

1077 **Figure 10.** The size distribution of pH and all analyzed chemical components in the daytime (a, e,  
1078 e) and (b, d, f) nighttime in summer, autumn and winter.

1079



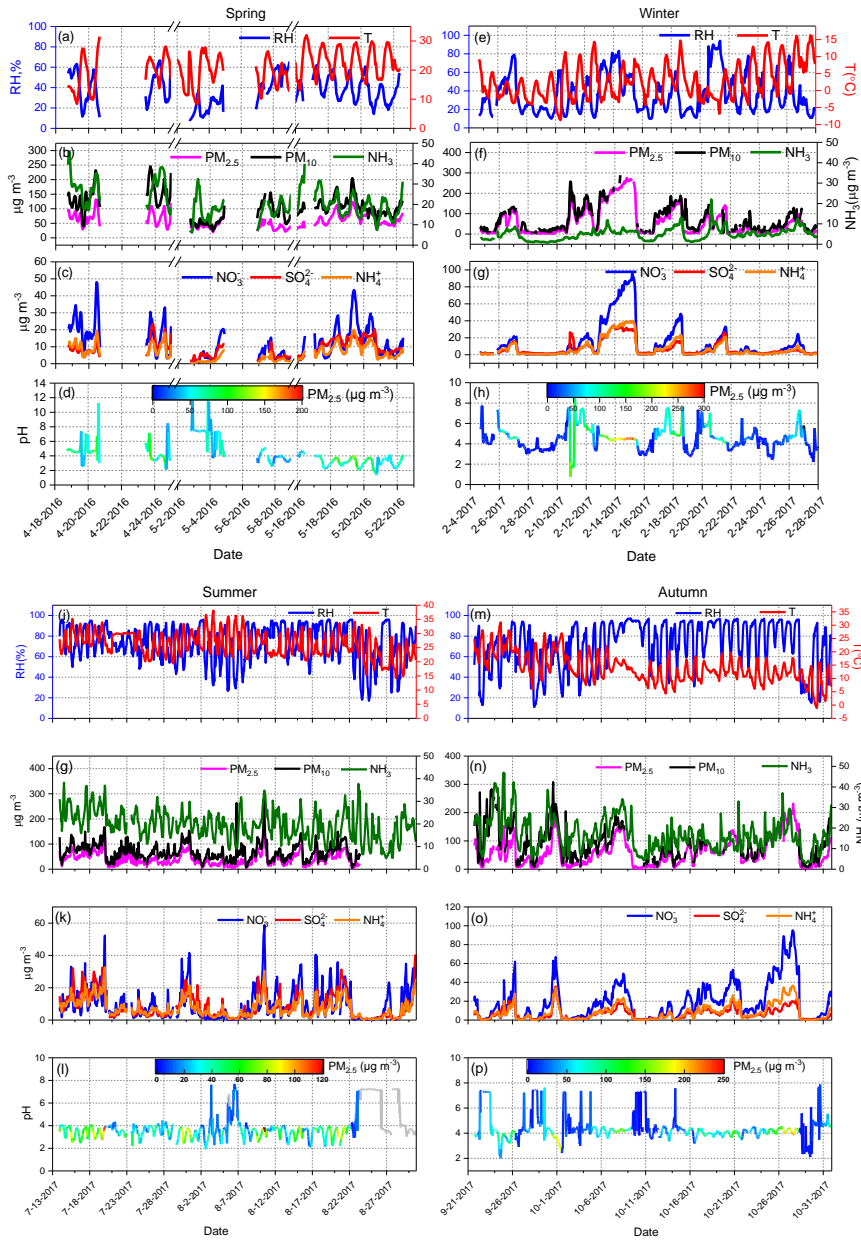


Figure 1.

带格式的: 两端对齐

1080

1081

1082

1083

1084

1085

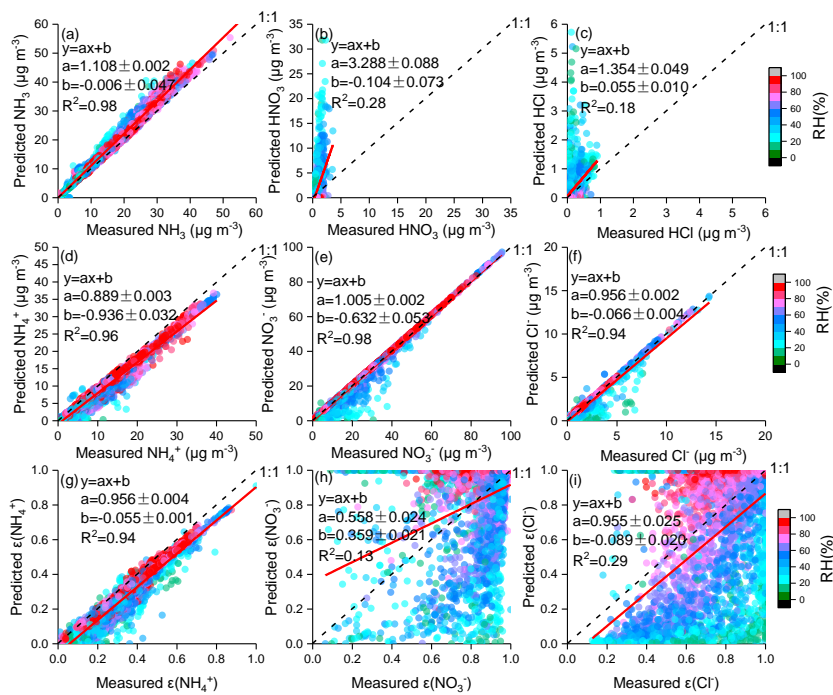
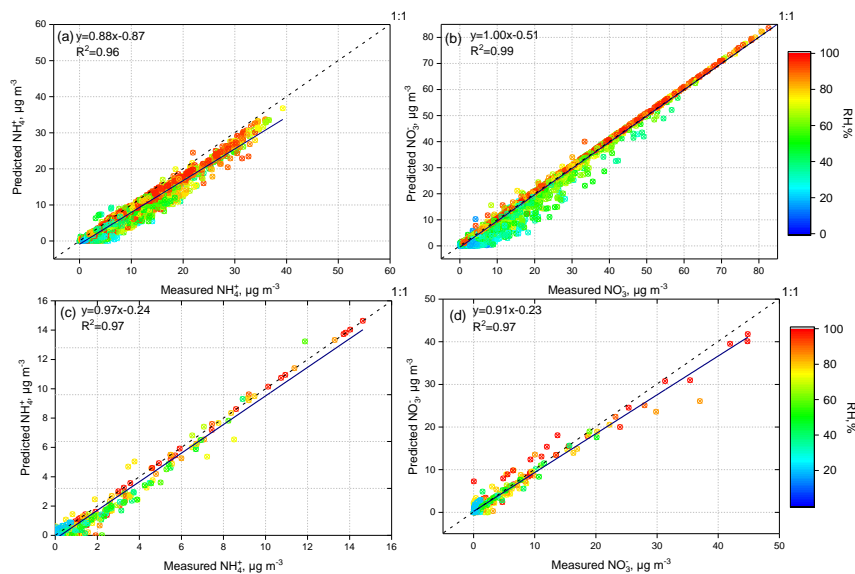
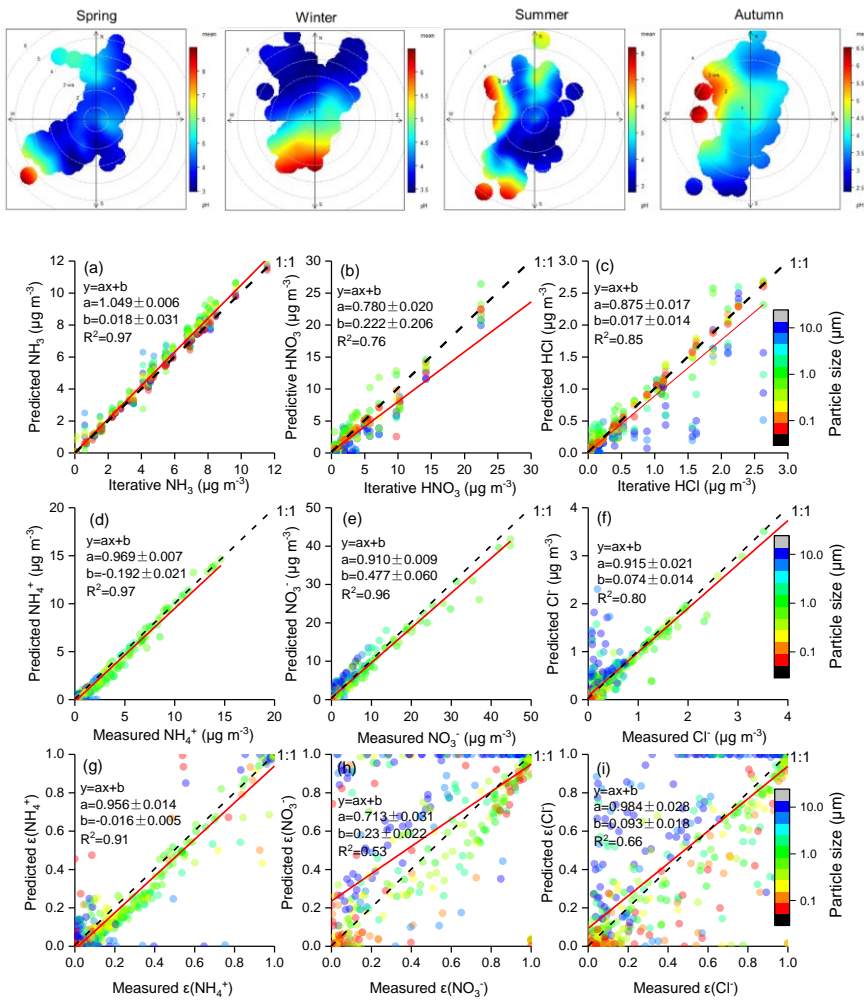


Figure 2.

带格式的: 缩进: 首行缩进: 0 字符

带格式的: 字体: Times New Roman

1090  
1091  
1092



1094  
1095  
1096

Figure 3

- 带格式的
- 带格式的: 段落间距段前: 0 磅, 段后: 0 磅, 无孤行控制
- 带格式的: 字体: 加粗

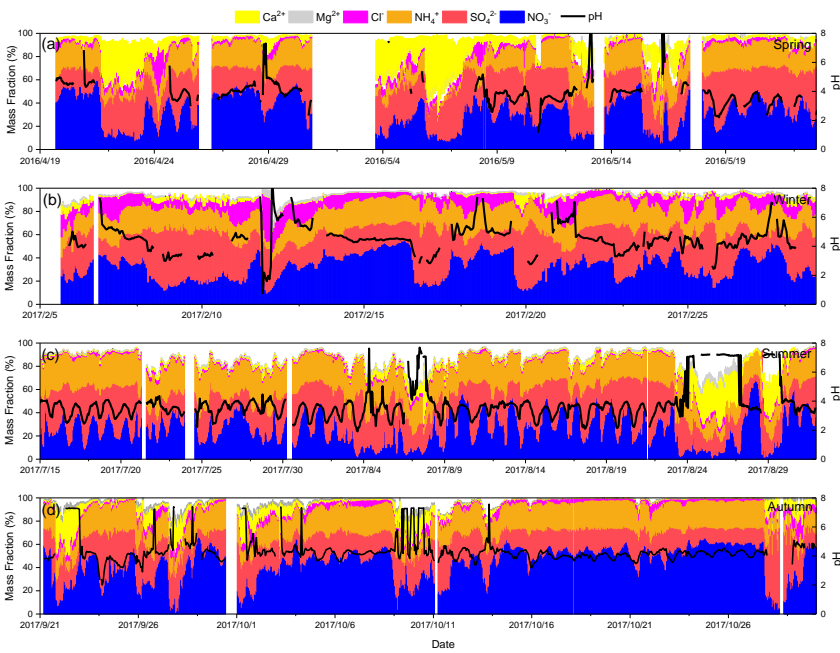
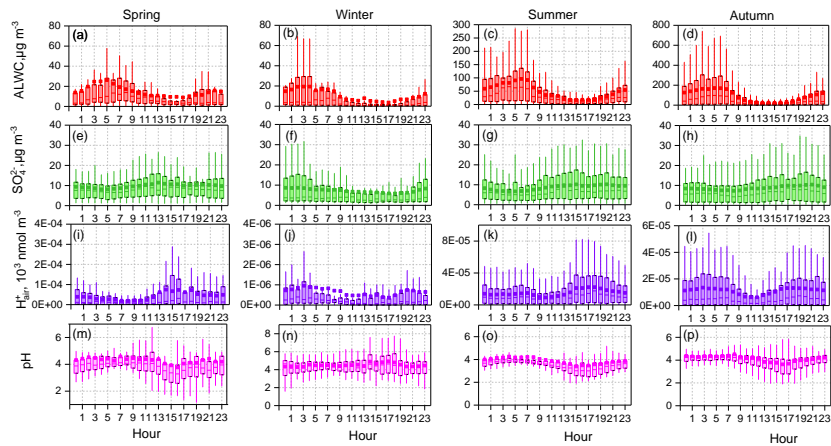


Figure 4.

带格式的: 字体: 加粗  
 带格式的: 段落间距段前: 0 磅, 段后: 0 磅  
 带格式的: 缩进: 首行缩进: 1 字符, 行距: 1.5 倍行距

带格式的: 字体: Times New Roman, 加粗  
 带格式的: 行距: 1.5 倍行距

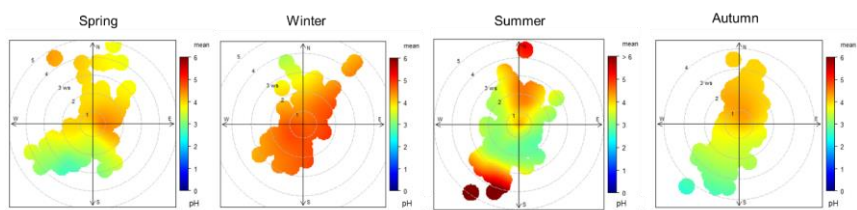
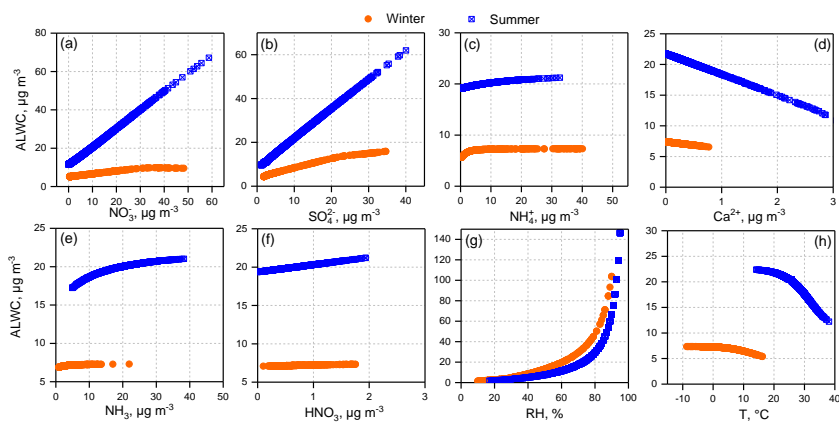
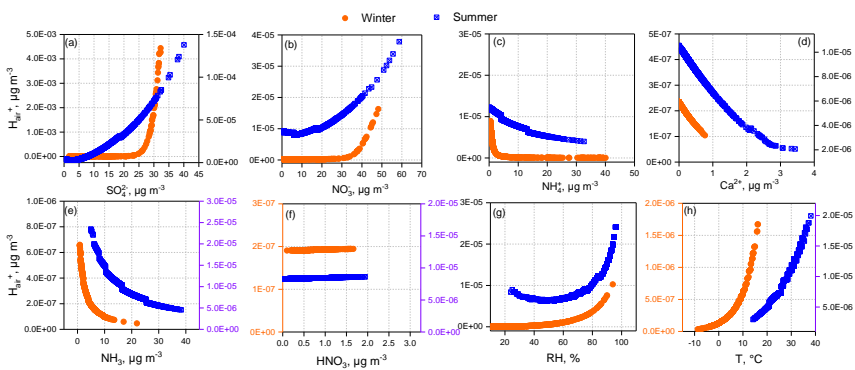


Figure 5.



带格式的: 缩进: 首行缩进: 0 字符

带格式的: 字体: 加粗

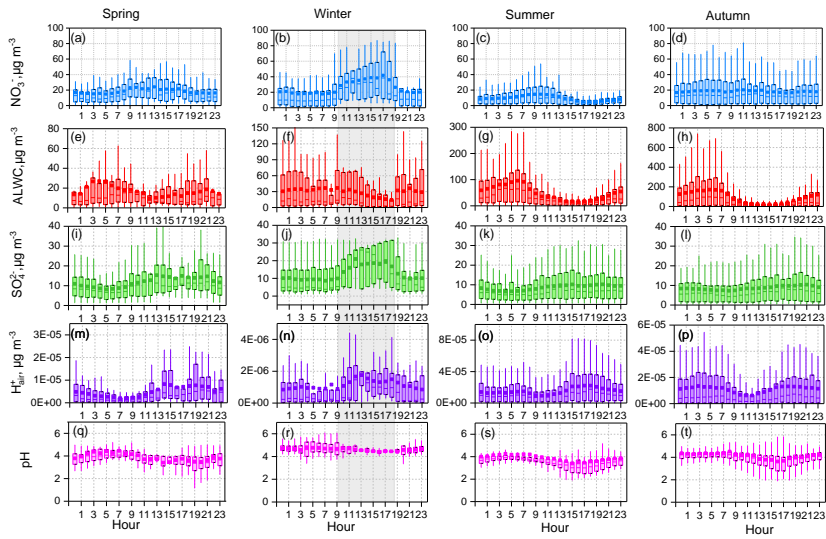
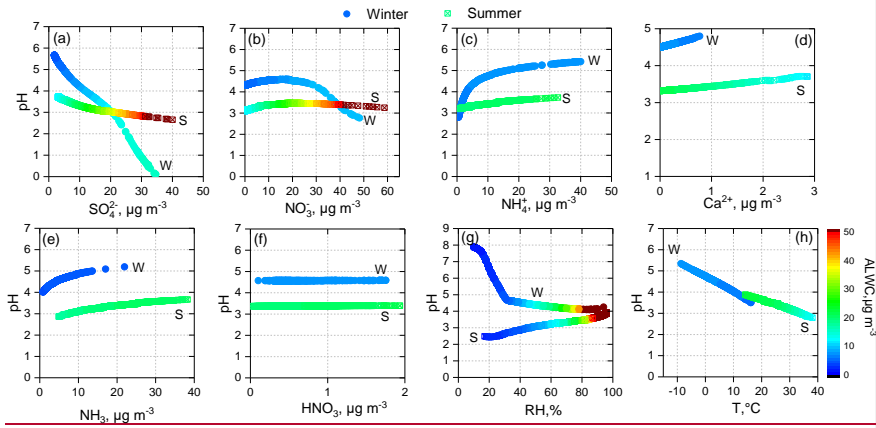


Figure 6.

带格式的: 缩进: 首行缩进: 0 字符



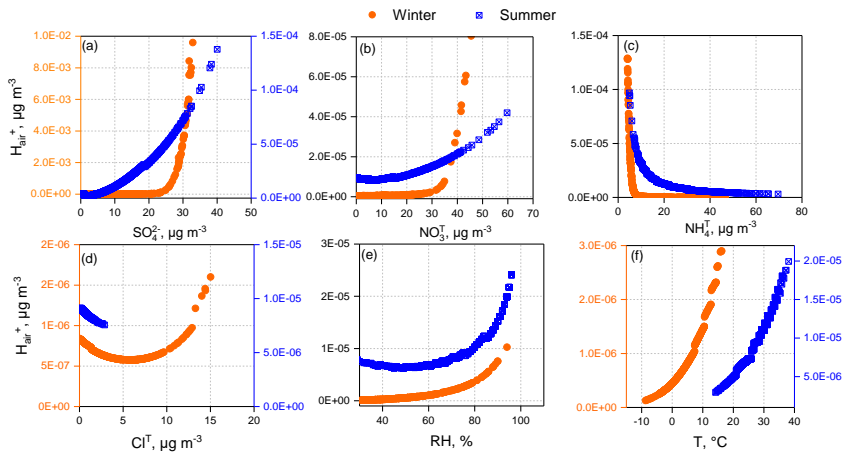
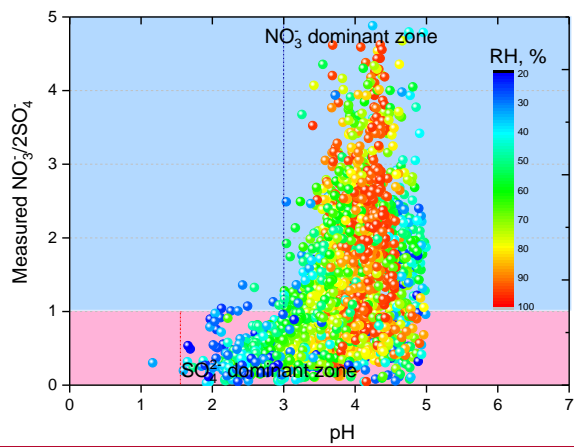


Figure 7.

带格式的: 缩进: 首行缩进: 0 字符

带格式的: 字体: Times New Roman



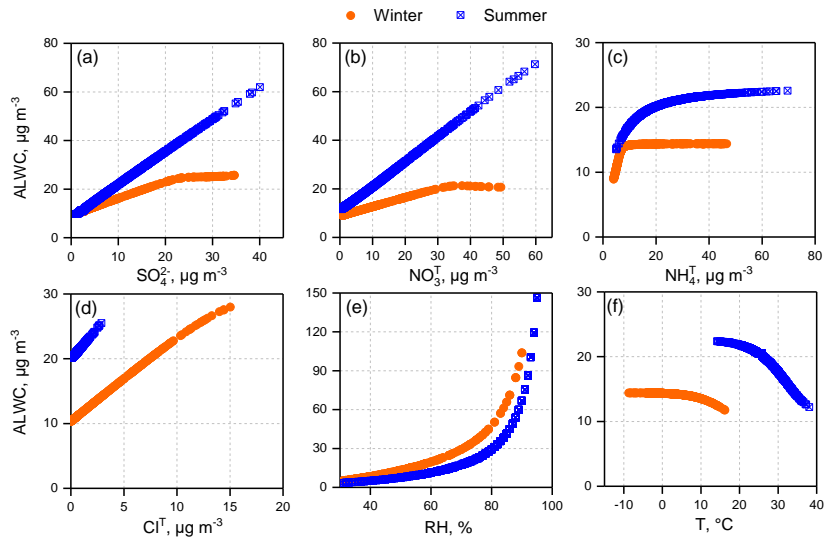


Figure 8.

带格式的: 字体: 加粗

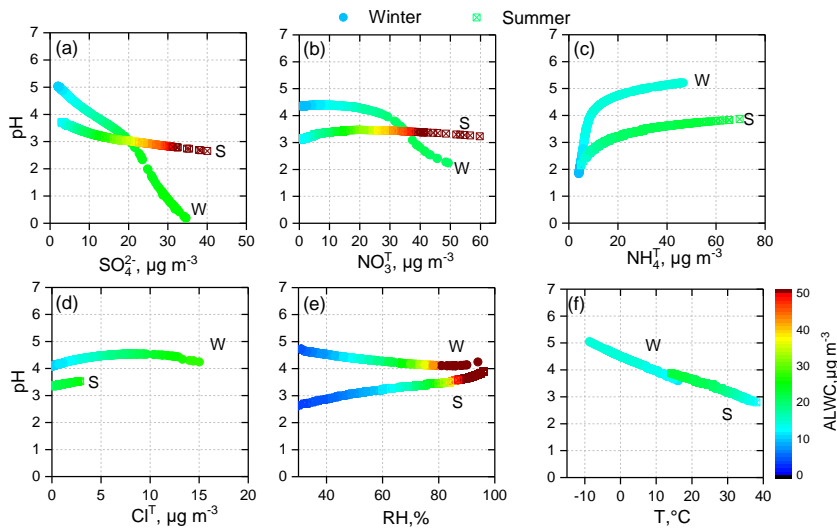


Figure 9.

1125  
1126  
1127  
1128

1129  
1130



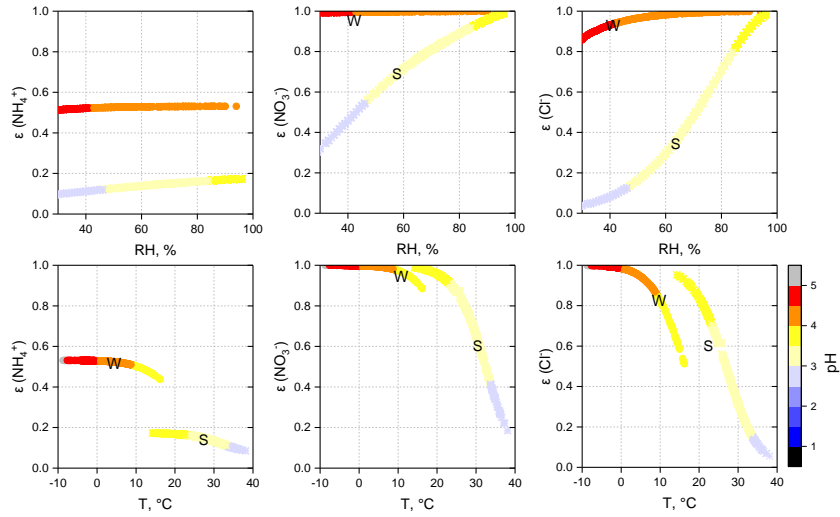
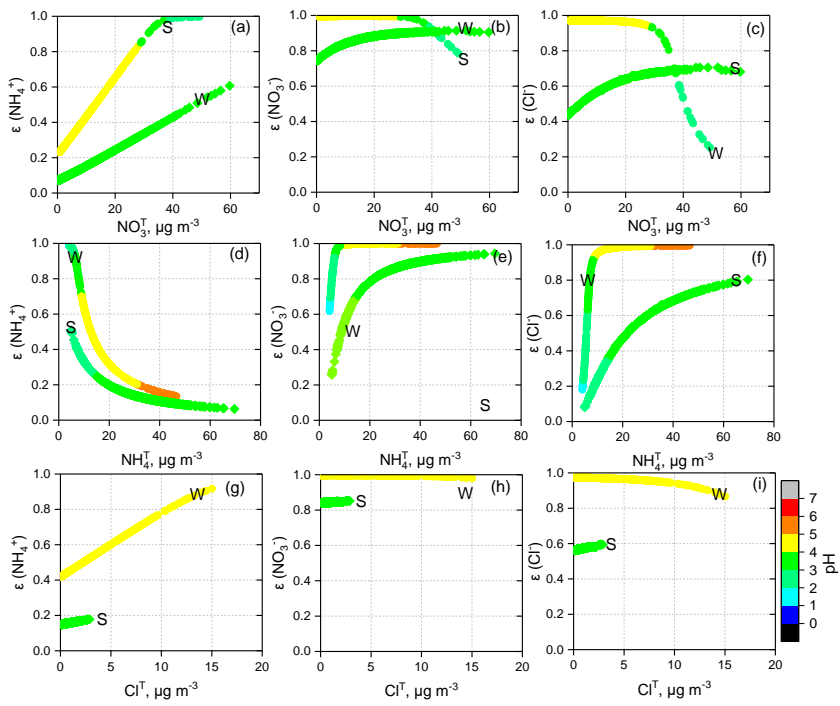


Figure 10.



1131

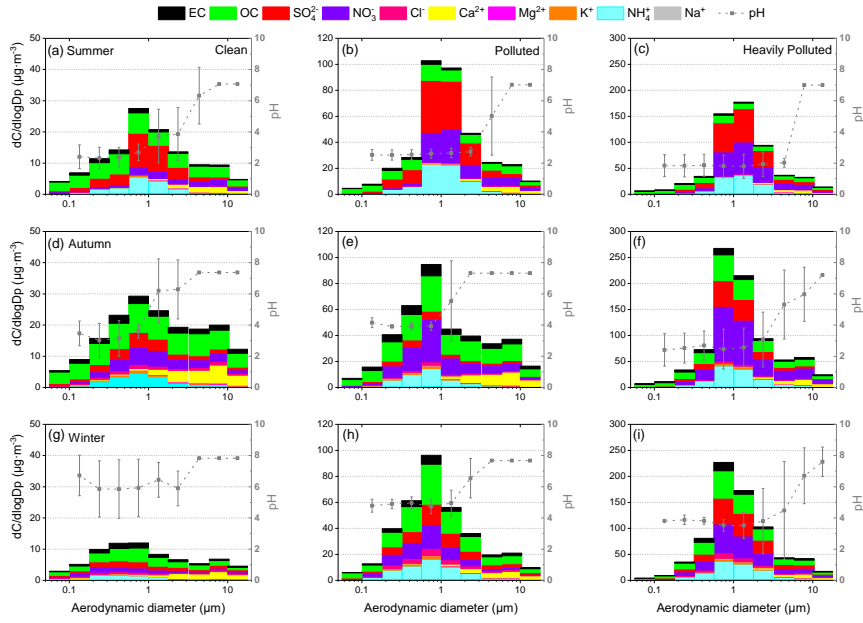
1132

1133

1134

1135  
1136  
1137  
1138

**Figure 11.**



1139  
1140

**Figure 912.**

带格式的: 字体: 加粗

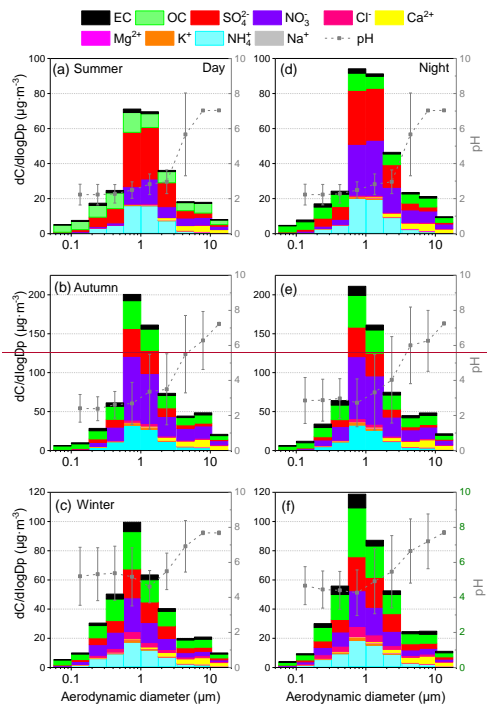


Figure 10.

1141

1142